REPAIRING AND RETROFITTING OF NON-SEISMICALLY DESIGNED REINFORCED CONCRETE CIRCULAR BRIDGE PIERS WITH LOW GRADE GLASS FIBRE REINFORCED POLYMER

by

Md. Mosharef Hossain

B.Sc., Bangladesh University of Engineering and Technology, 2014

A THESIS SUBMITTED IN PARTIAL FULFILLMENT OF

THE REQUIREMENTS FOR THE DEGREE OF

MASTER OF APPLIED SCIENCE

in

THE COLLEGE OF GRADUATE STUDIES

(Civil Engineering)

THE UNIVERSITY OF BRITISH COLUMBIA

(Okanagan)

September 2017

The undersigned certify that they have read, and recommended to the College of Graduate Studies for acceptance, a thesis entitled:

REPAIRING AND RETROFITTING OF NON-SEISMICALLY DESIGNED REINFORCED CONCRETE CIRCULAR BRIDGE PIERS WITH LOW GRADE GLASS FIBRE REINFORCED POLYMER

Submitted by Md. Mosharef Hossain in partial fulfillment of the requirements of the degree of

Master of Applied Science

Dr. M. Shahria Alam, Associate Professor, School of Engineering, UBC
Supervisor

Dr. Ahmad Rteil, Assistant Professor, School of Engineering, UBC
Supervisory Committee Member

Dr. Kasun Hewage, Professor, School of Engineering, UBC
Supervisory Committee Member

Dr. Thomas Johnson, Assistant Professor, School of Engineering, UBC
University Examiner

Dr. Rudolf Seethaler, Associate Professor, School of Engineering, UBC
Neutral Chair

21 September 2017
(Date Submitted to Grad Studies)

Abstract

Many of the highway bridges in Canada have passed their anticipated service life and do not meet the current seismic standard because of seismic design code upgradation. These bridges either need to be demolished or seismically upgraded causing a huge impact on the economy. A cost-effective alternative to current rehabilitation materials is required that can serve the purpose reliably. Glass Fibre Reinforced Polymer is a composite material that has emerged as a viable solution to this with its attractive mechanical properties, corrosion resistance and ease of application. This thesis presents an experimental investigation on the effect of repairing and retrofitting on the performance of damaged and deficient reinforced concrete circular bridge piers using a low grade GFRP. Market available bi-directional GFRP fabrics, commonly used for non-structural application like boat and yacht strengthening were used and their mechanical and bonding properties were obtained by laboratory test. The effect of this GFRP confinement thickness on the compressive strength of concrete was evaluated by testing cylinders confined with GFRP layers having a variable thickness. The effect was further investigated on the performance of 1/3 scale circular bridge piers by repairing and retrofitting with 2 layers and 150 mm overlap length of GFRP. Performance of these piers was compared in terms of lateral load capacity, drift, ductility and energy dissipation capacity with deficient pier. Finally, the performance of repaired and retrofitted piers under simulated seismic aftershocks was investigated and compared. Results of this study show that GFRP repaired pier can restore its strength with increased ductility and retrofitting it before damage improves the flexural capacity by 27%, energy dissipation capacity by 140% and ductility by 73%. Also, the retrofitted pier was capable of withstanding six consecutive seismic loading whereas the repaired pier failed after only two sets of seismic loading.

Preface

Major portions of the research work outlined in this thesis have been submitted to peer-reviewed technical journals for publication. All analytical work, literature review, modelling process, and writing of the initial draft of all papers presented in the following journal papers have been solely carried out by the author. The thesis supervisor was responsible for the research guidance and supervision of the work and helping in the development of the final versions of the publications.

List of publications related to this thesis

A portion of Chapter 3 has been published in the 6th International Conference on Engineering Materials and Mechanics, May 31- June 3, 2017, Vancouver, Canada. **Hossain, M.M.** and Alam, M.S. Compressive Strength Enhancement of Low-Strength Concrete Subjected to Freeze-Thaw Effect Using Glass Fibre Reinforced Polymer. I wrote the manuscript which was further edited by Dr. Alam.

A portion of Chapter 4 will be submitted to the ACI Structural Journal, 2017. **Hossain, M.M.** and Alam, M.S. Will a Seismically Damaged Deficient RC Bridge Pier After Repairing Perform Similarly Compared to that of a Retrofitted RC Bridge Pier? I wrote the manuscript which is being further reviewed and edited by Dr. Alam.

A portion of Chapter 5 will be submitted to the ASCE Journal of Bridge Engineering, 2017. **Hossain, M.M.** and Alam, M.S. Performance of GFRP Repaired and Retrofitted RC Circular Bridge Pier Under Simulated Earthquake Aftershocks. I wrote the manuscript which is being further reviewed and edited by Dr. Alam.

Table of Contents

List of Tables

List of Figures

Acknowledgements

I convey my profound gratitude to the almighty Allah for allowing me to bring this effort to realization. I cannot express greatly enough my appreciation to my supervisor, Dr. M. Shahria Alam for providing me with an opportunity to work with him at The University of British Columbia. I could not have asked for a better mentor and guide for my Master program and I really appreciate all the support, guidance, and motivation that he has provided me throughout my graduate studies. He has been instrumental with knowledge, support, and mentoring that made my graduate experience at UBC so immaculately productive and rewarding, and made a great contribution to the success of this research.

I would like to thank my thesis committee members, Dr. Ahmad Rteil and Dr. Kasun Hewage for always supporting my research work and providing me with great feedback from time to time, helping me improve the quality of my work immensely. Graduate school and experimental research facility at UBC's Okanagan campus has provided an excellent educational experience.

I have been fortunate to get the opportunity to work with an excellent group of graduate students in the research group who have offered technical knowledge, lively discussions, and friendship. I offer my enduring gratitude to the assistance of UBC Structures Laboratory Technicians especially Alec Smith and Kim Nordstrom, and graduate student Anant Parghi for assistance with the test setup and specimen preparations.

I am truly grateful for the unconditional support of my family members; my mom, brother and sister, whom I feel to be the key source of inspiration for all my achievements. They have offered endless support, wise advice, and love. Their support, sacrifice, and enduring love have meant the world to me throughout this process and always.

DEDICATED TO MY MOM

Chapter 1

Introduction

1.1 General

The highway transportation system is a critical foundation for a country's economic development. They act as the arteries, just like a human body to establish link between different cities and across the country. The continuity of this transportation system is maintained by constructing bridges over lakes, tunnels and rivers. There are more than 685,000 reinforced concrete (RC) bridges in North America, among them about 80,000 are in Canada (Huijbregts 2012). About 40% of the civil infrastructure including highways bridges in Canada have passed their service lives and they are deficient either structurally or functionally (Huijbregts 2012). In addition to that, updating the seismic design made many of the existing bridges not to meet the current seismic standard. These bridges either need to be demolished or seismically upgraded. Therefore, huge amount of bridge rehabilitation and replacement work need to be done in the near future in North America in order to ensure a safe and continuous transportation facility.

Recent earthquakes, including 2012 Emilia earthquakes Italy, 2011 Tohoku earthquake, 2011 Christchurch earthquake New Zealand, and 2011 Sikkim earthquake India have made people aware of the catastrophic damages and collapse of the buildings and bridges designed and built according to older seismic design codes. Piers are the most critical elements of a bridge and many of the concrete bridges failed during past earthquakes due to the failure of piers. Many existing bridges were designed without following any seismic guideline as they were constructed prior to seismic resistance design code. Again, many bridges may become

deficient as they might not have been designed as per the principle of the capacity design, or they may have been constructed in a location where the seismic hazard level has been reevaluated and augmented (ATC-32 1996, CAN/CSA-S6 2014). Research studies reported that the inadequate lap splice length at the plastic hinge zone and inadequate transverse reinforcement are the most significant factors causing a lateral deficiency in resisting seismic force leading poor flexural ductility and/or insufficient shear capacity (Priestley and Seible 1995, Elsanadedy and Haroun 2005).

In order to avoid catastrophic damage during a seismic event that may occur in the near future, these deficient bridges need to be replaced with a new one or strengthened up to the current seismic standards. However, new construction is quite expensive, time consuming and even impractical in some cases. Hence, strengthening the existing deficient bridges with proper retrofitting technique is the viable solution to avoid any devastation during earthquakes.

1.2 Objective of the Study

Researchers and engineers are using fibre reinforced polymer with high mechanical properties for rehabilitation of structures. Extensive research has been done on the application of this technique. But up to the best knowledge of the author, no one has investigated the effect of low grade GFRP on the performance of concrete and bridge piers as well. Also, the performance of rehabilitated bridge piers under earthquake aftershocks has not been studied before. The primary objectives of the current study include:

1. Investigating the effect of market available low grade GFRP confinement on the compressive strength of concrete. This aims to find a cost-effective and available

alternative to retrofit bridge infrastructures as compared to high strength FRP composite materials.

2. Seismic performance comparison between a GFRP retrofitted deficient RC bridge pier and a seismically damaged deficient RC bridge pier repaired and strengthened with GFRP. Evaluating the effectiveness of an easy and simple repairing method of bridge piers where damaged concrete is replaced with new repair concrete but yielded and bucked reinforcements are kept in place.
3. Performance investigation of GFRP repaired and retrofitted RC circular bridge pier under repeated seismic loading that represents the earthquake aftershocks and their comparison with deficient pier.

1.3 Scope of the Research

This research plays an important role in investigating and improving the seismic performance of bridges designed according to old bridge design codes by using a cost-effective alternative. In order to achieve the goals of this study, the deficiencies in existing old bridge piers were identified and their corresponding effects on the bridge performance were obtained from literature. Experimental investigations on low grade GFRP confinement thickness effect, how it improves the seismic performance of deficient piers during earthquake and its aftershocks help to evaluate the effectiveness of market available low grade GFRP for retrofitting purpose. Also, the effectiveness of a quick and easy repairing method has been studied in this thesis.

1.4 Thesis Organization

This thesis is organized in six chapters. The outline of the thesis is presented in Fig. 1.1. In the present chapter (**Chapter 1**), a brief preface, research objectives and scope are presented. The content of this thesis is organized into the following chapters:

In **Chapter 2**, a comprehensive review of the currently available literature on FRP retrofitted piers is presented. Review on common seismic deficiencies found in existing old bridges along with a detailed review of researches related to the application of bridge pier retrofit and strengthening techniques is presented. This chapter also describes the application of various retrofitting techniques developed for bridge strengthening and their comparative performance evaluation.

In **Chapter 3**, an experimental investigation on the effect of market available low grade GFRP confinement with varying thickness on the compressive strength of concrete is presented. The GFRP used for this study is low grade and has low mechanical properties as compared to other FRPs available in the market. The mechanism behind FRP confinement is explained and the mechanical properties of GFRP are tested. The effect of layer thickness on the compressive strength of concrete is investigated by experiment. The optimum overlapping length for developing full tensile strength in fibres is also determined. These results are used in the process of repairing and retrofitting technique discussed in Chapter 4. Finally, these confinement effects are applied on a bridge pier and its performance for varying number of layers (i.e. thickness) under lateral loading is analyzed using finite element modeling.

Chapter 4 demonstrates the cyclic performance comparison of reinforced concrete circular bridge pier repaired and retrofitted with low grade GFRP confinement. Mechanical and bond properties obtained in Chapter 3 are used in the process of repairing and retrofitting. A seismically deficient prototype bridge pier is considered for the study and it was further scaled down for experimental investigation. The test setup, instrumentation layout, and loading protocol are presented. The steps involved in repairing and retrofitting are also described briefly. The results of the experiments are presented in terms of cyclic response, strain response, moment-curvature, ductility analysis, energy dissipation and residual drift and compared for three conditions of pier: deficient, repaired and retrofitted. The effectiveness of a proposed repairing technique is evaluated by comparing the results. The failure modes of the tested specimens are also presented at the end.

Chapter 5 presents the performance of a GFRP retrofitted reinforced concrete circular bridge pier under repeated sets of cyclic lateral loading. These repeated sets represent the aftershocks associated with earthquakes. Once a repaired or retrofitted pier is damaged during a main shock, its capacity to prevent collapse during the associated aftershocks is studied which has not been done before. For this purpose, the tested specimen in Chapter 4 are subjected to several sets of cycling loading until they reach failure using the same test setup. Test results of repaired and retrofitted pier under several sets of lateral loadings are presented and compared.

Finally, **Chapter 6** presents the summary and conclusions attained from this study. The limitations of this study are discussed and some recommendations for future studies on this topic are also suggested in this chapter.

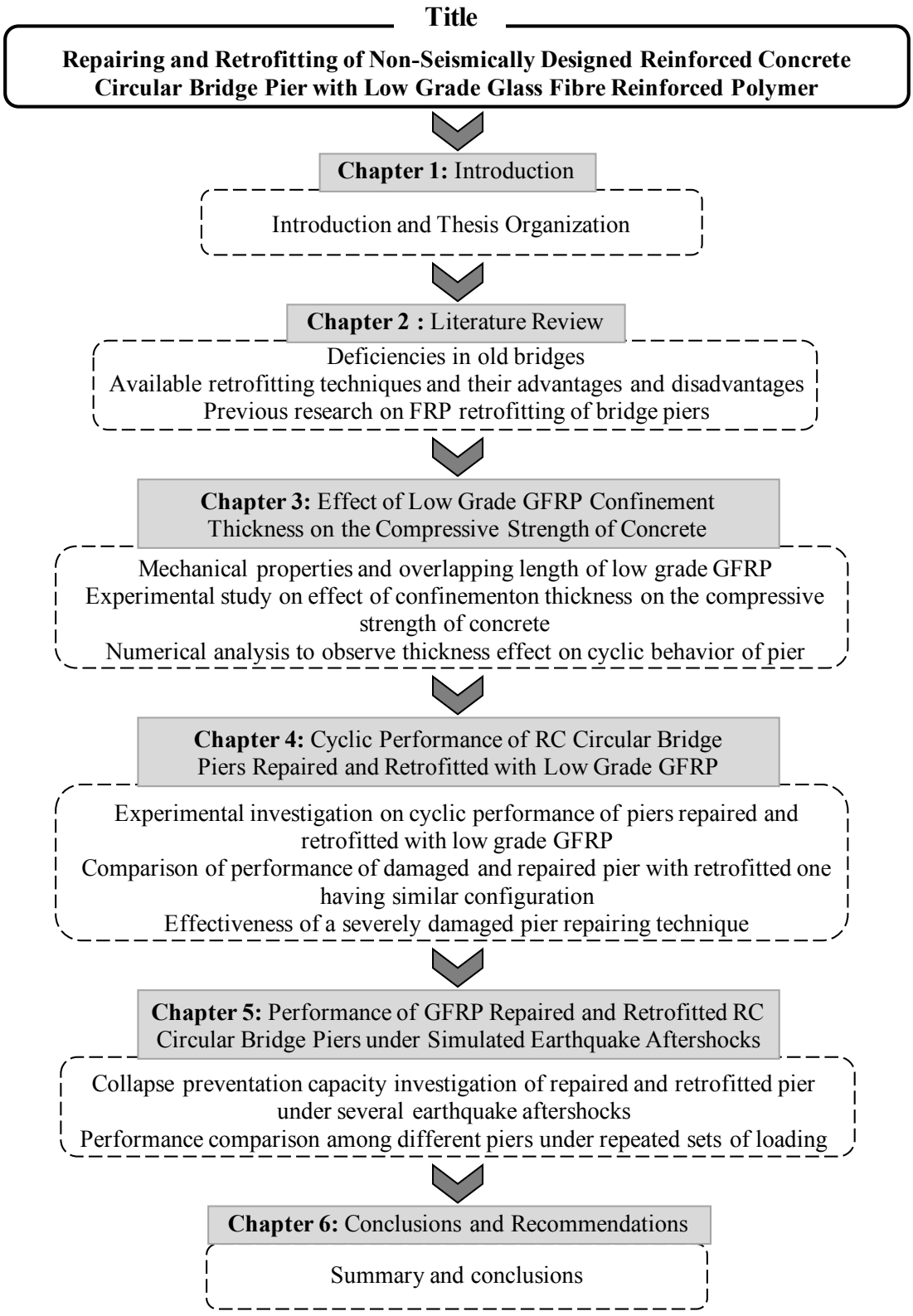

Figure 1.1: Outline of the thesis

Chapter 2

Literature Review

2.1 General

This chapter provides a comprehensive literature review on seismic deficiencies found in existing bridges along with a detailed review of researches related to the application of bridge retrofit and strengthening techniques and their consequences in performance.

2.2 Seismic Deficiencies of Existing Bridges

Researchers have reported the deficiencies in existing bridges through extensive studies. Their studies include the damages occurred during major earthquakes like- 1971 San

Table 2.1: Deficiencies in existing old bridges

Location	Deficiency	Consequences
Column	Large spacing of transverse reinforcement	Inadequate confinement of core concrete. Unable to prevent longitudinal bar buckling. Susceptible to shear failure.
	Longitudinal bar splicing in PH region	Limited hinging length. Inadequate splice length unable to transfer the full tensile force.
	Absence of intermediate cross ties	Inadequate shear strength. Inadequate control of bar buckling.
Cap Beam	Insufficient anchorage length of longitudinal reinforcement	Insufficient flexural capacity.
	Inadequate shear reinforcement	Insufficient shear capacity.
	Inadequate embedment of bottom bars in joints	Insufficient development of flexural reinforcement.
Bent Joint	Lack of vertical and horizontal shear reinforcement	Insufficient shear strength.
	Large diameter bends necessary for large bar sizes	Reduction of effective depth of joint region. Formation of weak shear plane through joint.
	Poor anchorage detailing of transverse and flexural reinforcement	Insufficient shear and flexural strength of joint.

Fernando earthquake (Housner 1971), 1989 Loma Prieta (Bruneau 1990, Mitchell et al. 1991), 1994 Northridge (Mitchell et al. 1995, Seible and Priestley 1999) and 1995 Kobe earthquake (Anderson et al. 1996, Taylor 1999). According to a study conducted by Mitchell et al. (1994), columns have many deficiencies in existing bridges built before 1970. The deficiencies observed in different elements of bridges are presented in Table 2.1.

2.3 Limitations of Old Bridge Design Codes

Many of the bridges in North America built before 1971 San Fernando earthquake may not have adequate seismic resistance as specified by previous design code (ATC-32 1996), and the recent design guidelines (CAN/CSA-S6 2014). This is because of the application of elastic design philosophy in earlier days. In recent guidelines, bridge piers are required to be designed with sufficient energy dissipation capacity during an earthquake. Bridge piers with poor reinforcement detailing are susceptible to loss of axial and lateral load carrying capacity at 2 to 3 % drift level during a design level earthquake (Boys et al. 2008). In most of the bridges designed using pre-1971 guidelines, the axial capacity of the pier was the focus of design criteria. Lateral loads were not considered in design and bridges were built with sufficient longitudinal reinforcement, but with traditional hoop spacing of 300 mm, irrespective of column size, strength, or deformation demands. These hoops were often closed by lap splices in the cover concrete instead of being anchored by bending back into the core concrete. Such transverse reinforcement provides inadequate confinement for the core concrete under compression and insufficient clamping action to the longitudinal reinforcement to prevent buckling. As a result, the ultimate curvature developed within the potential plastic hinge region is limited by the strain at which the cover concrete begins to spall, which is typically around0.5 percent strain (Chai et al. 1991). Thus, the failure of pier

is initiated by cover concrete spalling, leading to crashing, and later buckling of reinforcement due to the splitting action under fully reversed cyclic loads. The inadequate transverse reinforcement and inadequate lap splice length at the plastic hinge zone were the most significant factors causing a lateral deficiency in resisting seismic force (Priestley and Seible 1995, Elsanadedy and Haroun, 2005).

The maximum spacing of transverse reinforcement specified in CAN/CSA-S6 (1974) code was the least of 16 times the diameter of longitudinal reinforcement, 48 times diameter of stirrup or smallest dimension of the pier. CSA CAN3-S6-M (1978) code provisions specified the tie spacing of 300 mm or the smallest dimension of the member, and tie must cover every alternate bar. According to CAN/CSA-S6 (2006), the maximum spacing of transverse reinforcement is the smallest of six times the longitudinal bar diameter or one-fourth of the minimum dimension of pier or 150 mm and tie must cover every longitudinal bar. Thus, recent Canadian bridge design code CAN/CSA-S6 (2014) has specified lower tie spacing than that of 1974 and 1978 code provisions.

2.4 Performance of RC Bridge Piers in Past Earthquakes

Past earthquake reconnaissance report showed that many of the damaged bridges experienced structural collapse because of poor detailing. The 1971 San Fernando, 1989 Loma Prieta, and 1994 Northridge earthquakes in California; the 1995 Kobe earthquake, the 2004 Niigata-Keb Chuetsu earthquakes in Japan; the 1999 chi-chi earthquake in Taiwan; the 1999 Kocaeli and Duzce earthquakes in Turkey; the 2010 Chile earthquake in Chile resulted significant damages to many of the bridges that lead to structural collapse. In many cases, the failure occurred at the base of the piers because of inadequate confinement from transverse

reinforcement (Kawashima 2011). Another common reason of failure was insufficient development length (20 times bar diameter) of longitudinal rebar terminated at mid-height of piers (Kawashima 2011). Some bridges designed following recent codes but with poor detailing also suffered serious damages. According to Taiwanese Highway Bureau's preliminary report, minimum 9 bridges were severely damaged, including 3 bridges that were under construction during 1999 Chi-Chi earthquake in Taiwan. Five of them collapsed due to fault rupture, and seven were moderate damaged (Yen 2002). As mentioned before, the past earthquake records proved that existing bridges built prior to the 1971 seismic design code provisions have shown many drawbacks. Studies on these records (Chai et al. 1991, Priestley et al. 1994, Maekawa and An 2000) concluded that insufficient flexural ductility and shear capacity are the two main reasons for the failure of RC bridge piers. Inadequate transverse confinement and insufficient lap splice length at the plastic hinge region are main causes for low flexural ductility, and shear failure in many collapsed bridge piers (Priestley and Seible 1995, Seible et al. 1997, Elsanadedy and Haroun 2005).

2.5 Existing Seismic Retrofitting Techniques for RC Bridge Piers

Seismic retrofitting of existing bridges is a challenging job that requires defining the seismic performance level and the goals. Over the years, engineers have developed various rehabilitation techniques for upgrading the seismic performance of existing RC structures. Extensive analytical and experimental studies have been carried out by researchers to reveal the influential factors behind seismic performance improvement of bridges. A common method to improve the seismic performance of poorly designed RC piers is proving an external confining layer at the potential plastic hinge region. Priestley et al. (1996) presented

different seismic rehabilitation methods for reinforced concrete bridge piers using concrete, steel and fibre reinforced polymer (FRP) confinement.

Confinement approaches could be divided into two major types, namely, active confinement and passive confinement techniques. In active confinement technique, the confining pressure is applied prior to the application of axial compression load. This delays damages sustained by the concrete. The feasibility of active confinement technique for seismic retrofitting of RC structures has been studied by several researchers (Gamble et al. 1996, Saatcioglu and Yalcin 2003). Although, there are benefits for active confinement, its field application is limited due to difficulties associated in application at job site. The passive confinement can be defined where the confinement reacts to the expansion of concrete under axial compression load. Steel plates and FRP jacketing are the most common methods for passive confinement techniques to improve the ductility of vulnerable piers (Chai et al. 1991, Norris et al. 1997, Elsanadedy and Haroun 2005). The passive confinement technique is easier to apply and widely used all over the world.

2.5.1 Active Confinement Techniques

It is well established that, inadequate confinement, insufficient transverse reinforcement and lack of proper reinforcement splicing are the most common causes of failure of existing bridges under earthquake motions. Researchers reported that, active confinement technique is superior to the passive confinement techniques for seismic retrofitting.

2.5.1.1 External Prestressing

External prestressing can be an effective method of confining concrete and improve its compressive and ductile behavior. This is done by wrapping prestressing wire under tension around a column. Reliable anchorage of the wire ends is essential for this method to be effective in field application. This helps to increase the flexural ductility of circular columns with lap splices at the critical region, though its effect on shear strength has not yet been investigated. Figure 2.1 shows the active confinement technique using prestressing wire.

Figure 2.1: Circular reinforced concrete piers prestressed with steel wires (Zong-Cai et al. 2014)

Several researchers conducted experimental study in order to investigate the viability of applying active confinement in the field of seismic retrofitting. Coffman et al. (1991) demonstrated the application of prestress steel hoops to retrofit circular bridge columns. They reported that, this technique is effective for long columns with flexural failure behavior. Saatcioglu and Yalcin (2003) conducted experimental investigation on two full-scale square columns, and five circular columns externally confined with prestressing strands under lateral cyclic load along with a constant axial load. Results from their study showed improvement in flexural strength and ductility. This is because of the additional confinement and shear reinforcement provided by external prestressing system.

2.5.1.2 Shape Memory Alloy (SMA) Spirals

Shape Memory alloy can be an alternative material for actively confining circular bridge piers. The large strain recovering capacity of SMAs helps to restore the strength, stiffness, and flexural ductility of deficient piers. Shin and Andrawes (2011) tested 1/3 scale RC circular pier in as-built condition and actively confined with shape memory alloy spiral wires. They reported improvement in strength and ductility because of the active confinement provided by SMA spiral, which could delay the propagation of further damage.

2.5.2 Passive Confinement Techniques

2.5.2.1 Concrete Jacketing

Concrete jacketing had been a popular method for rehabilitation of deficient structures in earlier days. It is more economical and the most suitable method for underwater retrofitting works. In this method, a thick layer of reinforced concrete jacket to improve the sectional properties of piers. It has some drawbacks when compared to FRP and steel jacketing. Itis more labor-intensive, time consuming, and could have shrinkage and bonding problem with substrate concrete. Another consideration is that, it reduces the available floor area and modifies the dynamic characteristics of the entire structure by increasing the member size. If applied with appropriate reinforcement and anchorage, this method can enhance the stiffness, flexural and shear strength as well as the deformation capacity. Figure 2.2 illustrates the concrete jacketing technique.

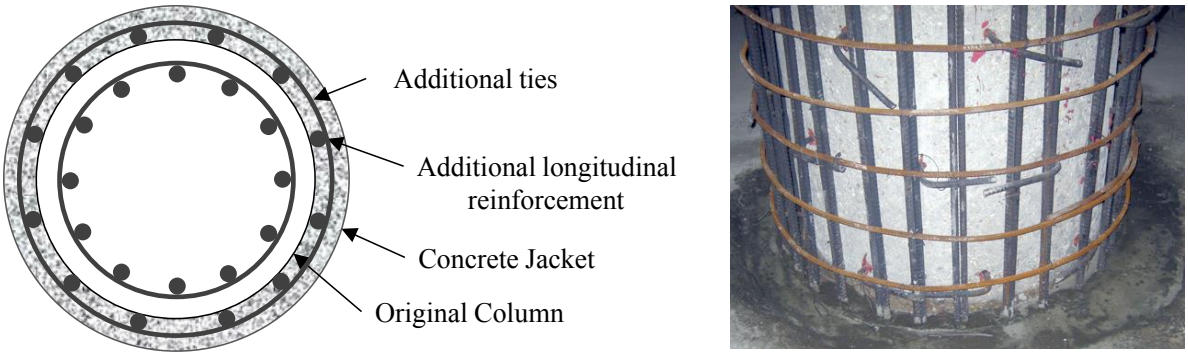

Figure 2.2: Column retrofitting technique using concrete jacket

Rodriguez and Park (1994) conducted experimental investigation on rectangular RC pier retrofitted with concrete jacketing under simulated seismic load. They observed improved strength, stiffness and ductility of damaged and undamaged piers encased with concrete jacket. Priestley et al. (1996) provided a detailed description about concrete jacketing technique for both rectangular and circular columns. They reported that the construction and effectiveness of concrete jacket is convenient for circular column using closely spaced ties. Bousias et al. (2006) concluded that, the concrete jacketing is effective for retrofitting piers with a lap splice length of, as short as 15-bar diameter.

2.5.2.2 Steel Jacketing

The strength and ductility of deficient piers can be enhanced using steel jackets. This method was originally developed for circular columns and further modified for rectangular column with elliptical steel jacket. Figure 2.3 depicts typical steel jacketing for circular pier.

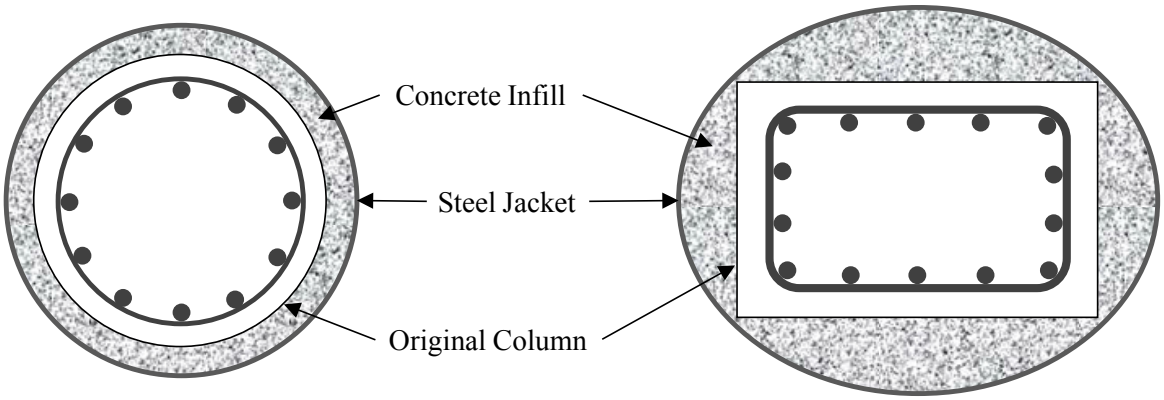

Figure 2.3: Steel jacketing technique for circular and rectangular column.

Many researchers experimentally investigated the effectiveness of steel jacketing for retrofitting seismically deficient RC column. Chai et al. (1991) found in their study that, columns retrofitted with steel jacket exhibit ductility similar to that of columns designed following current seismic codes. Later, Priestley and Seible (1991) conducted more experimental investigation and introduced steel jacketing technique as a retrofitting method for both circular and rectangular columns. Tsai and Lin (2001) introduced octagonal steel jacket that improved ductility and cyclic strength of deficient RC rectangular bridge piers.

2.5.2.3 Engineered Cementitious Composite Jacketing

Engineered Cementitious Composite (ECC) has emerged as a technique to increase the ductility of Ultra High Performance Concrete (UHPC). UHPC has been used for construction of tall buildings and large bridges from the last decades. But, the brittle nature of UHPC limited its use in structural applications. To change this nature of concrete, Li (1992) and his research team developed a concept of high performance fibre reinforced cementitious composites with micromechanical principles. These principles allow it to strain harden in tension and exhibit much higher strain capacity (0.03-0.05) than normal concrete (Li et al. 2001, Kesner and Billington 2004, Boshoff 2014). Minimum amount of reinforcing fibres

(less than 2% by volume) is required to represent high performance with extreme ductility (Kesner and Billington, 2005). ECC has high tensile ductility, high damage tolerance and much finer crack development that make ECC superior than ordinary concrete.

ECC has been used in many structural applications because of its appealing properties. Example includes RC coupling beams (Canbolat et al. 2005 and Yun et al. 2005) and beam-column connections (Parra-Montesinos and Wight 2000). The use of ECC has been proposed to provide energy dissipation to systems that do not possess such characteristics, such as frames or members reinforced with FRP bars that do not yield (Fischer and Li, 2003) and for retrofitting applications of seismically deficient structures (Kesner and Billington, 2005). Billah et al. (2013) and Billah and Alam (2014) conducted fragility analysis of multicolumn bridge bent retrofitted with four different techniques. From their nonlinear dynamic analysis and developed fragility curve, they reported that the bridge bents retrofitted with ECC and CFRP jacketing possess less vulnerability at different damage states under both near-fault and far-field earthquakes.

2.5.2.4 Ferro Cement Jacketing

Ferro cement is a thin composite concrete shell reinforced with continuous wire mesh. Hydraulic cement is used to prepare the mortar for ECC and the mesh is closely spaced. It has isotropic behavior in two principal directions. Small diameter wires are uniformly distributed over the entire volume of mortar. These wires lead to a higher specific surface area which offers more effective confinement. This confinement makes the material isotropic and homogeneous in both principal directions leading to much higher ductility. Ferrocement is moderately cost effective and does not require any advance technique for application. Low

material cost, special fire and corrosion protection characteristics of ferrocement make it an appropriate mean for jacketing materials (Williamson and Fisher 1983, ACI 549.1R 1993).

The potential applications of ferrocement jacketing have been reported by numerous researchers in their rehabilitation studies. Kaushik et al. (1990) revealed that the ferrocement confined short concrete piers could enhance the strength and ductility of piers for both axial and eccentric loadings. Xiao et al. (2011) reported that the ferrocement confined piers produce a more ductile behavior than the fibre-reinforced polymer confined piers. Kumar et al. (2005) conducted an experimental investigation on RC bridge piers strengthened with ferrocement. Their observation revealed that, enhanced stiffness, strength, energy dissipation and ductility can be achieved using ferrocement jacketing.

2.5.2.5 FRP Composite Jacketing

Fibre Reinforced Polymer (FRP) composites are manufactured by combining high strength fibres and resins. These composites were initially developed for application in mechanical and aerospace engineering (Fardis and Khalil 1982). FRP materials have several advantages over concrete and steel jacketing such as, high strength to weight ratio, high elastic moduli, resistance to corrosion, and ease of application (Billah 2011). These qualities made FRP composites a suitable candidate for structural retrofitting and confining material. Table 2.2 shows a comparison of mechanical properties of commonly available FRP's for structural application.

Figure 2.4: Retrofitting of RC circular bridge piers using CFRP (Priestley et al. 1996)

Researchers have investigated the viability of FRP passive confinement techniques for seismic upgradation of deficient bridge piers (Saadatmanesh et al. 1994, Ma and Xiao 1997, Samaan et al. 1998, Bakis et al. 2002, Chang et al. 2004, Haroun and Elsanadedy 2005, Han et al. 2014). Nanni et al. (1999) retrofitted RC bridge piers with near surface mounted carbon FRP rods as well as jackets made of continuous FRP sheets and tested them up to failure. Gallardo-Zafra and Kawashima (2009) conducted experimental investigation on CFRP retrofitted rectangular RC bridge piers under near-fault ground motions. Their study reported that flexural strength and ductility of piers retrofitted with CFRP composites increased with the increasing CFRP confinement ratio. Parghi and Alam (2016) studied the effect of different design parameters and their interactions on the limit states of CFRP confined deficient RC circular bridge piers. In another study, Parghi and Alam (2017) studied the seismic vulnerability of FRP retrofitted piers. Both the study showed that, the shear span-depth ratio, yield strength and longitudinal reinforcement ratio, axial load and CFRP confinement significantly affect the lateral load capacity, ductility and the failure mode of retrofitted bridge piers under seismic load.

Table 2.2: Mechanical properties of FRPs available for structural application

Type of FRP	Tensile Strength (MPa)	Elastic Modulus (GPa)	Strain at Break (%)
CFRP	1720-3690	120-580	0.5-1.9
GFRP	480-1600	35-51	1.2-3.1
AFRP	1720-2540	41-125	1.9-4.4
BFRP	1035-1650	45-59	1.6-3.0

2.6 Comparative Assessment of Retrofitting Techniques

This section describes a comparative assessment of different retrofitting techniques. Among the available retrofitting techniques, steel jacketing is the most popular around the world. This method is used by CALTRANS and a good number of bridges have been retrofitted using this technique. Concrete jacketing is the oldest form of retrofitting technique and more effective for circular column. Now-a-days, FRP composites have become an attractive alternative technique of seismic retrofitting because of their attractive mechanical properties, lightness and corrosion resistance. Table 2.3 shows the advantages and disadvantages of popular retrofitting methods.

Table 2.3: Advantages and disadvantages of concrete based jacketing

	Technique	Advantage	Disadvantage
Concrete Based	Concrete jacket	Increased flexural and shear strength, low cost, suitable for underwater work.	Reduced compressive strength of column as a result of biaxial stress state coming from additional tensile stress in jacket.
	Ferro-cement jacket	Low cost, easy application, flexible for circular or rectangular column.	Low durability, poor aesthetics.
	ECC jacket	Ductile, high energy dissipation and damage tolerance, strain hardening property.	High cost, limited design guideline, lack of experience.
Steel Based	Steel based	Readily available, low cost, durable.	Corrosion, heavy weight.
	Circular jacket	Effective, practical application.	High installation cost, difficult to weld.
	Elliptical jacket	Suitable for rectangular column, provides adequate confinement.	Limited application, high installation cost, special forms and bracing required.
	Plates and angles	Readily available, easy to work with.	Enormous welding, quality assurance, high installation cost.
	Jacket and stiffeners	Good aesthetics, readily available, easy to handle.	Difficulty in cutting and welding.
	Prestressed external hoops	Effective on flexural strength and stiffness improvement.	Applicable to circular column only, reliable anchorage required.
FRP Based	Advanced composite	Strong, lightweight, durable, low labor cost.	High material cost, temperature sensitive, moisture prone.
	Carbon Fibre	Easy application, high tensile strength, high modulus of elasticity, flexural and shear enhancement.	High material cost.
	Glass Fibre	Moderate cost, improved ductility of column.	Susceptible to moisture absorption.
	Aramid Fibre	Light and easy application, good fatigue behavior, suitable for column with varying cross-section.	High cost, susceptible to moisture absorption.

2.7 Previous Research on GFRP Retrofitted RC Bridge Piers

Researchers have conducted numerous experimental investigations on the seismic behavior of GFRP retrofitted RC bridge piers. Priestley and Seible (1993) carried out tests on 2/5 scale substandard bridge piers retrofitted with GFRP confinement. They applied reversed cyclic load along with 18% axial load and tested the piers up to failure. Diagonal cracks were observed and the piers were damaged with spalled concrete. After that, they repaired the piers by removing lose concrete and patching with cement-sand mortar, and injecting epoxy in the cracks. Their study concluded that the strength of retrofitted and repaired piers was restored with a high ductility compared to as-built specimen. Saadatmanesh et al. (1997) performed tests on GFRP retrofitted RC circular bridge piers under seismic load along with constant axial load. They observed that the piers experienced severe damage with debonding of starter bars, spalling and crushing of concrete, buckling and separation of longitudinal rebar from the core concrete. They repaired the piers with active GFRP confinement straps after testing in as-built condition. They reported that GFRP active strap confining technique is effective and enhances both flexural strength and ductility. Xiao et al. (1999) studied the influence of prefabricated GFRP jacket on deficient ½ scale RC circular bridge piers for enhanced shear strength. Their experimental results showed that the full height GFRP jacketed specimen exhibited improved hysteretic behavior with high ductility. The stable performance in hysteretic loops can prevent shear failure of the piers. Sheikh and Yau (2002) conducted investigation on circular RC deficient piers confined with GFRP and CFRP composites under simulated seismic lateral cyclic load with constant axial load (27 and 57% of axial capacity). Their study reported that the CFRP and GFRP retrofitted piers showed more ductile and stable behavior compared to the as-built piers. The retrofitted specimen,

which was tested with 27% axial load, exhibited significantly more ductile behavior and higher energy dissipation capacity than a specimen with an axial load of 54%. Shin and Andrawes (2011) carried out tests on 1/3 scale deficient RC circular piers under lateral cyclic load and 5% constant axial load. The piers once tested were repaired using mortar and epoxy injection and retrofitted using varying layer of GFRP up to different height. They concluded that strength of the GFRP retrofitted piers was restored and ductility and energy dissipation capacities were significantly improved compared to as-built pier.

2.8 Summary

The relevant research reported in the existing literature was summarized in this Chapter. The deficiencies in the existing bridges are shown; limitations of old bridge design codes are marked, performance of bridge piers in the past earthquakes are described. The existing techniques of repairing and retrofitting are described with their relative advantages and disadvantages. Finally, an overview on GFRP composite materials is given with its detailed mechanical and environmental properties.

Chapter 3

Effect of Low Grade GFRP Confinement Thickness on the Compressive Strength of Concrete

3.1 General

Concrete is one of the major role playing composite materials in the field of infrastructure development. It has a very good compression taking capability which makes it the most suitable material for construction of buildings, bridges, highways and runways. Reinforced with steel or any other reinforcing material, it forms different structural elements. In this fusion, concrete plays the role of taking major compressive loads while the reinforcements take most of the tensile loads. This compression taking capability of concrete can be significantly improved by adding a confinement effect that basically comes from the shear reinforcement in structural elements when it is designed properly. When structural members are designed with low shear demand or without considering the seismic requirements, concrete doesn't get the confinement from inadequate shear reinforcement.

Earlier before 1970, there was no strict provision for seismic code. Thus, many of the bridges were built without considering the seismic effect and minimum requirements needed for withstanding the damage event of an earthquake. This deficiency in confinement can be resolved by adding external confinement using different techniques using steel tube and composite materials like GFRP and CFRP. Among these GFRP is cost-effective and most convenient for easy application. Thus, the structures that need retrofitting and repairing works, can meet the shear requirements without demolishing.

The confinement also helps to improve the performance of low strength concrete that cannot meet the design strength because of improper mix design, curing and other environmental impacts like freeze-thaw effect. Poorly detailed and deteriorated RC structural elements are vulnerable to loss of axial load carrying capacity at drift levels (2-3%) during a design level earthquake (Boys et al. 2008). Before 1970, the tie spacing of 300 mm was commonly used in the bridge piers. The inadequate lap splice length at the plastic hinge zone and inadequate transverse reinforcement in these piers were the most significant factors causing a lateral deficiency in resisting seismic force (Priestley and Seible 1995, Elsanadedy and Haroun 2005).

Passive confinement is one of the effective techniques for strengthening and has been popular and widely used all over the world. FRP wraps are the most common materials used to improve the ductility capacity of vulnerable piers (Chai et al. 1991, Norris et al. 1997, Elsanadedy and Haroun 2005). Several researchers like Elsanadedy and Haroun, Gallardo-Zafra and Kawashima conducted experimental investigation on the effectiveness of passive confinement using FRP composites. While other studies attempted to describe analytically the constitutive behavior and stress-strain model of concrete confined with FRP (Spoelstra and Monti 1999, Fam and Rizkalla 2001, Chun and Park 2002, Marques et al. 2004, Binici 2005, Youssef et al. 2007, Teng et al. 2007).

Even though passive confinement with GFRP is a very common method of retrofitting, its effectiveness for improving the compressive strength of low strength concrete has not been well investigated. This chapter describes the methods and results from the investigation carried on the effect of low-grade GFRP confinement on the compressive strength of concrete. Market available materials were used to form low grade GFRP. The mechanical

properties and proper overlapping length for this GFRP are obtained by coupon test in the laboratory. Cylinders having compressive strength of 22 MPa and 32 MPa were wrapped with different layers of GFRP following standard method and tested under compression. Results from these tests shows that the compressive strength of concrete can be improved more than 100% with the GFRP confinement. But, the failure mode changes with increasing thickness of GFRP.

3.2 Research Significance

This study guides enhancing compressive strength of concrete using a market available low grade GFRP composite. Concrete strength may not be achieved because of improper mix design, inadequate curing and deterioration because of environmental effects like freezing and thawing. These can be enhanced by using confinement effect. Also, the performance of old structures made of low strength concrete can be improved by enhancing the compression carrying capacity of concrete using GFRP confinement. Also, the capacity of non-seismically designed structural elements can be significantly improved by applying this kind of low grade external confinement.

3.3 Mechanism of FRP Confinement

Confining concrete with external FRP jacket is a passive approach to increase its strength and ductility. In such FRP confined concrete (FCC), at lower axial strain, the confinement is negligible due to small transverse strain (Afifi et al. 2015). When the axial stress/strain surpasses particular limits, significant micro cracking occurs in the concrete core with increasing transverse strains due to Poisson's effect, which becomes noticed and results in a lateral pressure (Benzaid et al. 2010, Lam and Teng 2003a). When This confining lateral

pressure develops as an outcome of a restrain provided by the confinement to the radial dilation of the concrete when subjected to axial compression. Figure 3.1 shows the schematic representation of the confinement action exerted on the FCC. At the FRP-concrete interaction, the confinement pressure, f_l on the concrete core can be computed based on the force equilibrium and the displacement compatibility characteristic using Eq. (3.1)

$$f_l = \frac{f_h t_{frp}}{R} \qquad \text{Eq. (3.1)}$$

where, f_h is the hoop tensile stress in FRP jacket, and R is the radius of the core concrete section. The FRP composites show linear stress strain relationship until rupture, thus the hoop stress of FRP jacket is proportional to the hoop strain $\varepsilon_{h,frp}$, which could be calculated as $f_h = E_{frp} \times \varepsilon_{h,frp}$, where E_{frp} is the elastic modulus of FRP composite.

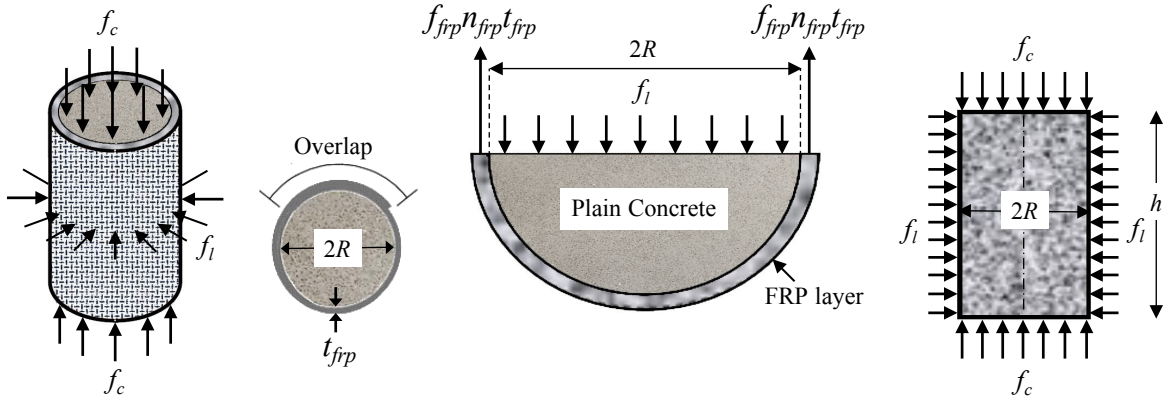

FRP wrapped cylinder | Overlapping on final layer | Free body diagram of FRP confined concrete | Tri-axial stress stage of concrete

Figure 3.1: Confinement action of FRP-confined concrete in circular section

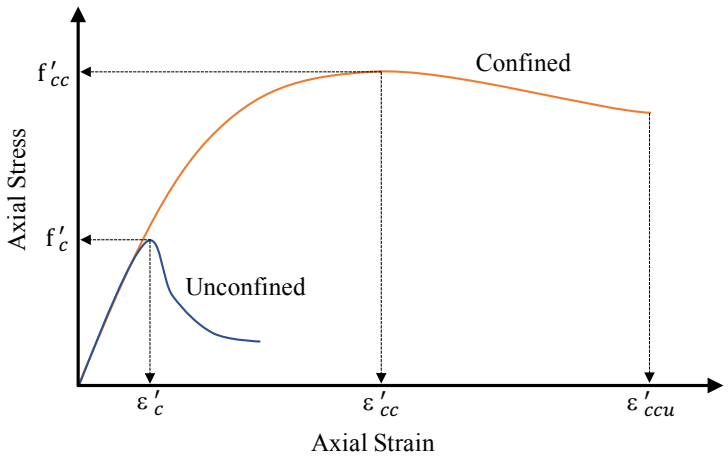

Figure 3.2: Schematic demonstration of confinement model by Mander et al. (1988)

The axial compressive stress increases due to the uniform radial stress exerted by FRP jacket, which produces hoop tensile stresses (De Lorenzis and Tepfers 2003, and Teng and Lam 2002). The extreme confinement stresses exerted by the FRP is achieved when the peripheral strain in the FRP reaches its ultimate strain capacity and the rupture of fibre leads to brittle failure of the confined concrete (Benzaid et al. 2010). At the ultimate strength (f_{lu}) of FCC, the lateral confining pressure could be estimated using Eq. (3.2). However, numerous researchers, (Mirmiran et al. 1998, Matthys et al. 1999 , Xiao and Wu 2000, Pessiki et al. 2001, Harries and Carey 2002, Lam and Teng 2003b, De Lorenzis and Tepfers 2003, Lamand Teng 2004, Theriault et al. 2004, Matthys et al. 2006, and, Ozbakkaloglu and Oehlers 2008) reported that the hoop strain ($\varepsilon_{h,rup}$) at rupture of FRP jacket in confined concrete is considerably lower than the ultimate hoop rupture statin of (ε_{frp}) of FRP coupons (Benzaid et al. 2010 and, Seffo and Hamcho 2012).

$$f_l = \frac{2E_{frp}t_{frp}\varepsilon_{fu}}{d} = \frac{2t_{frp}f_{frp}}{d} = \frac{f_{frp}\rho_{frp}}{2} \qquad \text{Eq. (3.2)}$$

where, f_l, E_{frp}, ε_{fu}, f_{frp}, and t_{frp} are the lateral confining pressure, modulus of elasticity, ultimate tensile strain and strength, and nominal thickness of the FRP jacket, respectively. d

is the diameter of the core concrete, and ρ_{frp} is the volumetric ratio of FRP jacket to the core concrete that can be estimated using Eq. (3.3) (Xiao and Wu 2001).

$$\rho_{frp} = \frac{\pi d t_{frp}}{\pi d^2/4} = \frac{4t_{frp}}{d} \quad \text{Eq. (3.3)}$$

3.4 Experimental Investigation on Confinement Thickness Effect of GFRP

3.4.1 Selection of Specimens

To carry out the investigation on the effect of GFRP confinement on the compressive strength of concrete, two different types of cylinders were chosen: Type 22 with compressive strength of 22 MPa and Type 32 with compressive strength of 32 MPa. Type 22 cylinders were not properly cured after construction. That is why they could not gain the required strength and had compressive strength of only 22 MPa. Cracks were formed on the surface of the cylinders. This group of cylinders represents concrete from old infrastructures. Also in practical condition it might happen that, required compressive strength cannot be achieved because of improper mix design, curing and environmental conditions. Other cylinders were properly cured and not subjected to any environmental impact. Thus, they could attain the design compressive strength of 32 MPa.

3.4.2 Preparation of Polymer Matrix and GFRP

Aropol K 1951-22 polyester resin and CSM 1.5 OC woven fabric glass fibre (Fig. 3.3) was used as a binder and reinforcing material respectively, to form the GFRP matrix. Luperox DDM-9 from Arkema Inc., a Methyl Ethyl Ketone Peroxide, is used as a catalyst for the resin for curing where 1:1 ratio (w/w) is used for fabric and resin. The amount of catalyst used was 1.5% of the resin (w/w) which lies between 1.5-2% as specified by the producer. The smaller

percentage of catalyst ensures a slow rate of reaction that allows the matrix to have sufficient curing time. The prepared matrix was cured for 48 hrs before they were used for preparing specimens for tension and bond test.

Figure 3.3: Bi-directional woven roving fibres used to prepare GFRP

3.4.3 Tensile Strength Test of GFRP

The GFRP plates once cured are cut into specific dimensions using water-jet machine for coupon test. Fig. 3.4(a) shows the dimensions of coupons made for tensile strength test. Coupons were made with two different thicknesses, i.e. one, two and three layers, and their strength and modulus of elasticity were calculated according to CSA S806. Fig. 3.4(c) shows the failure of a coupon under tensile test.

3.4.4 Bond Test between GFRP Layers

For developing the full fibre strength in tension, the proper overlap length of prepared GFRP was tested using Bond Test Coupon. The dimensions of Bond Specimens with varying overlap length are shown in Fig. 3.4(b). The overlap length was varied between 25 mm to 200 mm, i.e. 6 different lengths where each had 3 specimens. These coupons were also tested under tension according to CSA S806 and their developed strength were calculated for

varying overlap length. Fig. 3.4(d) shows the bond failure between adjacent GFRP layers where the overlap length was 75mm.

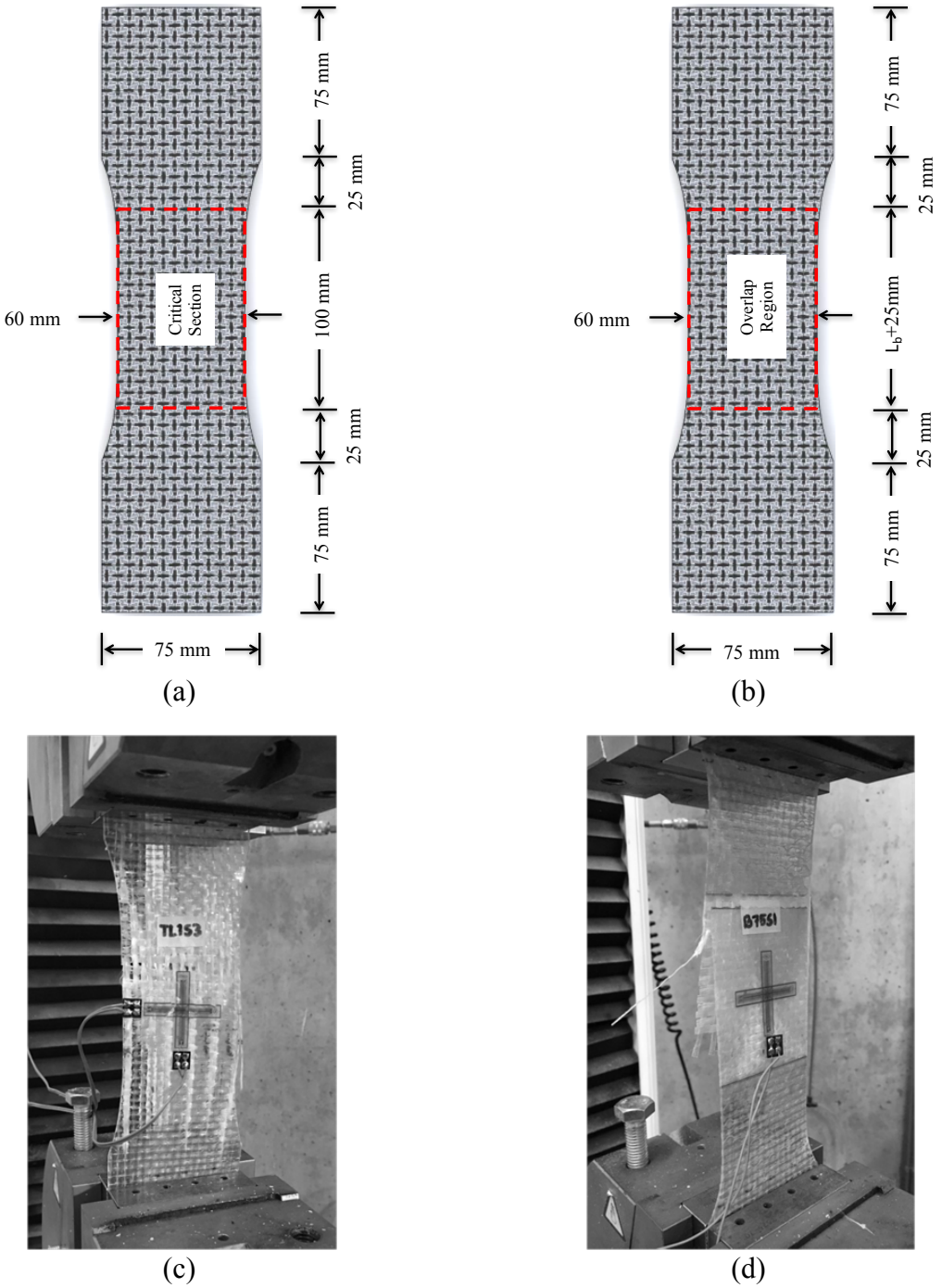

Figure 3.4: GFRP Coupons for (a) tensile test (b) bond test between GFRP layers; (c) coupon after tensile failure (d) coupon after bond failure

3.4.5 Application of GFRP on Cylinders

The prepared cylinders were confined with different thickness of GFRP by applying one, two and three layers of GFRP on them. Fig. 3.5 illustrates the standard procedure used to confine the specimens. Each cylinder was first coated with a prime layer of epoxy to ensure the fibre would bond to the concrete. The fibre was covered with epoxy glue and then wrapped around the specimen. A grooved roller was used to press the fibre against the concrete for a good bond. When more than one layer was applied, the above operation was repeated, with a 150 mm overlap between final two adjacent layers (Aire et al. 2010). Fig. 3.6 shows the specimens with strain gauges attached before and after applying GFRP confinement.

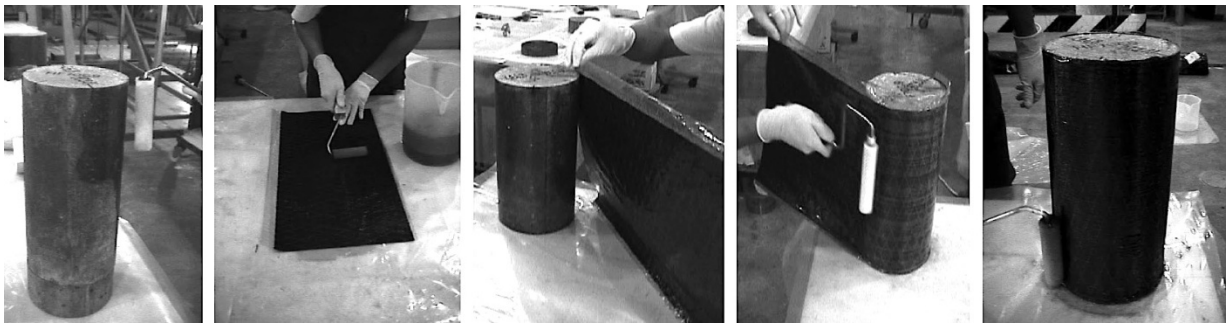

(a) (b) (c) (d) (e)

Figure 3.5: Standard method of GFRP confinement application: (a) Priming; (b) Applying epoxy on glass fibres; (c) wrapping the first layer of GFRP around the specimens; (d) Pressing with a grooved roller; (e) Applying last layer of epoxy.

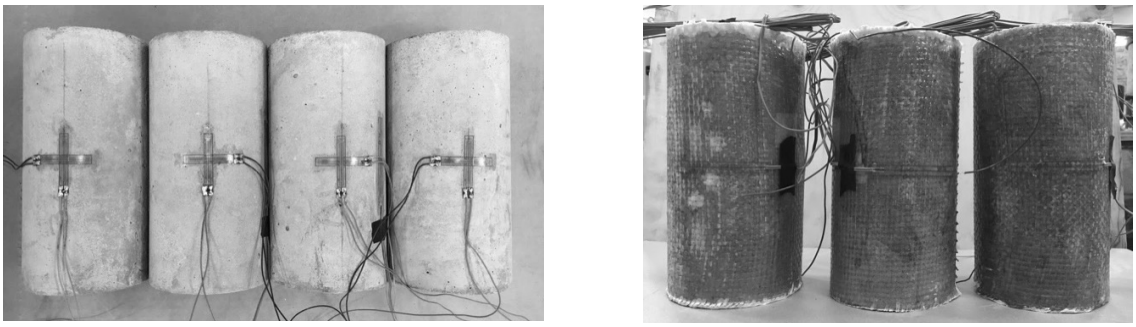

(a) Control cylinders (b) GFRP confined cylinders

Figure 3.6: Specimens with strain gauges and GFRP confinement

3.4.6 Test for Compressive Strength

The control cylinders and GFRP confined cylinders were tested according to CSA A23.2-9C (Fig. 3.7). Concrete cylinders having 100 mm x 200 mm dimension with strain gauges attached on them were tested under compressive load. The rate of loading applied was 2 kN/sec up to the maximum capacity. After reaching the maximum load, displacement controlled loading was applied with a rate of 2 mm/min to get the post peak behaviour.

(a) (b)

Figure 3.7: Test of cylinders under compression (a) control cylinder (b) GFRP confined cylinder

3.5 Results

3.5.1 Tensile Properties of GFRP

Coupons for tensile test were tested under uniaxial tension to get the tensile properties of GFRP. The tensile test results for 1, 2 and 3 layers of GFRP are shown in Fig. 3.8(a). The nonlinear behavior of GFRP is because of the misalignment of fibres during preparation and the failure of resin at around 50 MPa stress. After that, the fibres started to take complete tension and align with the direction of load application. From the graph it is found that, increasing the number of layer (i.e. thickness) increases the strength and stiffness of GFRP.

This is because, these properties are calculated based on the gross cross-sectional area of the coupons, which does not have a linear relationship with number of layer. For instance, the thicknesses of one and two layers are 0.85 mm and 1.55 mm. Thus, the area for two layers is less than twice the area of one layer. But in terms of load carrying capacity, two layers of GFRP can take twice the load of one layer. Thus, dividing load by gross area for calculating the strength gives higher strength value for two layers compared to one layer. Similar behavior is observed for three layers of GFRP. The mechanical properties of GFRP for varying number of layers are shown in Table 3.1. The properties obtained from the prepared coupons are much lower than the commonly used GFRP's for structural application (Table 2.2). The standard deviations (σ) of strength and strain at break for each layer are also shown in the graph. From the values of standard deviation, it can be concluded that GFRP coupons with similar thickness had similar strength and stain capacity.

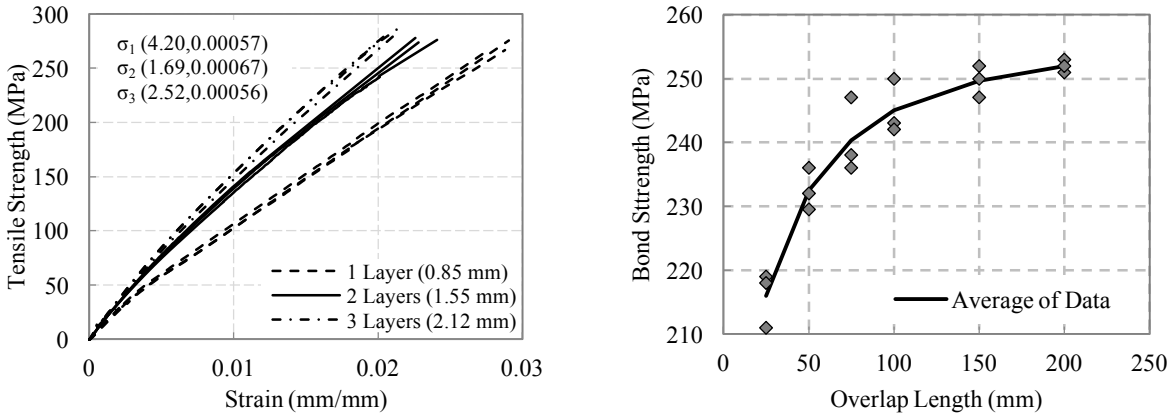

(a) (b)

Figure 3.8: Graphs showing mechanical and bond properties of GFRP (a) Stress-Strain curves for different number of layer; (b) Bond between layers.

3.5.2 Bond Properties between Layers

For each of the overlap lengths, bond failure was observed between two adjacent layers. The strength developed in the GFRP specimens were very low while the overlap length was

below 50 mm beyond which, it gradually increased to 252 MPa for 200 mm. Fig. 3.8 (b) shows the gradual bond strength development with increasing overlap length of GFRP. The asymptotic behavior of bond strength developed for increasing overlap length demonstrate an optimum overlap length of 150 mm which follows recommendation from previous research (Aire et al. 2010).

Table 3.1: Properties of GFRP obtained from tests

Properties	**Value**
Tensile strength (MPa)	270-290
Young's modulus of elasticity (GPa)	13.5-18.0
Fracture strain (%)	2.2-2.9
Epoxy strength (MPa)	50
Overlapping length (mm)	150

3.5.3 Compressive Properties of GFRP Confined Cylinders

All the GFRP-confined specimens are found to fail by rupture of the GFRP jacket outside of the overlapping zone. Fig. 3.9 and 3.10 show the stress-strain curves of Type 22 and Type 32 respectively for different confinement layers considered in this study. The following sign convention is adopted: compressive stresses and strains are positive in concrete. It is found that, the compression carrying capacity of concrete increases with the number of GFRP layer (i.e. thickness). For type 22 cylinders with low compression capacity, traditional nonlinear curve is observed, while type 32 exhibits the well-known bilinear stress-strain curve of ascending type.

The compressive strength of confined concrete is obtained by dividing the maximum load by the cross-sectional area of the specimen. By increasing the number of layer, confinement on concrete can be increased which results in improvement of compression carrying capacity.

This improvement is very significant for concrete that has a very low strength because of improper mix design and deterioration due to environmental effect.

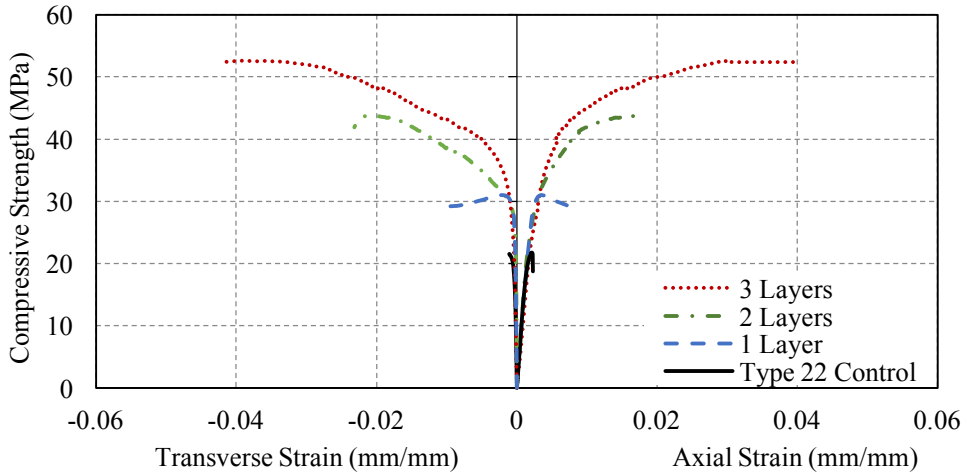

Figure 3.9: Effect of GFRP confinement on the compressive strength of Type 22 concrete

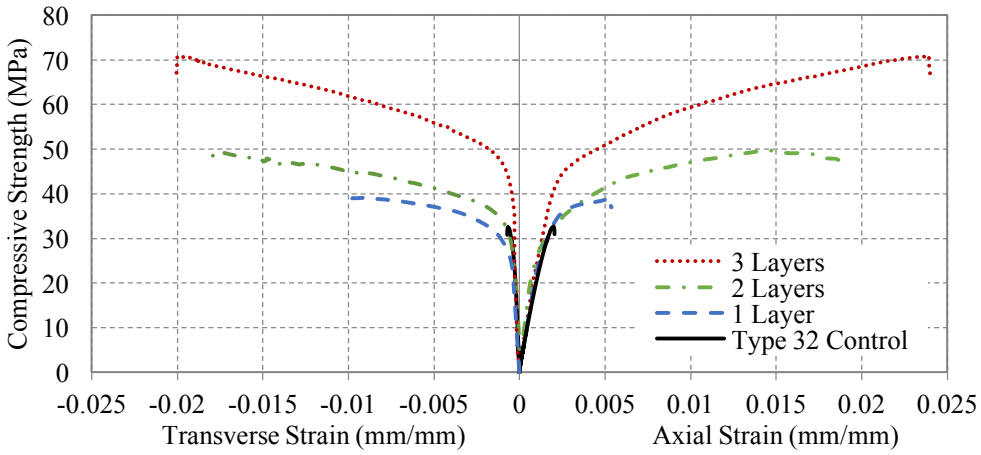

Figure 3.10: Effect of GFRP confinement on the compressive strength of Type 32 concrete

About 142.4% improvement in compressive strength was achieved in the experiment for 3 layers of GFRP which provides a confinement factor of about 2.42. Confinement also improves the strain capacity of concrete which can be up to 0.04 for 3 layers of tested confinement. Also, it is found that, the maximum strength is achieved at the maximum strain of concrete. This improvement in strain capacity makes the material more ductile and improves the ductility of structural elements as well.

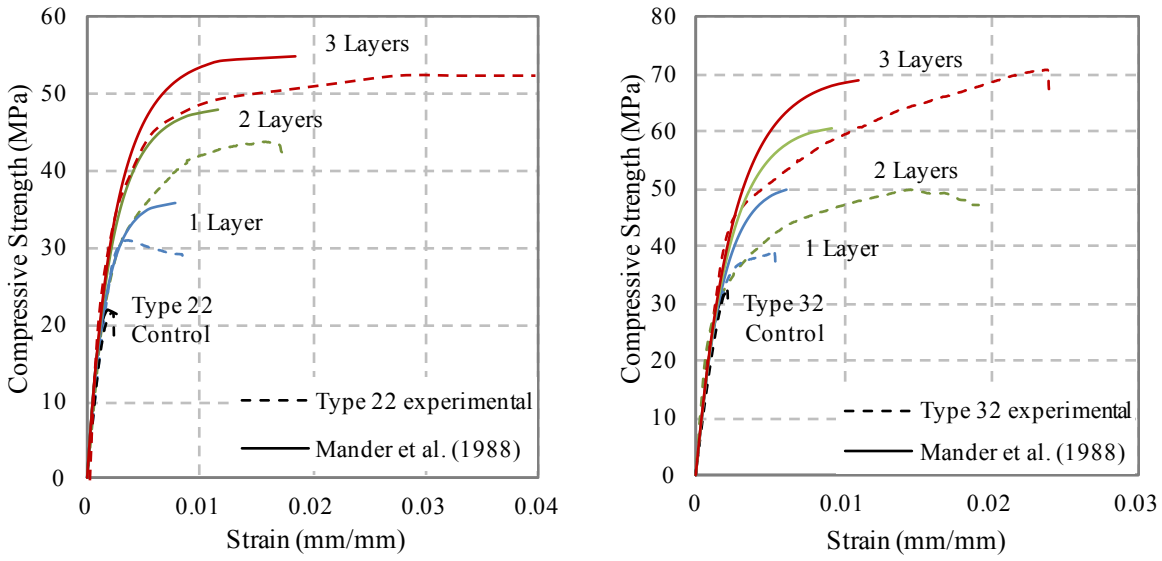

Type 22 Type 32

Figure 3.11: Comparison of stress-strain behavior of confined concrete between experimental result and Mander's confined model (1988)

The obtained compressive stress-strain behaviors from tests were compared with Mander et al. (1988) model as shown in Fig. 3.11. From the comparison it was found that, Mander's model could not accurately predict the stress-strain behavior of concrete confined with low grade GFRP. For both type of specimen, the model predicted higher compressive strength and lower strain capacity as compared to the experimental results. Also it was found that, the model did not show ascending type bilinear stress-strain curve under higher confinement effect.

Table 3.2: Compressive strength improvement and confinement factors

No. of Layer	Compressive Strength* (MPa)	% Improvement	Confinement Factor	Compressive Strength* (MPa)	% Improvement	Confinement Factor
	Type 22 Cylinder			Type 32 Cylinder		
0	21.7	-	1	32	-	1
1	32.1	47.93	1.48	39	21.88	1.22
2	41	88.94	1.89	51	59.38	1.59
3	52.6	142.4	2.42	72	125	2.25

* Average of 3 specimens

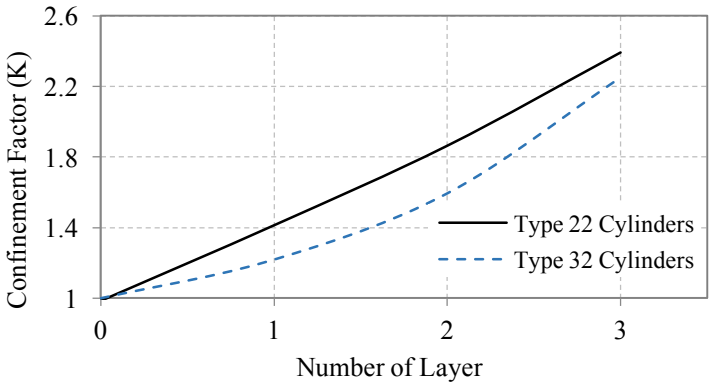

Figure 3.12: Confinement Factors for different number of layers

Table 3.2 shows the values for compressive strength and confinement effect for different number of layers. The confinement factors calculated from this table are used for modelling the retrofitted piers with different number of GFRP layers in section 3.6. Fig. 3.12 shows that confinement factor is almost linearly proportional with the number of GFRP layer for Type 22 cylinders and there is a logarithmic relationship for Type 32 cylinders.

3.5.4 Failure Mode

For the control specimens, the middle section is slightly bloated during failure, and many vertical cracks are formed on the outer surface of the specimens. For the confined specimens, there is no significant change in the phenomenon during the initial loading stage of the test. When the load is approaching to the maximum axial force, the fibres at the middle section of the specimens produce a "sizzling" noise lasting for a certain period of time. The ultimate failure is initiated by tearing of GFRP at the middle section of the specimens, and the specimens in the middle bloated and failed. The thickness of GFRP layer has a significant role in the failure mode of the concrete. Gradual tearing of GFRP fibres were observed for 1 and 2 layers but a loud explosive noise is heard for cylinders with 3 layers of GFRP confinement (Fig. 3.13). Both the coarse aggregate and the bonding interface between the

aggregate and cement paste are damaged simultaneously. Thus, it can be concluded that, increased thickness of GFRP brings more brittle characteristic to the failure mode. There was no bond failure observed between the outer layers of GFRP. This means, 150 mm overlap length in the final layer was sufficient for developing required tensile strength in the fibres.

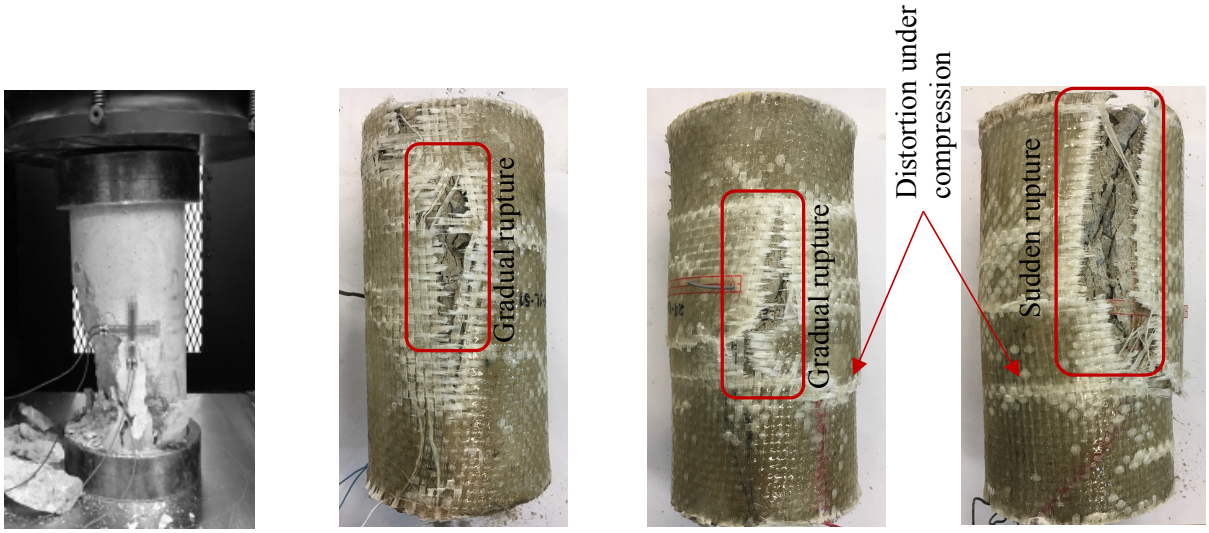

(a) (b) (c) (d)

Figure 3.13: Failure mode of cylinders for varying layer of GFRP confinement; (a) control; (b) 1 layer of confinement; (c) 2 layers of confinement; (d) 3 layers of confinement.

3.6 Performance of a Non-Seismically Designed Deficient Bridge Pier Retrofitted with Varying GFRP Thickness

Under strong seismic excitations, reinforced concrete bridge piers designed using earlier codes are commonly deficient in flexural ductility, shear and flexural strength. While confinement technique is proved to be effective under monotonic loading by extensive experimental investigation (Mirmiran and Shahawy 1997, Spoelstra and Monti 1999, Xiao and Wu 2000, Moran and Pantelides 2002), their cyclic response has yet to be investigated. Later, researchers conducted cyclic loading test on reinforced concrete columns retrofitted with various external confinement method (Kawashima et al. 2000, Yoneda et al. 2001, Sheikh and Yau 2002, Haroun et al. 2003, Li and Sung 2004, Haroun and Elsanadedy 2005,

Gu et al. 2010 and Wang et al. 2010). The FRPs used in these studies were formed using carbon, glass and aramid fibres. The test column detailing from test of Kawashima et al. is used to check the effectiveness of GFRP confinement in enhancing seismic performance of deficient bridge columns. In this study, adopted numerical modeling is validated with the test result of Kawashima et al. and later retrofitted with different thickness of GFRP to investigate their seismic performance.

3.6.1 Design and Geometry of Bridge Pier

The dimensions and material properties of deficient bridge pier are selected from previous experimental work (Kawashima et al. 2000). The detailing of the adopted bridge pier is presented in Fig. 3.14. The pier is 400 mm in diameter with an effective height of 1350 mm. It is reinforced with 12-15M rebar providing a longitudinal reinforcement ratio of 1.89% and

Table 3.3: Summary of the properties used in numerical modeling of piers

Description of properties	Values	Units
Dia. of pier	400	(mm)
Effective height of pier	1350	(mm)
Longitudinal reinforcement ratio	1.89	(%)
Volumetric ratio of lateral reinforcement	0.128	(%)
Compressive strength of concrete	30	(MPa)
Modulus of elasticity of concrete	27.7	(GPa)
Yield strength of steel	374	(MPa)
Modulus of elasticity of steel	200	(GPa)
Thickness of GFRP layer	0.85	(mm)
Tensile strength of GFRP	270	(MPa)
Initial stiffness of GFRP	13.5	(GPa)
Maximum elongation of GFRP	2.8	(%)
Axial Load	135	(kN)

0.128% volumetric ratio of transverse reinforcement (6 mm diameter) with 300 mm center-to-center spacing. The clear cover maintained around the transverse reinforcement is 35 mm. The foundation of the pier is assumed to be infinitely rigid. An axial compressive load of 135 kN representing 8% of axial capacity is applied at the top of the pier which represents dead load coming from deck. Table 3.3 shows a summary on the geometry and material properties used for this study.

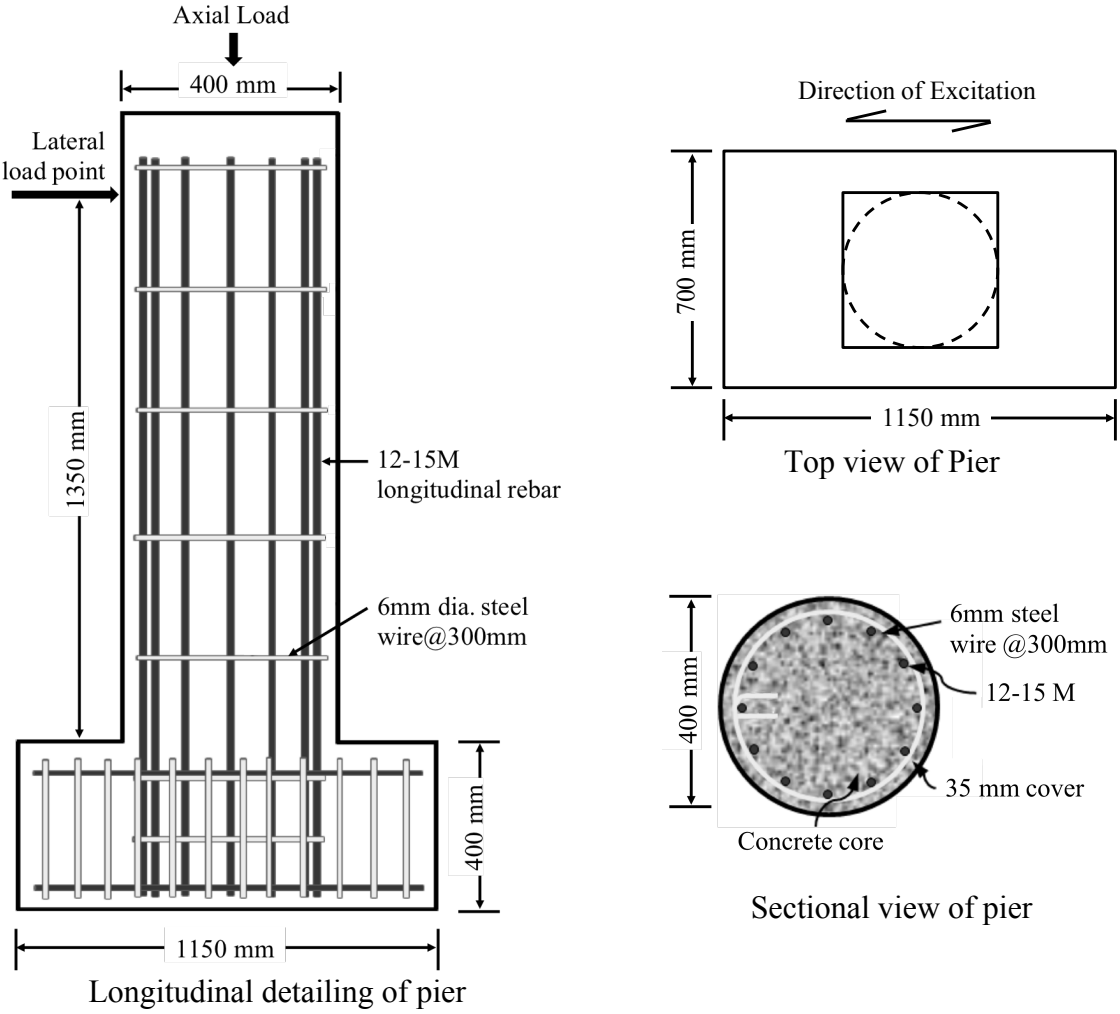

Figure 3.14: Detailing of the bridge pier adopted in this study

3.6.2 Material Modelling

3.6.2.1 Constitutive Model of Concrete

For the uniaxial cyclic behavior of confined concrete with different loading and unloading cycles, Mander et al. (1988) cyclic model is adopted. The materials properties of concrete used in Mander et al. (1988) are depicted in Table 3.4. For developing a cross-section discretization scheme, the concrete is assumed to crack at a tensile stress of zero.

Table 3.4: Parameters used in Mander et al. (1988) model in SeismoStruct (2016)

Parameter	Value
Mean compressive strength (MPa)	35
Young's modulus of elasticity (GPa)	27.8
Mean tensile strength (MPa)	0
Strain at peak stress (mm/mm)	0.002
Specific weight (kN/m^3)	24

3.6.2.2 Constitutive Model of Steel

To simulate the behaviour of steel reinforcement under cyclic load, Menegotto and Pinto (1973) steel model with Zulfiqar and Filippou (1990) isotropic strain hardening property is adopted as the constitutive model, which can be expressed as a bilinear kinematic hardening model. This model can capture the hysteretic behavior of steel reinforcing bars under simulated cyclic load. In addition, this model has a clear yielding point with a transient state from elastic to plastic response. Table 3.5 shows the parameters used in Menegotto and Pinto (1973) model for longitudinal steel reinforcement.

Table 3.5: Parameters used in Menegotto and Pinto (1973) model in SeismoStruct (2016)

Parameters	Value
Yield strength (MPa)	374
Young's modulus of elasticity (GPa)	200
Strain hardening parameter	0.035
Transition curve initial shape parameter	20.0
Transition curve shape calibration coefficient, A1	18.5
Transition curve shape calibration coefficient, A2	0.15
Isotropic hardening calibration coefficient, A3	-0.01
Isotropic hardening calibration coefficient, A3	15
Fracture strain (mm/mm)	0.22
Specific weight (kN/m^3)	78

3.6.2.3 Constitutive Model of GFRP

The properties of the GFRP confinement used for modelling the retrofitted piers with varying number of layers are chosen from experimental results obtained in section 3.5.1 and 3.5.2. Table 3.1 shows the properties of GFRP adopted in the modelling of retrofitted piers.

3.6.3 Finite Element Modelling

The finite element model of the adopted bridge pier is approximated as a continuous 2-D finite element frame using the computer software, SeismoStruct (2016). Fibre modeling approach is employed in order to represent the distribution of material nonlinearity along the height and cross-sectional area of the members. The advantage of fibre modeling approach is that yielding height and the exact value of plastic rotation can be estimated without considering the idea of equivalent plastic hinge length (Mortezaei and Ronagh 2012).

The pier is modeled using a linear beam element with the stiffness corresponding to flexural yielding and a fibre element is used to idealize flexural hysteretic behavior at the plastic hinge region. The length of the fibre element is assumed to be half of the column diameter from the base of the column. In addition to the fibre elements, a nonlinear zero length rotational spring element was used in the model to capture the bond-slip rotations at the pier-footing interface. This spring depicts the longitudinal reinforcement pullout from the footing due to lap splicing of rebar. Its properties are used from Gallardo-Zafra and Kawashima (2009). The gravity load is assumed to be lumped at the point of application of lateral load. All these considered components are defined in the model with corresponding material properties.

3.6.4 Analysis under Lateral Cyclic Loading

3.6.4.1 Loading Protocol

The seismic performance of the adopted pier is analysed using a displacement controlled quasi-static cyclic loading with an increment of 0.5% drift until reaching a maximum drift of 5.5%. The displacement loading at each drift level is applied for 3 cycles. Fig. 3.15 shows the loading protocol used in the cyclic test of Kawashima et al. (2000) which is used for lateral loading in the later part of this study.

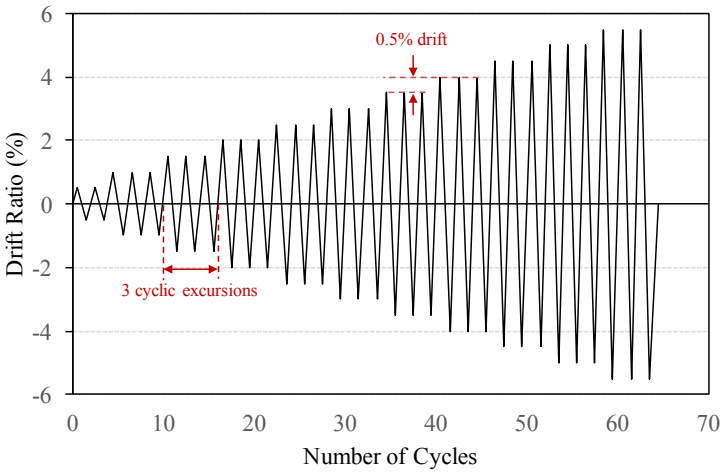

Figure 3.15: Cyclic loading protocol applied on the pier from Kawashima et al. (2000).

3.6.4.2 Cyclic Response

Fig. 3.16 illustrates the hysteretic behavior of deficient column considered in this study and the numerical results obtained by Kawashima et al. (2000). Under the same displacement-controlled reverse cyclic loading history, the modeled pier demonstrates a good agreement with the experimental results reported by Kawashima et al. (2000). This means, the modeled pier can simulate the initial stiffness, post-elastic stiffness and the ultimate load carrying capacity of the pier with a sufficient level of precision.

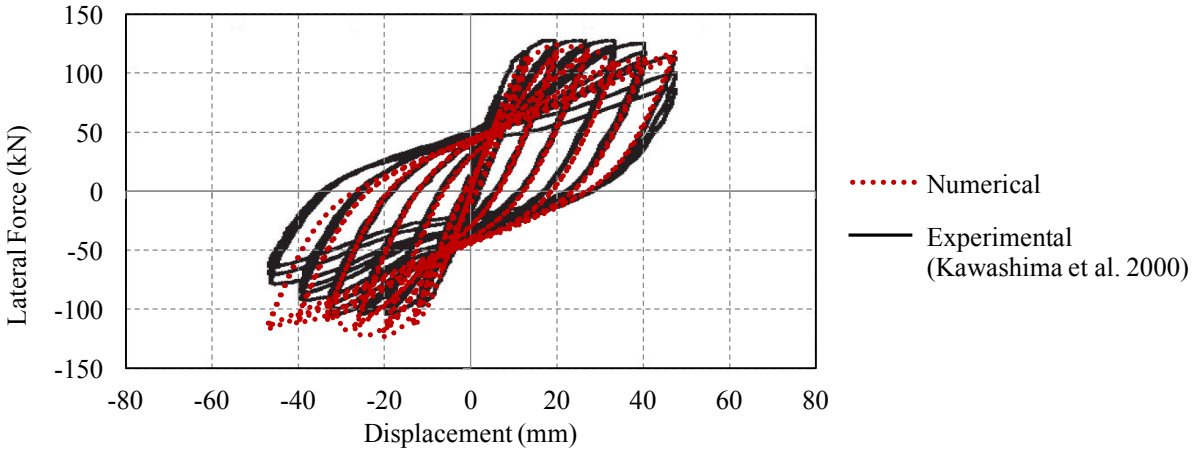

Figure 3.16: Validation of the bridge pier modeled in SeismoStruct (2016)

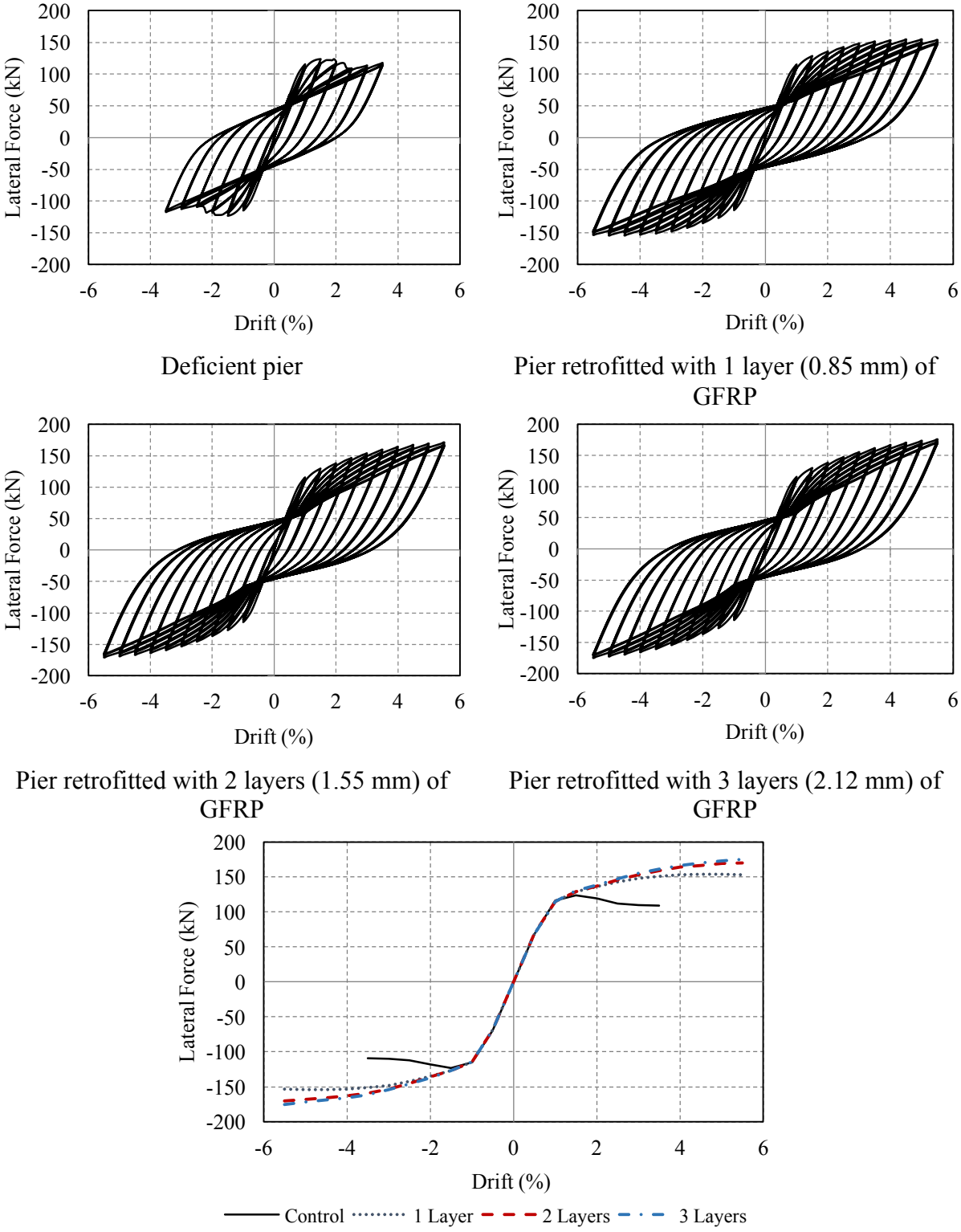

Figure 3.17: Hysteretic response of the piers under lateral cyclic loading

Fig. 3.17 shows the computed lateral force vs. drift under cyclic loading obtained for deficient and retrofitted piers with one, two and three layers of GFRP. The deficient pier reaches its maximum strength of 124 kN at 1.45% drift and is stable until 2.2% drift. The strength deteriorated by 13.7% at 2.5% drift. The strength of the pier deteriorated significantly after 3.5% drift which depicts the failure of the pier by concrete crushing. Compared to deficient pier, the retrofitted piers exhibit a stable response in the entire loading range because of the confinement effect from GFRP with varying thickness. The hysteresis reaches its maximum strength of 153 kN, 170 kN and 175 kN for one, two and three layers of GFRP retrofitting respectively. The lateral capacity of the pier increased by 23.4%, 37.1% and 41.1% respectively for 1, 2 and 3 layers of GFRP confinement. The increased thickness of GFRP enhanced the capacity of concrete under compression leading to improvement in shear capacity of piers. No deterioration of the restoring force is observed for these piers in the entire range of applied displacement. This depicts increased flexural and shear strength and ductility capacity can be attained with increased GFRP confinement effect. The reduction in strength gaining with increasing number of layers predicts that the effectiveness of confinement becomes saturated after a certain number of layers. From this result, it is predicted that 2 layers of GFRP confinement with 150 mm overlap length should enhance the seismic performance of deficient pier significantly in the experimental section described in Chapter 4.

3.7 Summary

A combined experimental and numerical study has been conducted and presented in this chapter on improving the compression carrying capacity of concrete using low grade GFRP confinement. Material properties were tested prior to application of GFRP on cylinders. Based on the properties obtained from experiment and previous literature, a deficient bridge pier is modeled and later retrofitted with varying thickness of GFRP. The nonlinear behavior of these circular piers under an applied axial load and unilateral cyclic loading is simulated using fibre element analysis. Result from the numerical analysis also supports the effectiveness of performance enhancement using 2 layers of GFRP for this study. The mechanical properties and optimum overlapping length obtained from tests will be used in the experimental investigation on bridge pier described in next chapter.

Chapter 4

Experimental Investigation on Cyclic Performance of RC Circular Bridge Piers Repaired and Retrofitted with Low Grade GFRP

4.1 Introduction

In most of the bridges designed using pre-1971 guidelines, the axial capacity of the pier was the focus of design criteria. Lateral loads were not considered in design and bridges were built with sufficient longitudinal reinforcement, but with traditional hoop spacing of 300 mm, irrespective of column size, strength, or deformation demands. These hoops were often closed by lap splices in the cover concrete instead of being anchored by bending back into the core concrete. Such transverse reinforcement provides inadequate confinement for the core concrete under compression and insufficient clamping action to the longitudinal reinforcement to prevent buckling. As a result, the ultimate curvature developed within the potential plastic hinge region is limited by the strain at which the cover concrete begins to spall, which is typically around 0.5 percent strain (Chai et al. 1991). Thus, the failure of pier is initiated by cover concrete spalling, leading to crashing, and later buckling of reinforcement due to the splitting action under fully reversed cyclic loads.

To repair damaged piers and retrofit deficient circular RC bridge piers with inadequate lateral confinement, various retrofitting means have been developed by researchers and practicing engineers; for example, jacketing with concrete, steel, fibre reinforced polymer (FRP), engineered cementitious composite and near surface mounted reinforcement, prestressing hoops etc. Concrete based jacketing techniques are cheaper, suitable for underwater work and increase flexural and shear capacity but have biaxial stress state, low durability and poor

aesthetics. Steel jacketing has been proven by Chai et al. (1991) to be an effective method of retrofitting columns with inadequate lateral confinement and insufficient lap-splice lengths. Even though steel jacketing has been widely used in practice in US and Canada, difficulties in cutting and welding, and complexity during installation doesn't make it a cost-effective retrofitting technique. Moreover, the corrosion of the steel jacket is a major drawback in the present day of sustainable infrastructure.

Researchers (Mander et al. 1988) have established that closely spaced lateral confinement reinforcement in the potential plastic hinge regions increases both the compressive strength and effective ultimate compressive strain in the core concrete. The ultimate compressive strain increases from a value of about 0.005 in unconfined concrete to a value of 0.03 or higher in confined concrete. The increase in ultimate compressive strain significantly enhances the ductility capacity of the concrete section. Priestly et al. (1984) have shown that columns designed with reasonable volumetric ratios of confinement reinforcement ($0.005 \leq \rho_s \leq 0.03$) can develop stable hysteresis loops during inelastic cycling to displacement ductility exceeding 6.

Confining the concrete columns with external jacket is a passive approach to increase their strength and ductility. In such confined columns, at lower axial strain, the confinement is negligible due to small transverse strain. With increasing the axial and lateral load, significant micro cracking occurs in the concrete core with increasing transverse strains due to Poisson's effect, which becomes noticed and results in a lateral pressure. This confining lateral pressure develops as an outcome of a restrain provided by the confinement to the transverse dilation of the concrete when subjected to axial and lateral load.

This chapter discusses an effective method of retrofitting existing structures using strength and ductility enhancement by a passive confinement provided by GFRP jackets. Performance of repaired and retrofitted piers is compared with as-built one and measures are suggested for preventing bridge collapse during earthquakes. Detailed experimental investigation, test method and setup, performances of non-seismically designed, repaired and retrofitted specimens have been properly investigated.

4.2 Research Significance

Poor performance of deficient reinforced concrete bridge piers, primarily due to lack of adequate lateral reinforcement, caused many bridge failures during recent earthquakes. These bridges were designed using old bridge design codes and many of them do not even meet the current seismic standards. To ensure a continuous and safe transportation system during earthquake, these bridges need to be demolished and new bridges are to be built requiring high cost and intensive labor. Rehabilitating these bridges could play a significant role in terms of economy and providing safety during earthquake. Among different retrofitting techniques external FRP confinement is one of the most popular now-a-days and widely used around the world. FRPs used for this purpose have high strength and are costly, thus a cheaper alternative should be adopted that can serve the purpose. As a quick, effective and convenient means for seismic upgrade of vulnerable piers, this study addresses the methodology for strengthening and analyzes the performance of repaired and retrofitted piers using market available low grade GFRP with lower mechanical properties compared to others. This low grade GFRP is usually used for strengthening of boats and yachts. Also, quick and easy repairing method for severely damaged bridge pier is explained where all the damaged concretes in the plastic hinge region were removed but the buckled bars were

straightened and kept in place. Results from this research provide an insight for repair and retrofit measures to enhance flexural strength and ductility of existing deficient RC circular bridge piers using low grade GFRP.

4.3 Materials

4.3.1 Concrete and Steel

Ready-mix concrete with an average compressive strength of 35 MPa (28 days strength) was used for building the test specimens. In order to obtain the actual mechanical properties of this concrete, cylinders were cast and tested after 28 days of moist curing. 10M steel rebar with yield strength of 450 MPa was used as reinforcement while casting the specimen. The stress-strain relationships of concrete and steel are shown in Fig. 4.1.

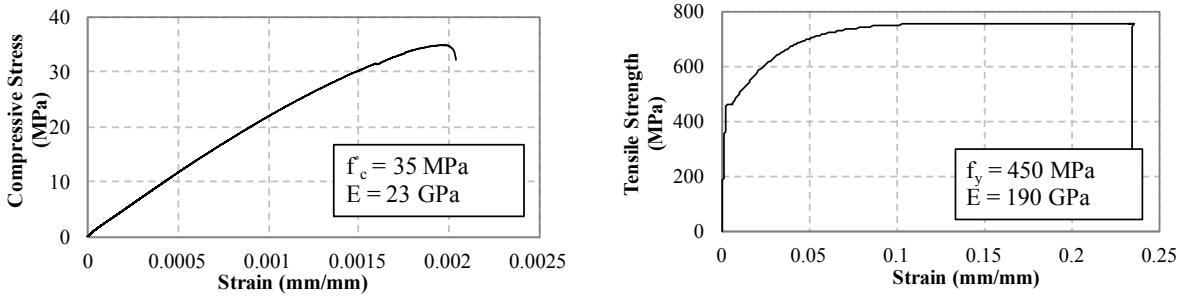

Figure 4.1. Stress-strain relationship of concrete (left) and steel(right) used in specimens

4.3.2 Glass Fibre Reinforced Polymer

Glass Fibre Reinforced Polymer (GFRP) is one of the most popular composite materials for strengthening structural elements. It has high modulus of elasticity, good tensile strength and excellent corrosion resistance. Bi-directional woven roving glass fibres with low mechanical properties were used to see its effect on improving the seismic performance of piers. This fibre is cost-effective, readily available and can reliably serve the purpose. From the results

of experimental investigation described in chapter 3, GFRP with following mechanical properties are used as a retrofitting material.

Table 4.1: Properties of GFRP used for confining the bridge piers

Properties	**Value**
Tensile strength (MPa)	285
Young's modulus of elasticity (GPa)	16
Fracture strain (%)	2.3
Epoxy strength (MPa)	50
Overlap length (mm)	150

4.3.3 High Early Strength Gain Repair Concrete

For repairing the damaged column, pre-mix repair concrete was used. There are different types of pre-mix repair concrete available in the market. They provide good workability and resistance to segregation and remarkable filling and passing ability. While repairing bridges, it is critical to reopen the transportation facility in the shortest possible time. Hence, quick repairing technique was adopted using high early strength concrete. Sakrete PSI 6000 premix from Basalite Concrete was used for restoration of damaged concrete. This has Self Compacting (SC) property which helps restoring element continuity and homogeneity. The maximum aggregate size of the mix was 10 mm and a water to cement (w/c) ratio of 0.4 was used. A 35 MPa mean compressive strength was achieved as the most similar value to that of the original pier. The strength development of repair concrete with time is shown is Fig. 4.2

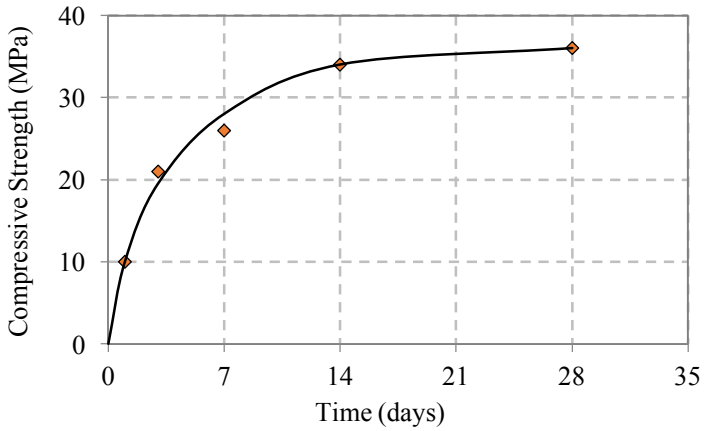

Figure 4.2: Strength developing of high early strength gaining repair concrete

4.4 Design and Geometry of Bridge pier

The test specimens were considered to be 1/3 scale models of a prototype pier with 900 mm diameter and traditional hoop spacing of 300 mm that demonstrates inadequate confinement from transverse reinforcement. Specimens were constructed with a footing to allow foundation influence or interaction to be monitored. Table 4.2 summarizes the comparison between test specimens and prototype pier.

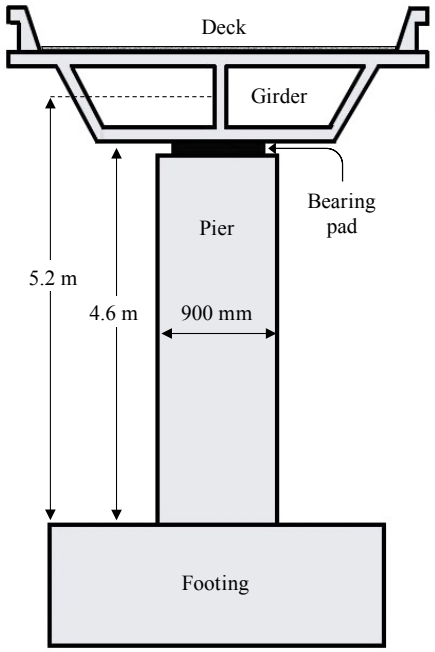

Figure 4.3: Geometry of prototype bridge pier considered in this study

Two scaled down cantilever piers with 300 mm diameter and effective height of 1730 mm were built. They were tested (either as deficient, repaired, or retrofitted as shown in Table 4.3) under constant axial and cyclic–lateral loading. The as-built pier (deficient) once tested up to failure was repaired using the method discussed in later section and tested again named as a repaired pier. Another specimen (retrofitted pier) was retrofitted before it was subjected to any kind of loading (i.e. no damage). The specimens were longitudinally reinforced with 18-10M rebar and laterally confined with 3.6 mm steel wire at 90 mm center to center spacing. Specimens were cast using ready-mix concrete with an average compressive strength of 35 MPa (28 days strength). One specimen after testing in as-built condition was repaired, and strengthened with external GFRP confinement and tested again. The other specimen was retrofitted with GFRP confinement and tested under same loading condition. The specimens during the test were subjected to a constant axial load based on 10% of f'cAg, where Ag is the cross-sectional area of the column, and f'c is the concrete compressive strength at 28 days. Fig. 4.4 shows the geometry and reinforcement layout of the specimens.

Table 4.2: Geometric comparison of prototype and test specimens

Description of properties	**Prototype**	**Test Specimens**
Diameter (mm)	900	300
Effective height (m)	5.2	1.73
Clear cover (mm)	60	20
Longitudinal reinforcement ratio (%)	2.52	2.55
Volumetric ratio of lateral reinforcement (%)	0.173	0.176
Tie spacing (mm)	10M @ 300	3.6 mm @ 90
Axial Load, P/f'_cA_g (%)	10	10
Yield Strength of Longitudinal reinforcement (MPa)	450	450
Yield Strength of transverse reinforcement (MPa)	400	400
Compressive strength of concrete (MPa)	35	35

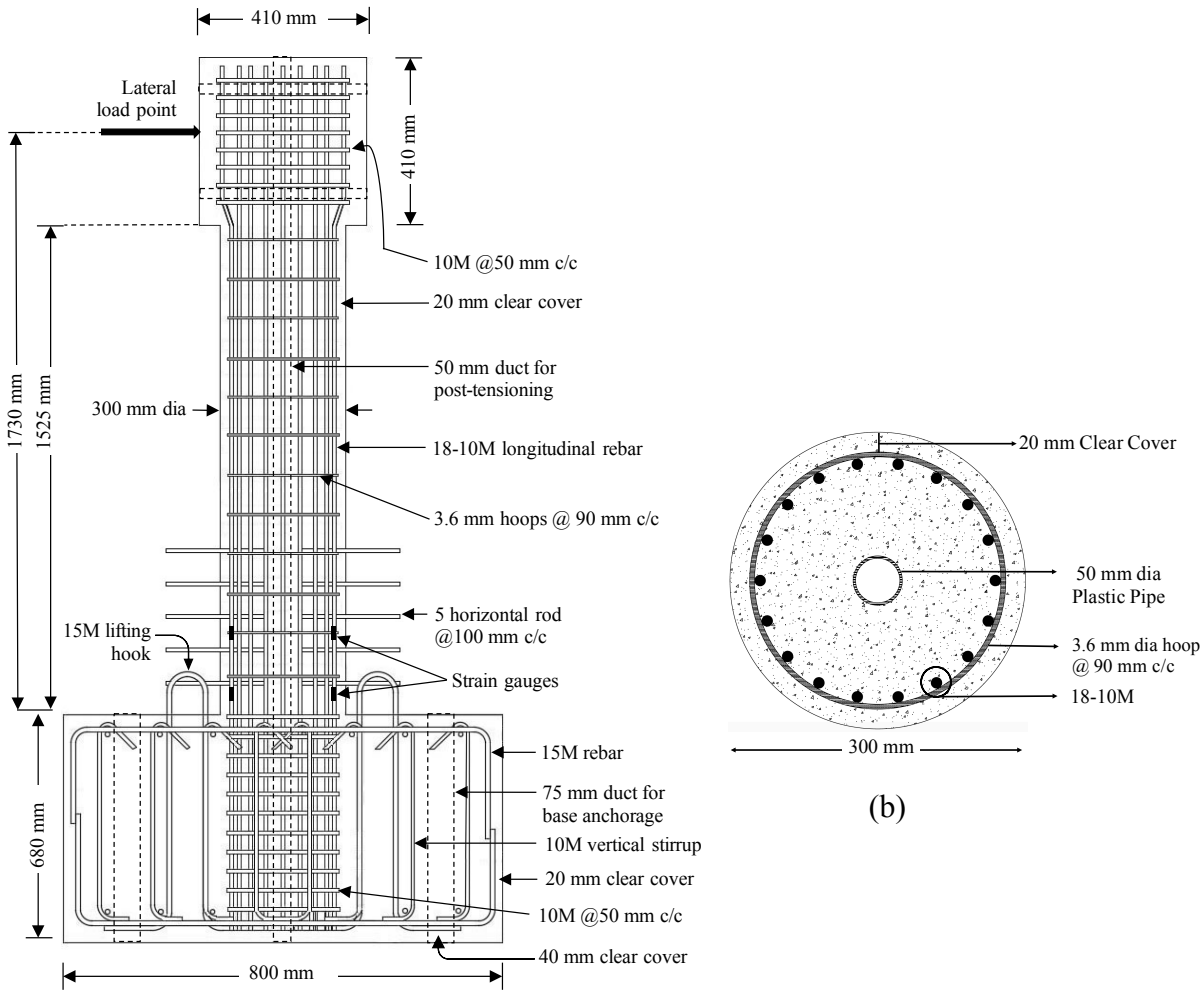

Figure 4.4: Specimen geometry and reinforcement layout: (a) reinforcement detailing; (b) cross-sectional detailing

Figure 4.5: Formworks for specimen casting and their curing process

Fig. 4.5 shows the formwork constructed for casting the specimens and the curing process using wet sack after the casting.

Table 4.3: Description of the specimens tested in the study

Specimen	Description	External Confinement
Deficient	As-built pier with inadequate confinement	No external confinement
Repaired	Damaged deficient pier repaired with new concrete and GFRP wrapping	2 layers (1.55 mm thick) of GFRP confinement after repairing
Retrofitted	Fresh pier retrofitted before any load application	2 layers (1.55 mm thick) of GFRP confinement before loading

4.5 Experimental Investigation on Bridge Pier

4.5.1 Test Setup and Instrumentation Layout

Fig. 4.6 shows the set-up of pseudo test. The footing of the specimen was anchored with specially designed strong floor by post-tensioning it on four corners using 36 mm diameter High Strength Steel (HSS) rebar. To simulate the effect of 10% axial load, a 26 mm diameter HSS rebar going through the center duct/hole of the specimen was post-tensioned to 238 kN and bolted at the bottom of the base and top of the column. Calibrated load cell was placed in between to monitor applied axial load on top of the pier. A hydraulic actuator with ±250 kN load capacity and ±125 mm displacement capacity was mounted from a reaction frame which was assumed to be infinitely rigid and had insignificant deformation during the test procedure. The actuator was placed in such a way that, once bolted with the pier, the actuator had similar displacement range on both push and pull. The lateral cyclic load was transferred to the specimen through steel plate. One side of the plate was tied to the actuator, and the other side was fitted to the column head through four strong bolts; the lateral loading was applied to the specimens gradually in the cases of pull and push. Deflections and load at the

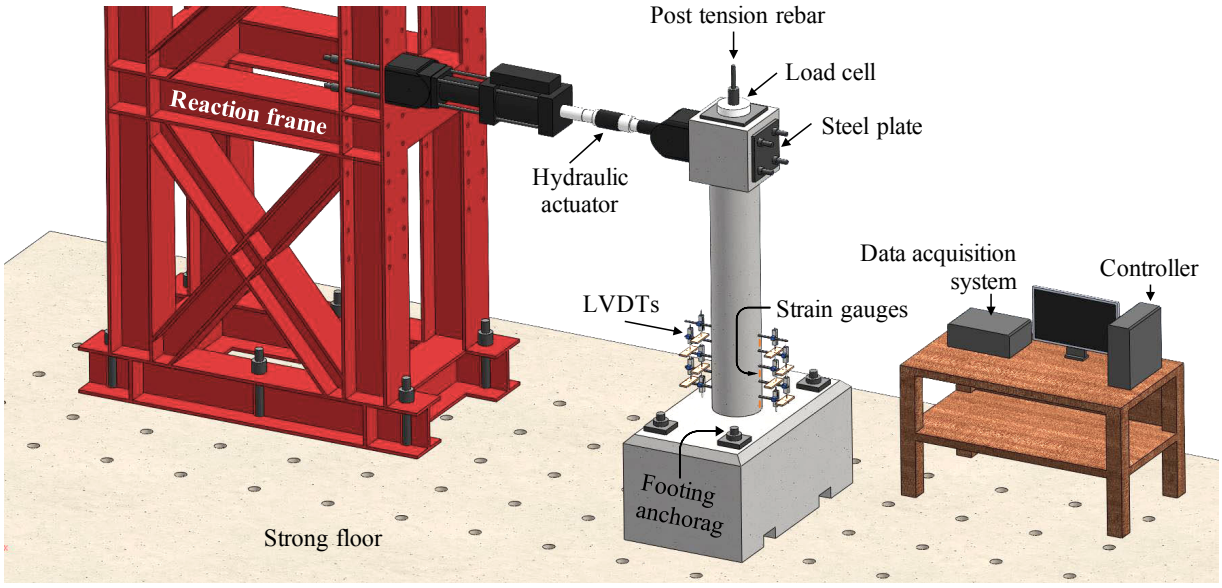

Figure 4.6: Experimental setup of bridge pier under lateral cyclic loading

Figure 4.7: Retrofitted pier under significant lateral drift during the test.

point of lateral load application were recorded by MTS controller. In addition, curvatures within the plastic hinge region were measured using pairs of Linear Variable Differential Transducers (LVDTs) mounted on horizontal rods cast through the columns in the potential plastic hinge region. Strains in the longitudinal rebar in the plastic hinge region, outer

concrete and jackets were measured with electrical resistance strain gauges using a National Instrument (NI) Data Acquisition System (DAQ). Fig. 4.7 shows the retrofitted pier under significant lateral drift during the test.

4.5.2 Loading Protocol

The seismic performance of the scaled down specimens was evaluated using a standard displacement controlled quasi-static cyclic loading with an increment of $0.5\Delta_y$ until reaching the failure. The displacement loading up to $2\Delta_y$ was applied for 3 cycles, later it was reduced to 2 cycles. The rate of loading for the protocol was 15.3 mm/min to make it a pseudo-static test (Ghannoum et al. 2012) and ignore the dynamic behavior of the piers, but a slower rate of 5.1 mm/min was applied up to the yielding of specimen in order to apply the displacement in that range accurately and observe the pier performance in the elastic range. Fig. 4.8 shows the standard loading protocol for cyclic test and the protocol adopted in this study.

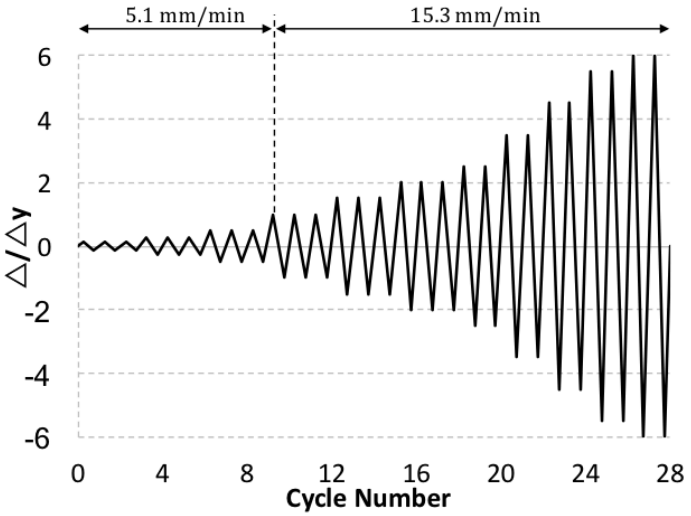

Figure 4.8: Loading protocol for lateral cyclic loading applied in this study

4.6 Repairing and Retrofitting Method

The operations for damage repairing of the deficient pier after testing it under lateral cyclic loading include: removal of loads (phase 1); mechanical removal of damaged concrete cover and cleaning of substrate from residue particles (phase 2); restoration of buckled reinforcement (phase 3); restoration of damaged concrete cover with high early strength gain concrete (phase 4); and GFRP strips application (phase 5).

4.6.1 Removal of loads by external support (Phase 1)

Before repairing, all the dead loads and live loads on the columns were removed using vertical wooden support (Fig. 4.9a). This helped to release the residual strain on damaged material and restoration of longitudinal reinforcements in phase 3. This also increased the effectiveness of external GFRP confinement applied at the initial stage of loading.

4.6.2 Damaged Concrete Removal (Phase 2)

Cracked and nearly detached part of concrete cover and core were completely removed over a height of 450 mm (visual and mechanical inspections are made to confirm the height of damaged area) from the pier base. Reinforcing bars have been accurately cleaned in order to guarantee optimal bond with the repairing material (Fig. 4.9b). The interface between the existing concrete and the repairing material could be a possible failure plane for re-loading. Proper bonding at this interface ensures durability and effectiveness of restoration. The interface was sufficiently roughened by mechanical removal followed by cleaning of substrate from residual particles.

4.6.3 Reinforcement Bar Restoration (Phase 3)

After removing the loads and damaged concrete, the buckled longitudinal reinforcements were almost in a restored position. The fractured ties were removed. The reinforcements were further pushed inward using some wires and externally applied load. New ties were provided with a lower spacing of 50 mm c/c (Fig. 4.9c). This change in spacing did not

(a) Phase 1

(b) Phase 2

(c) Phase 3

(d) Phase 4

(e) Phase 5

Figure 4.9: Steps involved in repairing of damaged pier after lateral cyclic loading

change the confinement factor for concrete section significantly (changed from 1.05 to 1.1 calculated from Mander et al. 1988), rather it helped to hold the reinforcement in place. Once restored, strain gauges with 350 Ω resistance and 5 mm gauge length were installed on rebars at the extreme sides of the pier.

4.6.4 Concrete Restoration (Phase 4)

The concrete restoration of pier includes: substrate preparation, formwork construction, concrete production, its application and ageing. Cylindrical formwork originally used to build the specimen (Fig. 4.9 d) was modified to include some openings allowing concrete pouring without interruption. The finished surface looked good although some imperfections were present after formwork stripping which was further improved by applying mortar. Vertical strain gauges were installed at 50 mm height on the loading sides of the columns to measure concrete strains.

4.6.5 GFRP Strengthening of Damaged Column / GFRP Retrofitting of Undamaged Column (Phase 5)

Same technique was adapted using GFRP to strengthen the damaged column or retrofitting of the undamaged deficient column. After proper curing of concrete (repair concrete for the damaged column), the column was wrapped with GFRP in the hoop direction. To ensure proper bonding of the FRP sheets to the concrete surface, the column surface was cleaned and completely dried before wrapping. The surface of the concrete was then coated with a thin layer of epoxy (priming). The bidirectional sheets were then saturated with epoxy, and applied directly on to the concrete surface using the wet lay-up method. To ensure full development of composite strength, complete saturation of the fibres was achieved by adding

another layer of epoxy to the exterior of the FRP sheets. The FRP sheet was applied over the total area (full wrapping), providing an overlap length of 150 mm in the circumferential direction (no overlap was provided in the longitudinal direction). This overlap length was determined based on the current test program presented earlier, which also meets the requirement of the standard (ISIS Canada 2008). This overlap in the circumferential direction was provided in order to avoid any premature failure of the concrete column at the overlap. The GFRP wraps were instrumented with conventional foil strain gauges, which had a resistance of 120 Ω and a gauge length of 30 mm to measure the strain along the hoop direction. Fig. 4.9(e) shows the GFRP strengthened pier ready for testing.

4.7 Test Results and Discussion

4.7.1 Cyclic Response

Fig. 4.10 shows the hysteretic behavior of deficient, repaired and retrofitted piers under cyclic loading obtained from the experiments. For deficient pier (Fig. 4.10a), the hysteresis reached its maximum strength of 62kN at 2.7% drift and was stable up to 3.9% drift. After that, significant strength degradation occurred on one side and the pier is considered as failed under lateral loading. The failing part of the curve shows that, the strength deteriorated from its maximum capacity by 11.6% at 4.64% drift and then suddenly by 29.4% at 5.2% drift, for as-built pier. Strength deterioration can be attributed to the spalling of cover concrete which initiated the buckling of the main rebars under compression at larger drift ratios. The pier showed symmetric strength behavior on both loading sides, except that, one more stable cycle was observed on pulling side.

After failure, the as-built pier was repaired according to the method described earlier and confined with GFRP for improved seismic performance. The other as-built pier was retrofitted in the same fashion before any load application. As depicted in Fig. 4.10 (b) and (c), the repaired and retrofitted columns demonstrated stable response in the entire loading displacement range tested. The hysteresis reached its maximum strength of 78 kN and 77.4 kN at the maximum drift of 6.9% for repaired and retrofitted piers, respectively. No degradation of the restoring force occurred up to the maximum drift capacity of 6.9% for the adopted test setup.

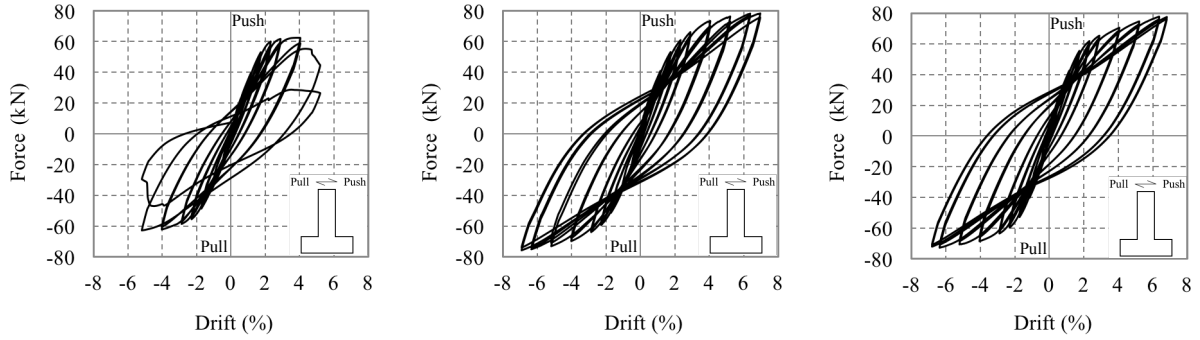

(a) Deficient (b) Repaired (c) Retrofitted

Figure 4.10: Hysteretic response of piers under lateral cyclic loading

To assess the influence of low grade GFRP confinement on the cyclic response of piers, lateral force-displacement skeleton curves of the specimens obtained from experiments are compared in Fig. 4.11. Increased flexural strength and ductility capacity were attained for both repaired and retrofitted specimens. However, there was no significant increase in lateral stiffness of piers. The lateral load capacity increased by 25% and a stable and ductile behavior is shown by both repaired and retrofitted piers. The enhanced compression carrying and strain capacity of GFRP confined concrete helped the piers withstanding more lateral load and drift. Not much difference was observed on the hysteretic response for the repaired

and retrofitted specimens. This indicates that repairing of a seismically damaged deficient column with GFRP composites could perform similarly to that of a GFRP retrofitted undamaged deficient column in terms of lateral load and drift capacity. Instead of demolishing the damaged concrete bridge column after a seismic event, the column could be retrofitted to increase its capacity and ductility to that of a retrofitted one. This could lead to a sustainable solution in terms of economy and reduced greenhouse gas emission by avoiding the works related to demolition and new construction. Proper care and safety protocols need to be followed while performing a repair work on a damaged bridge column. The superstructure needs to be supported by additional struts. In case of large permanent lateral and vertical drift, the whole structure needs to be jacked up and the bridge column needs to be pushed back to its original position.

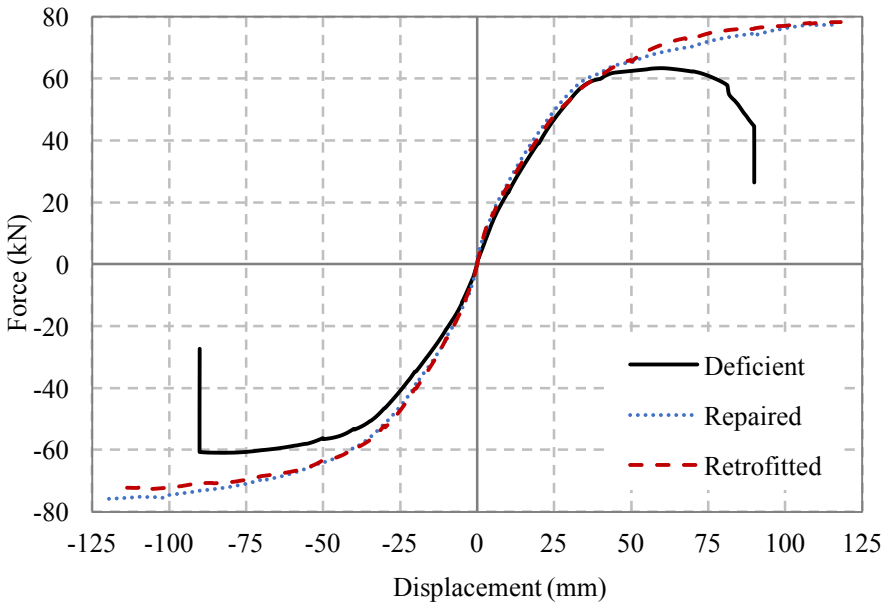

Figure 4.11: Skeleton curve of piers obtained from lateral cyclic loading.

4.7.2 Strain Response

Strains in the critical section of the plastic hinge regions of the specimens were measured using strain gauges installed on internal rebars, concrete and external GFRP reinforcements. The height of the strain gauges was 75 mm from support. Some strain gauge data were lost during the tests because of gauge failure or unreliable measurements caused by highly localized strains. The yield strain of longitudinal reinforcement was 0.00225. Fig. 4.12 shows the applied lateral load versus strain developed on steel and concrete for deficient specimen, and on steel, concrete and GFRP for repaired and retrofitted specimens, respectively. As shown in Fig. 4.12 (a) and (b), the strain response of steel reinforcement and concrete in deficient specimen follows the material constitutive behavior, with steel yielding at lateral load of 38.9 kN corresponding to 19.6 mm lateral displacement. Whereas, strain hardening is observed for strain response of repaired column as the reinforcements were already loaded and unloaded in previous test (Fig. 4.12 c and d). The full strain response of steel and concrete in this case couldn't be obtained because of strain gauge failure. The GFRP fibres were only subjected to tensile strain as they don't have any compressive resistance (Fig. 4.12 e and h). The strain response of steel, concrete and GFRP followed their constitutive behavior for retrofitted specimen (Fig. 4.12 f, g, h).

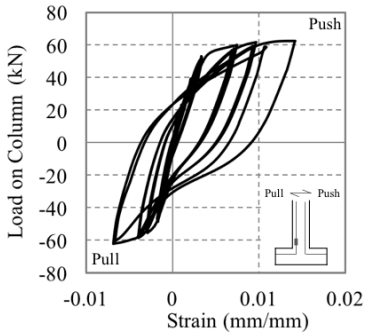

(a) Steel strain of deficient specimen

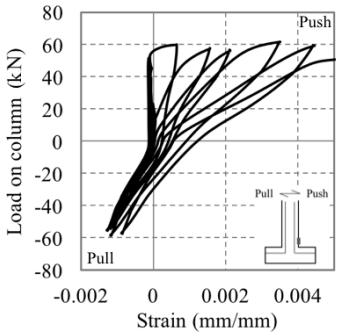

(b) Concrete strain of deficient specimen

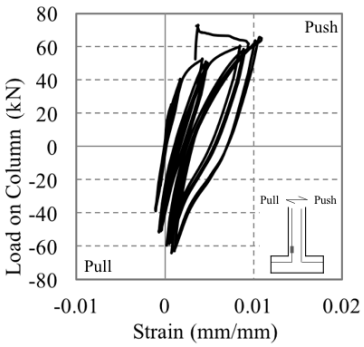

(c) Steel strain of repaired specimen

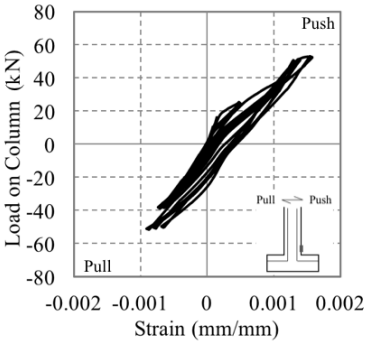

(d) Concrete strain of repaired specimen

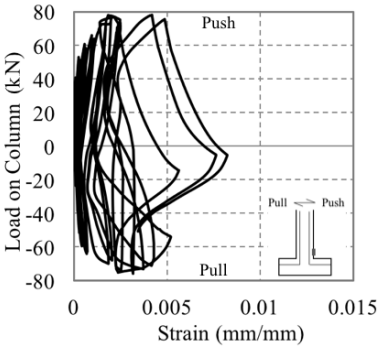

(e) GFRP strain of repaired specimen

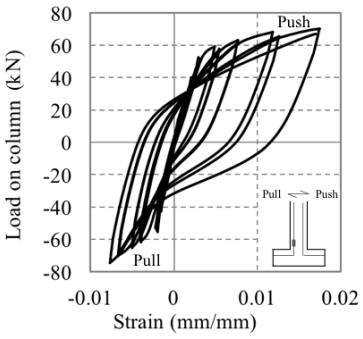

(f) Steel strain of retrofitted specimen

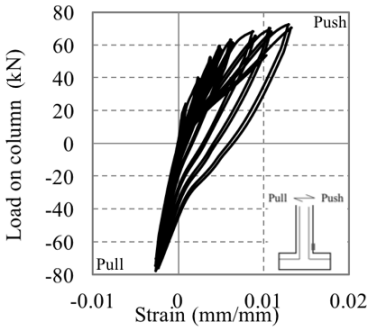

(g) Concrete strain of retrofitted specimen

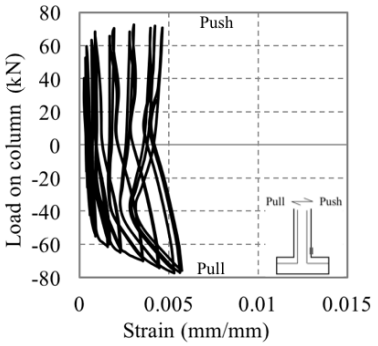

(h) GFRP strain of retrofitted specimen

Figure 4.12: Strain response of steel, concrete and GFRP observed on deficient, repaired and retrofitted pier.

4.7.3 Moment-Curvature Response

The curvature in the plastic hinge region was calculated based on the deformation measured by pair of transducer gauge mounted on the extreme sides of the specimens, where the plastic behavior is expected to occur. The curvature (φ) at the first critical section at 100 mm above the base was measured using the method explained in Fig. 4.13. The vertical elongation (Δ_t) and contraction (Δ_c) were measured on the extreme sides using pair of linear variable displacement transducers (LVDTs). The average strain (ε) was then calculated by dividing obtained elongation and contraction values by the considered gauge length (l) using formula: $\varepsilon = \Delta/l$. Once the strain profile at a section was developed, the average curvature (φ) was then calculated as the summation of the absolute values of two strains on opposite sides of the specimens, divided by the distance between two opposite LVDTs (Eq. 4.1); assuming that the angle of rotation for the section is very small. The corresponding moment (M) was obtained by multiplying the applied lateral load with the effective height of the considered section from lateral load point (Eq. 4.2).

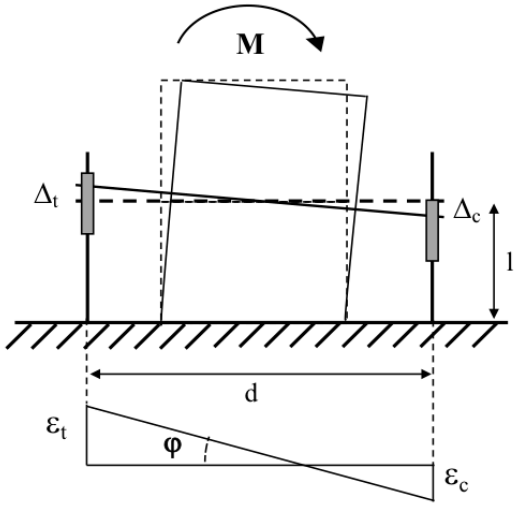

Figure 4.13: Technique used for measuring curvature of RC piers

$$\varphi = \frac{|\varepsilon_t| + |\varepsilon_c|}{d} \quad \text{Eq. (4.1)}$$

$$M = F * L_e \quad \text{Eq. (4.2)}$$

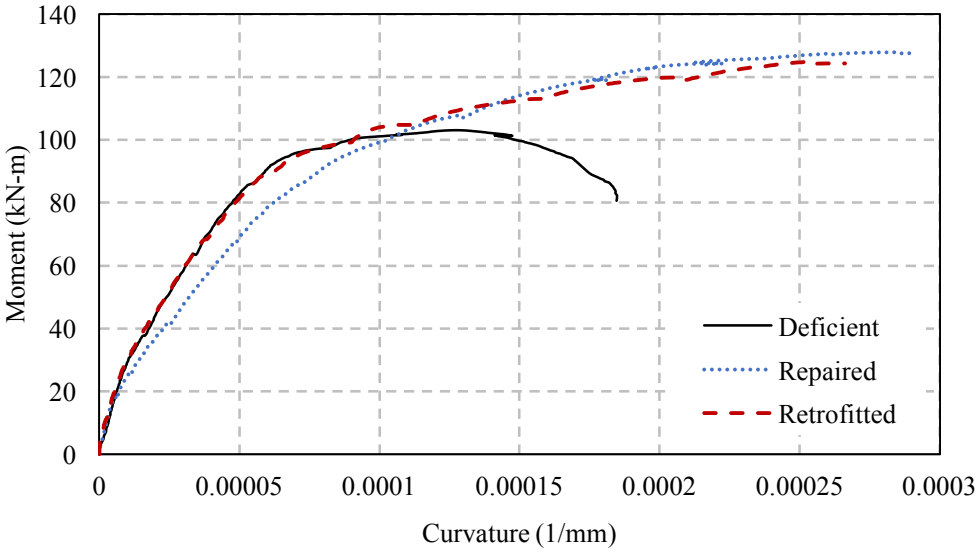

Figure 4.14: Moment-curvature response of non-seismically designed, repaired and retrofitted pier

The moment-curvature results for a section 100 mm above the base of piers subjected to a combination of constant axial load and varying lateral load are shown in Fig. 4.14. As shown in Fig. 4.14, the measured curvature for the specimens has differed from each other. The GFRP retrofitted specimen showed superior moment-curvature relationship compared to deficient and repaired specimen. The lateral load capacity of deficient specimen started to decrease after reaching a curvature value of 0.00013 per mm. The repaired specimen showed increased curvature value under similar loading but the moment capacity kept on increasing up to the whole range of loading. The retrofitted specimen showed similar moment-curvature relationship in the beginning stage of loading as deficient specimen and the moment capacity kept increasing for increased curvature value. This is because of the higher strain capacity of concrete provided by GFRP confinement that helped to improve the moment-curvature relationship of the section. When compared with the stress-strain graphs as shown in Fig. 3.8

and Fig 3.9, similar behavior can be found for confinement with higher number of layers.

4.7.4 Ductility Analysis

The displacement and curvature ductility of the piers are calculated based on the yielding and ultimate points of the test. The yield force was obtained from strain response of rebar (Fig. 4.12(a, c, f)) and corresponding displacement was found from load-displacement (Fig. 4.10) curve. The yield moment was calculated from yield force and the corresponding curvature was obtained from moment-curvature relationship (Fig. 4.14) obtained from tests. Table 4.4 shows the summary of displacement and curvature ductility.

Table 4.4: Ductility analysis of piers obtained under lateral cyclic load

Specimen type	**Yield**				**Ultimate**				**Disp. ductility**	**Curv. ductility**
	Force (kN)	Disp (mm)	Moment (kN-m)	Curv. (1/mm)	Force (kN)	Disp (mm)	Moment (kN-m)	Curv. (1/mm)		
Deficient	38.9	19.6	64.38	3.52×10^{-5}	62.3	69.3	103.11	9.64×10^{-5}	3.54	2.74
Repaired	43.13	25.2	71.38	5.25×10^{-5}	77.98	120	127.6	2.9×10^{-4}	>4.76	>5.52
Retrofitted	39.1	19.2	64.71	3.44×10^{-5}	79	120	130.75	2.66×10^{-4}	>6.25	>7.73

The stiffness and yield force of the retrofitted pier were slightly increased because of GFRP confinement effect. This resulted small reduction in displacement and curvature at yielding point and significant improvement of displacement and curvature at ultimate stage compared to deficient specimen. The displacement and curvature ductility were found as 3.54 and 2.74 respectively for control specimen, whereas the values were 6.25 and 7.73 respectively for retrofitted specimen. The enhanced strain capacity of confined concrete helped the pier to behave in a more ductile fashion as compared to deficient pier with inadequate confinement. The repaired specimen showed the effect of strain hardening because of previous loading and unloading during the test of control specimen. The value of force, displacement and

curvature at yielding point were higher than control specimen and at ultimate stage it showed comparable results with retrofitted one.

4.7.5 Energy Dissipation

Earthquakes impose tremendous amount of force on the structure. Energy dissipation capacity of a structure helps dissipating this force without significant structural damage, thus reduces the probability or prevents total collapse of the structure. Fig. 4.15 (a) and (b) depict the dissipated energy per cycle and cumulative energy dissipation for the deficient, repaired

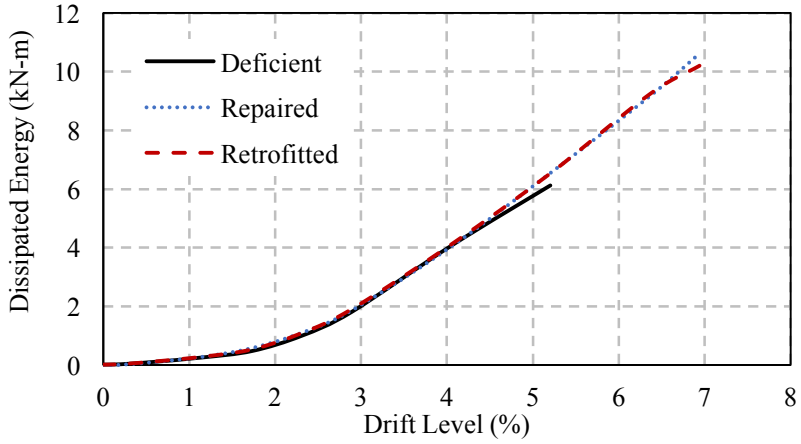

(a)

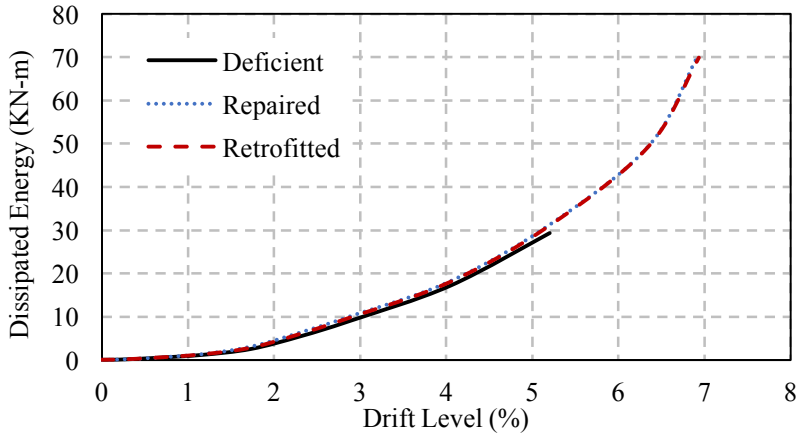

(b)

Figure 4.15: Energy dissipation capacity of piers under lateral cyclic loading: (a) energy dissipation per cycle; (b) cumulative energy dissipation.

and retrofitted columns, respectively. All the specimens exhibited similar energy dissipation capacity per cycle, but the repaired and retrofitted specimens could dissipate energy over more cycles than deficient specimen. Below about 1.5% drift, the piers dissipated a very small amount of energy as the materials were behaving in the elastic range and did not have significant residual deformation. Once nonlinearity of the materials came into action, the energy dissipation capacity of the pier started to increase significantly. As GFRP retrofitting is a passive confinement technique, confinement did not come into action at the beginning of loading and the initial behavior for all three specimens was similar. But later, it helped the repaired and retrofitted piers to take more loading cycles and dissipate more energy than the deficient pier. From cumulative energy dissipation graphs, it is evident that, repairing and retrofitting with GFRP confinement improved the energy dissipation capacity of a deficient pier as much as 2.4 times.

4.7.6 Residual Drift

Residual drift is an important criterion for determining the usability of a structure after a seismic event. Fig. 4.16 depicts the residual drift versus drift ratios. For the tested specimens, it can be observed that, all the piers experienced similar residual drift (1.5%) up to an applied drift of 3.9%. After that the residual drifts started increasing significantly with the applied load. After 3.9% applied drift, the deficient specimen started to fail by spalling of concrete, buckling of rebars and started to lose its restoring capacity. The deficient pier showed much higher residual drift than the repaired and retrofitted specimens. For instance, at 5.2% drift, the as-built column experienced 24% higher residual drift compared to the repaired and retrofitted specimens. The residual drift of the repaired specimen is slightly higher than the retrofitted specimen; however, follows a similar pattern and linear relationship with the

applied drift. This is because the repaired and retrofitted piers did not lose their restoring force up to the applied drift.

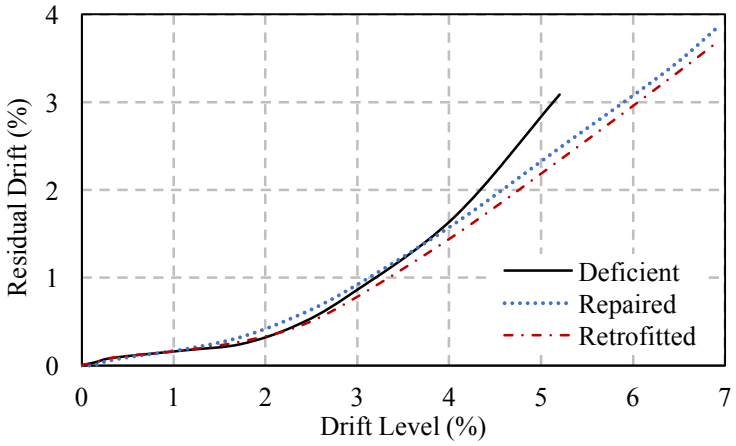

Figure 4.16: Residual Drift of tested specimen at different applied drift

4.7.7 Failure Mode

The failure mode for deficient specimen was characterized by the presence of small width horizontal cracks distributed both around and along the specimen's surface, and the diagonal shear cracks were located in the opposite direction of the loading. After reaching the maximum capacity, spalling of concrete started and it initiated the buckling of longitudinal reinforcement. This resulted in losing the restoring force of pier and increased residual drift and energy dissipation as discussed earlier. The buckling of the longitudinal reinforcements and crushing of core concrete caused hoop fracture in the plastic hinge region as well. At this point, there was a sudden drop in lateral load capacity of deficient pier. The failure modes of deficient pier are shown in Fig. 4.17 (a).

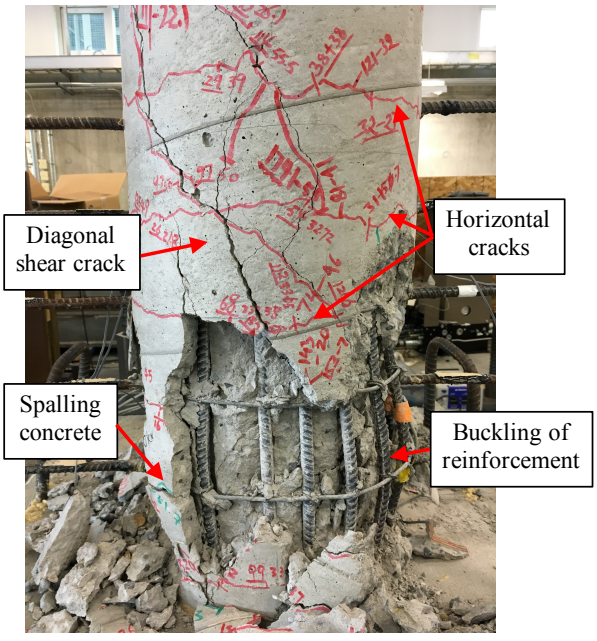

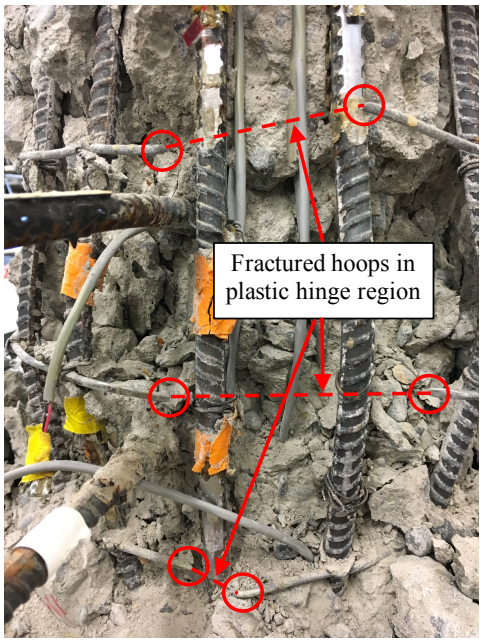

(a)

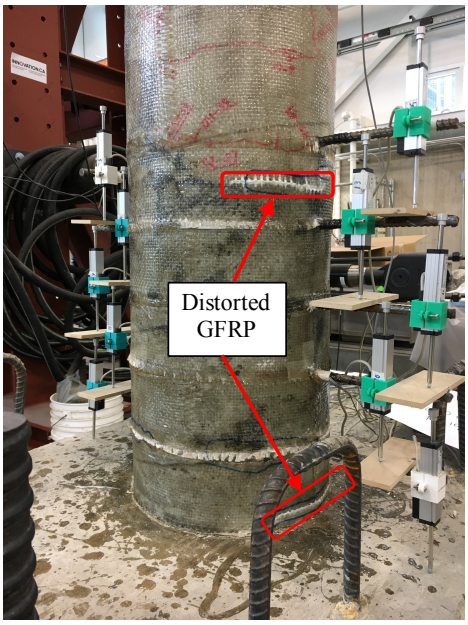

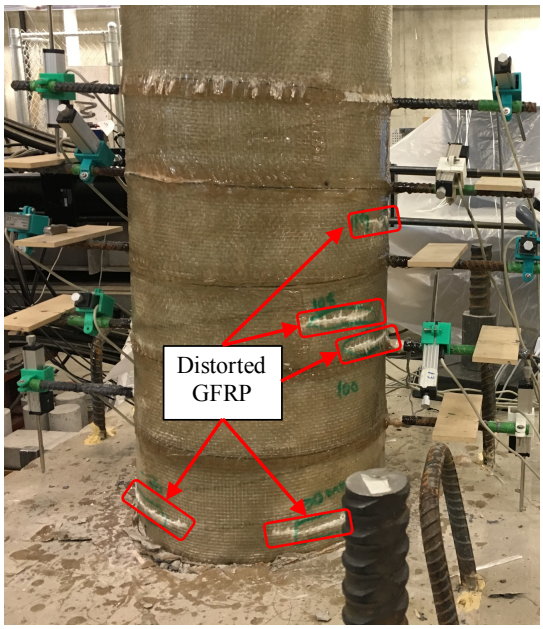

(b) (c)

Figure 4.17: Failure mode of tested piers after test (a) deficient, (b) repaired and (c) retrofitted.

The repaired and retrofitted specimens were tested up to the maximum displacement capacity (±120 mm or 6.9% drift) of hydraulic actuator. No specimen suffered any significant damage except some distortion of vertical fibres on the extreme sides under compression (Figs. 4.17 (b and c)). This was reported as a horizontal white line in the GFRP surface. This is because of the inability of fibres to take compression. It should be noted that these specimens were enhanced with GFRP confinement, which helped the specimens to take more shear force and have more ductility. There was no bond failure observed between the outer layers of GFRP. This means, 150 mm overlap length in the final layer was sufficient for developing required tensile strength in the fibres.

4.8 Summary

A detailed experimental investigation on seismic performance enhancement of non-seismically designed RC circular bridge pier is presented in this chapter. Using market available low-grade glass fibre reinforced polymer, it was found that seismic performance can be enhanced and damaged pier can be repaired and strengthened. Performance of repaired and retrofitted specimens was compared with deficient pier. The repaired specimen can perform similar to a retrofitted one when proper repair method is adopted and confinement is applied.

Chapter 5

Performance of GFRP Repaired and Retrofitted RC Circular Bridge Piers under Simulated Earthquake Aftershocks

5.1 General

Reinforced concrete bridge piers designed using pre-1971 guidelines are commonly deficient in flexural ductility, shear and flexural strength. Lateral loads were not considered in design guidelines and bridges were built with traditional hoop spacing of 300 mm, irrespective of column size, strength, or deformation demands. Such transverse reinforcement provides inadequate confinement for the core concrete under compression. As a result, the ultimate curvature developed within the potential plastic hinge region is limited by the strain at which the cover concrete begins to spall, which is typically around 0.5 percent strain (Chai et al. 1991). Thus, the failure of pier is initiated by cover concrete spalling, leading to crashing, and later buckling of reinforcement due to the splitting action under lateral motion.

Lateral confinement also helps to improve the performance of low strength concrete that cannot meet the design strength because of improper mix design, curing and other environmental impacts like freeze-thaw effect. Poorly detailed and deteriorated RC structural elements are vulnerable to loss of axial load carrying capacity at drift levels (2-3%) during a design level earthquake (Mander et al. 1988)). The inadequate lap splice length at the plastic hinge zone and inadequate transverse reinforcement in bridge piers are the most significant factors causing a lateral deficiency in resisting seismic force (Priestley and Park 1984, Boys et al. 2008).

Fibre-reinforced polymer (FRP) jackets are the most common materials used to improve the strength and ductility capacity of vulnerable piers (Chai et al. 1991, Boys et al. 2008, Priestley and Seible 1995) The confinement provided by an FRP jacket to a concrete core is passive rather than active, as the confining pressure from the jacket is induced by and increases with the expansion of the concrete core. Several researchers like Elsanadedy and Haroun (2005), Gallardo-Zafra et al. (2009), and Kawashima et al. (2000) conducted experimental investigation on the effectiveness of passive confinement using FRP composites. While other studies attempted to describe analytically the constitutive behavior and stress-strain model of concrete confined with FRP (Sheikh and Uzmeri 1980, Park et al. 1982, Mander et al. 1988, Fardis and Khalil 1982, Mirmiran and Shahawy 1987, Samaan et al. 1998, Spolestra and Monti 1999).

FRPs are generally constructed of high performance fibres such as carbon, aramid, or, glass which are placed in a resin matrix. By selecting among the many available fibres, geometries and polymers, the mechanical and durability properties can be tailored for a particular application. The performance of Glass Fibre Reinforced Polymer (GFRP) retrofitted reinforced concrete bridge piers have been studied for many years. Many studies have demonstrated that lateral confinement provided by GFRP confinement increases the compressive strength, ductility, and energy absorption capacity of the concrete (Herwig and Motavalli 2012, Rodsin 2015, Teng et al. 2013, Elwan and Rashed 2011, Gu et al. 2010, Sheikh and Yau 2002, Xiao et al. 1999). Although experimental studies were conducted to investigate the cyclic performance of GFRP-retrofitted columns, its fatigue performance under repeated set of lateral cyclic loading coming from several earthquake motions and their aftershocks has not been yet well investigated.

Earthquakes are often associated with number of foreshocks and aftershocks. Shear wave reflected from earth core is one of the main causes of aftershock. Retrofitted piers may prevent the collapse of bridges during an earthquake with severe damage. But what will happen to the damaged structures during several high magnitude aftershocks?

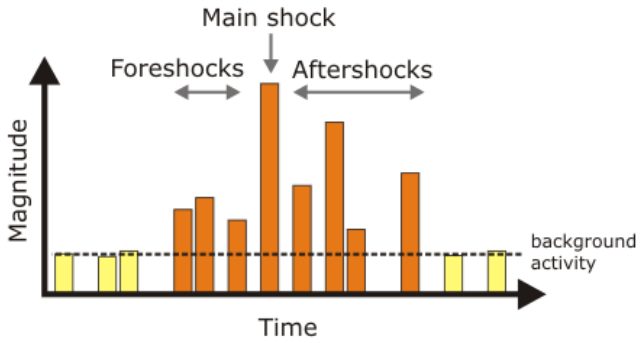

Figure 5.1: Demonstration of foreshocks and aftershocks associated with earthquake.

Researchers have conducted numerous investigations on effectiveness of GFRP retrofitting technique numerically and experimentally as well. It is established that this method can significantly improve the seismic performance of bridges that can prevents the collapse during an earthquake. But no one has investigated the performance of bridge piers under earthquake aftershocks that have significant magnitude as a main shock. These aftershocks can lead to collapse of bridges that are already damaged during the main shock.

This chapter discusses an effective method of retrofitting existing structures using strength and ductility enhancement by a passive confinement provided by GFRP jackets. Performances of a repaired and retrofitted pier under repeated sets of lateral loadings are analyzed and compared with as-built specimen. The influence of external GFRP confinement upon the hysteretic characteristics, ductile behavior, moment-curvature analysis, and ability of energy dissipation were analyzed. Detailed experimental investigation, test method and setup, performances of non-seismically designed and retrofitted specimens have been properly investigated.

5.2 Research Significance

Poor performance of deficient reinforced concrete bridge piers, primarily due to lack of adequate lateral reinforcement, caused many bridge failures during recent earthquakes. GFRP retrofitting is a quick, effective and convenient means for seismic repair of damaged piers and upgrade of vulnerable piers. Fatigue performance of a GFRP retrofitted pier is presented under repeated sets of lateral cyclic loadings. This represents the performance of repaired and retrofitted pier under several aftershocks during an earthquake event. Results from this research provide an insight for predicting the performance of repaired and retrofitted piers under earthquakes associated with several aftershocks.

5.3 Experimental Investigation on Piers

5.3.1 Design and Geometry of Pier

In order to investigate the performance of GFRP retrofitted bridge piers under earthquake aftershocks, the same bridge piers tested in Chapter 4 are considered. The design and geometry of these bridge piers are described in section 4.4. They were tested under repeated sets of loadings until failure to observe its performance under several aftershocks during an earthquake event. The specimens during the test were subjected to a constant axial load based on 10% of $f'_c A_g$, where A_g is the cross-sectional area of the column, and f'_c is the concrete compressive strength at 28 days.

5.3.2 Loading Protocol

The performance of the specimens was analyzed using a standard displacement controlled quasi-static cyclic loading as described in section 4.5.2. Each set of loading was consisting of

a protocol as section 4.5.2. This set was repeated several times to simulate the earthquake aftershocks. Fig. 5.2 shows repeated sets of loading protocol applied in this study.

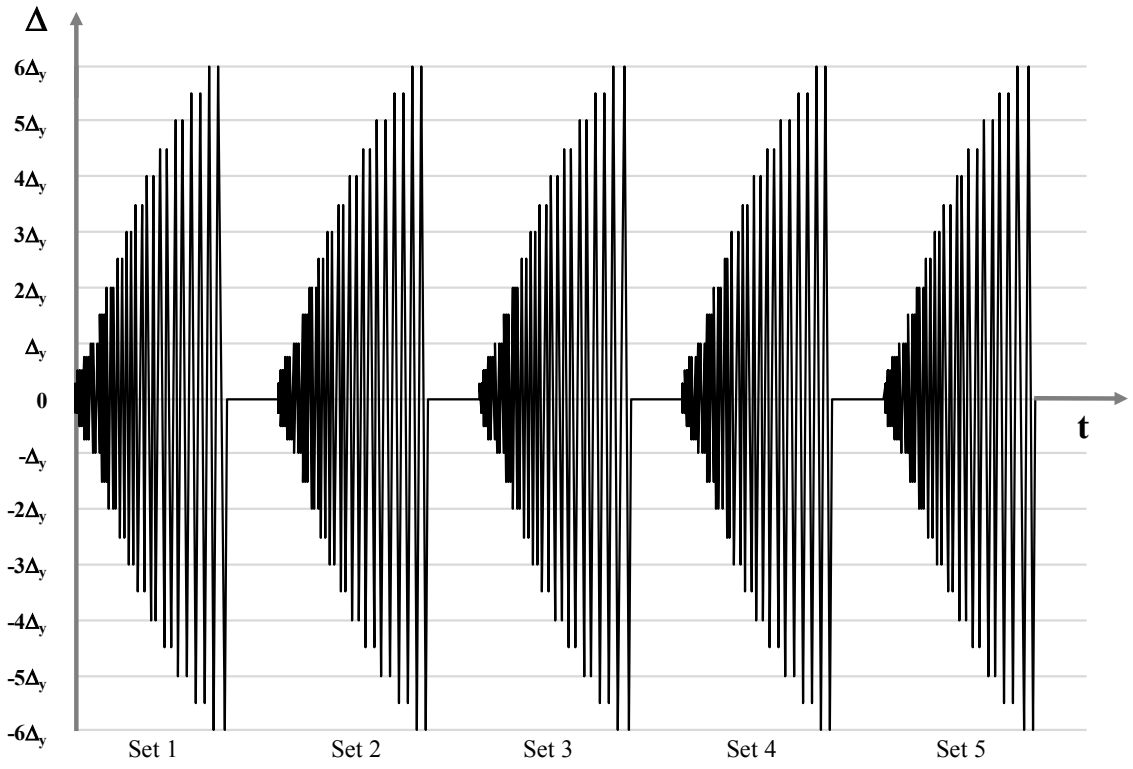

Figure 5.2: Repeated sets of loading protocol to simulate earthquake aftershocks.

5.4 Test Results and Discussions

5.4.1 Cyclic Response

Fig. 5.3 shows the hysteretic behavior of deficient, repaired and retrofitted piers under various cyclic loading sets up to failure obtained from the experiments. For deficient pier, the hysteresis reached its maximum strength of 62 kN at 2.7% drift and was stable until 3.9% drift. After that, significant strength reduction occurred on one side and the pier is considered as failed under lateral loading. The failing part of the curve shows that, strength deteriorated from maximum value by 11.6% at 4.64% drift and then suddenly by 29.4% at 5.2% drift.

Strength deterioration can be attributed to the spalling-off of cover concrete which initiated the buckling of the main bars under compression at these drift ratios. The pier showed symmetric strength behavior on both loading sides, except that, one more stable cycle was observed on pulling side. The deficient pier could not take one whole loading set and started to collapse after 3.9% drift.

The repaired specimen could take only 2 sets of cyclic loadings. Under first set of loadings, the repaired specimen showed significant improvement in lateral load carrying capacity and drift capacity. The maximum lateral load was observed 78 kN at 6.9% maximum drift. The specimen failed during the second set of loadings when the cycle of maximum drift was being applied. This can be attributed by the early progression in buckling of already yielded and buckled reinforcement in the repaired specimen. This early progression in buckling lead to extreme pressure on cover concrete and caused the GFRP to rupture under tension.

Under first set of loadings, the retrofitted column demonstrated stable response in the entire loading displacement range tested because of the confinement effect. The hysteresis reached its maximum strength of 77.4 kN at the maximum drift of 6.9%. No deterioration of the restoring force occurred up to the maximum drift capacity of 6.9% for the adopted test setup.

For second to fifth loading sets, hysteretic behavior with similar pattern were observed. The maximum lateral load reduced from 70 kN to 65.5 kN on pushing side and from 73.6 kN to 71.3 kN on pulling side at 6.9% drift. The slight reduction in stiffness occurred under 10 mm applied displacements, but it was significant in larger values of lateral displacement.

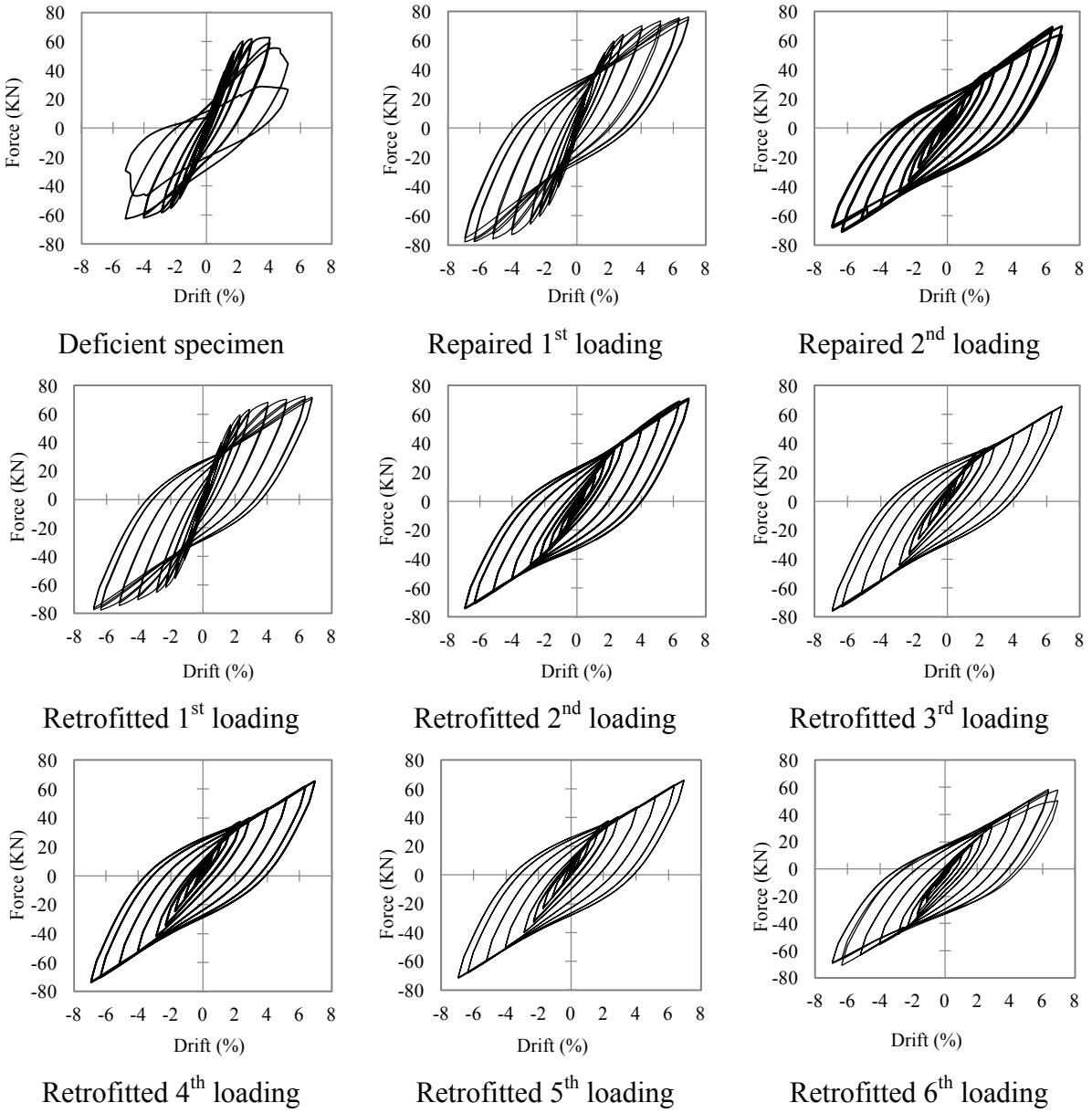

Figure 5.3: Hysteretic response of as built and retrofitted piers under lateral cyclic loading.

During sixth loading, before the failure of GFRP initiated, the specimen lost significant stiffness compared to previous loadings. Strength reduction was observed at the final cycle as GFRP started to rupture under tension on pulling side. This failure indicated the poor fatigue performance of GFRP. The lateral load reduced to 57.87 kN and then 49.88 kN during the final cycle.

To assess the influence of GFRP confinement on the seismic response of piers under repeated sets of cyclic loading, lateral force-displacement skeleton curves of the specimens obtained from experiments were compared in Fig. 5.4. Increased flexural strength and ductility capacity were attained for both repaired and retrofitted specimen under first set of loading. However, there was no significant increase in lateral stiffness of piers since the GFRP acted as a passive confinement. The lateral load capacity increased by about 24% and a stable

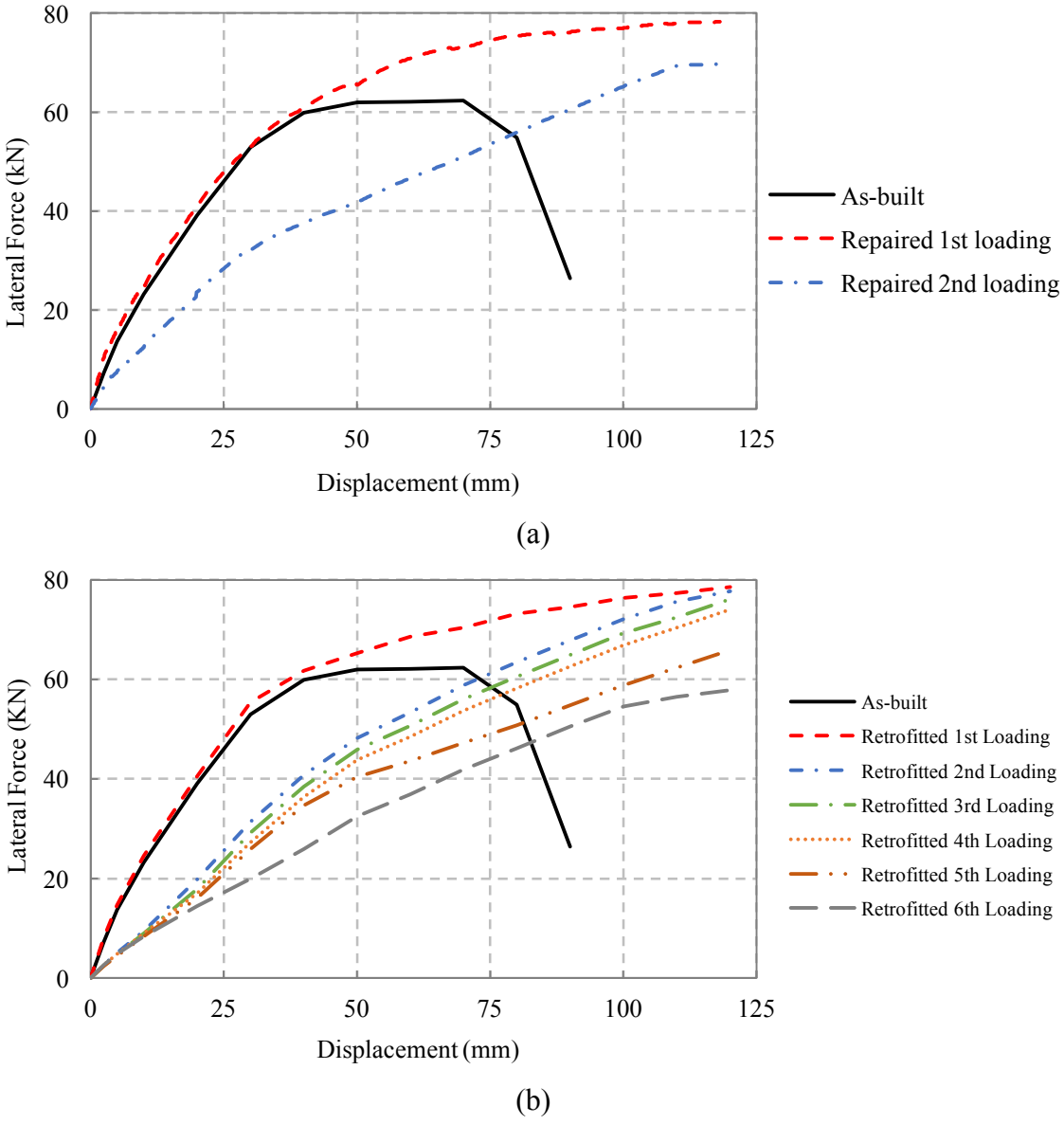

Figure 5.4: Skeleton curve obtained from load-displacement response of piers under repeated sets of loading; (a) repaired pier; (b) retrofitted pier

and ductile behavior was shown by piers. The stiffness of the specimens drastically reduced to one-third (from 2.93 kN/mm to 0.97 kN/mm) in the second set of loading, even though the maximum capacity was similar to first loading. Under other sets of loadings, the stiffness and maximum lateral load kept on decreasing until the GFRP ruptured on second cycle for repaired specimen and on sixth cycle for retrofitted specimen. This can be attributed by the damage occurred in concrete in each set of loading resulting in reduction of restoring force of piers. Failure for retrofitted specimen occurred at 6.9% drift when the lateral load was 57.87 kN. From the skeleton curve of retrofitted specimen, it can be concluded that, even though the stiffness of pier was reduced in each loading set, the confinement still helped the piers to maintain the ductility and load carrying capacity as compared to first loading set. This means, the retrofitted pier can prevent total collapse of bridges during earthquake aftershocks. The repaired pier showed poor performance in this case when compared with retrofitted one.

5.4.2 Moment-Curvature Response

The curvature in the plastic hinge region was calculated based on the deformation measured by pair of transducer gauge mounted on the extreme sides of the specimens, where the plastic behavior is expected to occur. The curvature at the first critical section at 100 mm above the base was measured using the method explained in section 4.7.3.

The moment-curvature response for a section at 100 mm height above the base of piers subjected to a combination of constant axial and varying cyclic load are shown in Fig. 5.5. The measured curvature values for the specimens under a certain applied moment were different for each specimen. The GFRP retrofitted specimen under first set of loadings showed superior improvement in moment-curvature relationship compared to the deficient

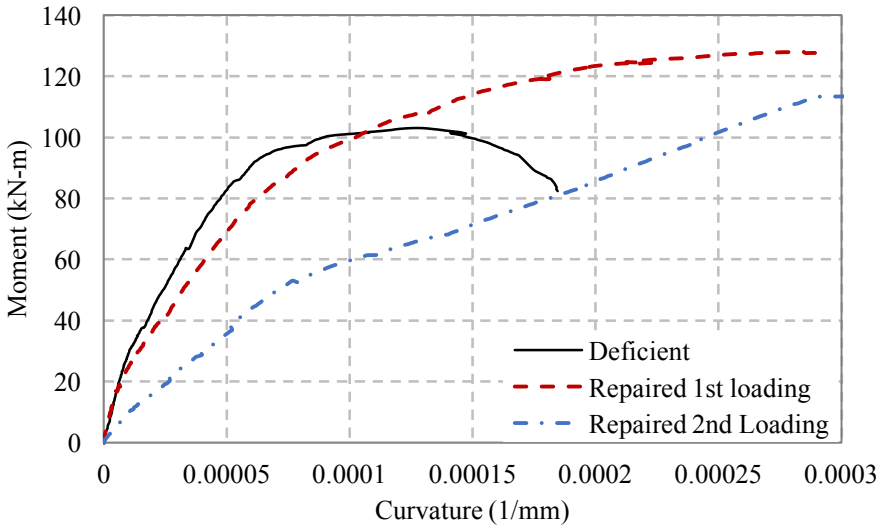

(a)

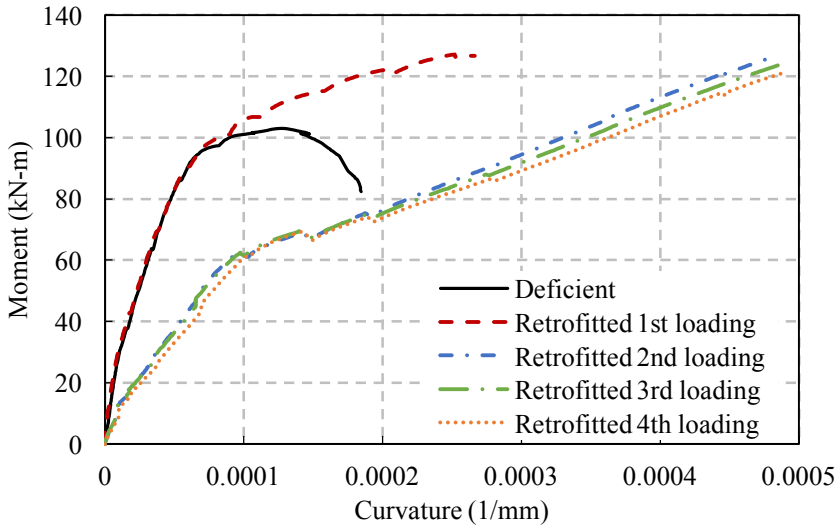

(b)

Figure 5.5 Moment-curvature response of deficient, retrofitted and repaired specimens under several sets of loading; (a) comparison between deficient and repaired pier; (b) comparison between deficient and retrofitted pier.

specimen and retrofitted specimens under other sets of loadings. The lateral load capacity of deficient specimen started to reduce after reaching a curvature value of 0.00013 per mm. The retrofitted specimen showed similar moment-curvature relationship at the beginning stage of loading, but after that the moment capacity kept increasing for increased curvature value. Similar bi-linear moment-curvature relationship is obtained for other sets of loadings. The

moment capacity dropped to 107.4 kN-m from 124.3 kN-m for forth loading. The moment-curvature relation for fifth and sixth loading could not be obtained because of program error in data acquisition system. From the moment curvature relationship of repaired and retrofitted specimen, it is found that the plasticity increases in the column under each set of loading, but the retrofitted specimen was capable of keeping similar moment-curvature relationship during each cycle until failure.

5.4.3 Energy Dissipation

Energy dissipation capacity of a structure helps dissipating energy without significant structural damage during an earthquake, thus reduces the probability of total collapse of the structure. As depicted in Fig. 5.6 and 5.7, the repaired and retrofitted specimens can withstand more loading cycles and dissipate more energy than deficient specimen. But the amount of energy dissipated per cycle kept on decreasing in each set of loadings. This is because of the reduction in lateral load capacity of piers in each loading set. The similar behavior is observed for cumulative energy dissipation curve. The retrofitted specimens dissipated more than double energy compared to deficient specimen, 2.4 times to be exact. The energy dissipation capacity of piers decreased slightly in each loading set; still they were able to maintain a very good energy dissipation capacity when compared to first loading. From Fig. 5.6 and 5.7 it was found that, there was a logarithmic increment in energy dissipation for increased drift. It can be concluded that, repairing and retrofitting with GFRP confinement can hold the improved energy dissipation capacity under several aftershocks as compared to the deficient pier.

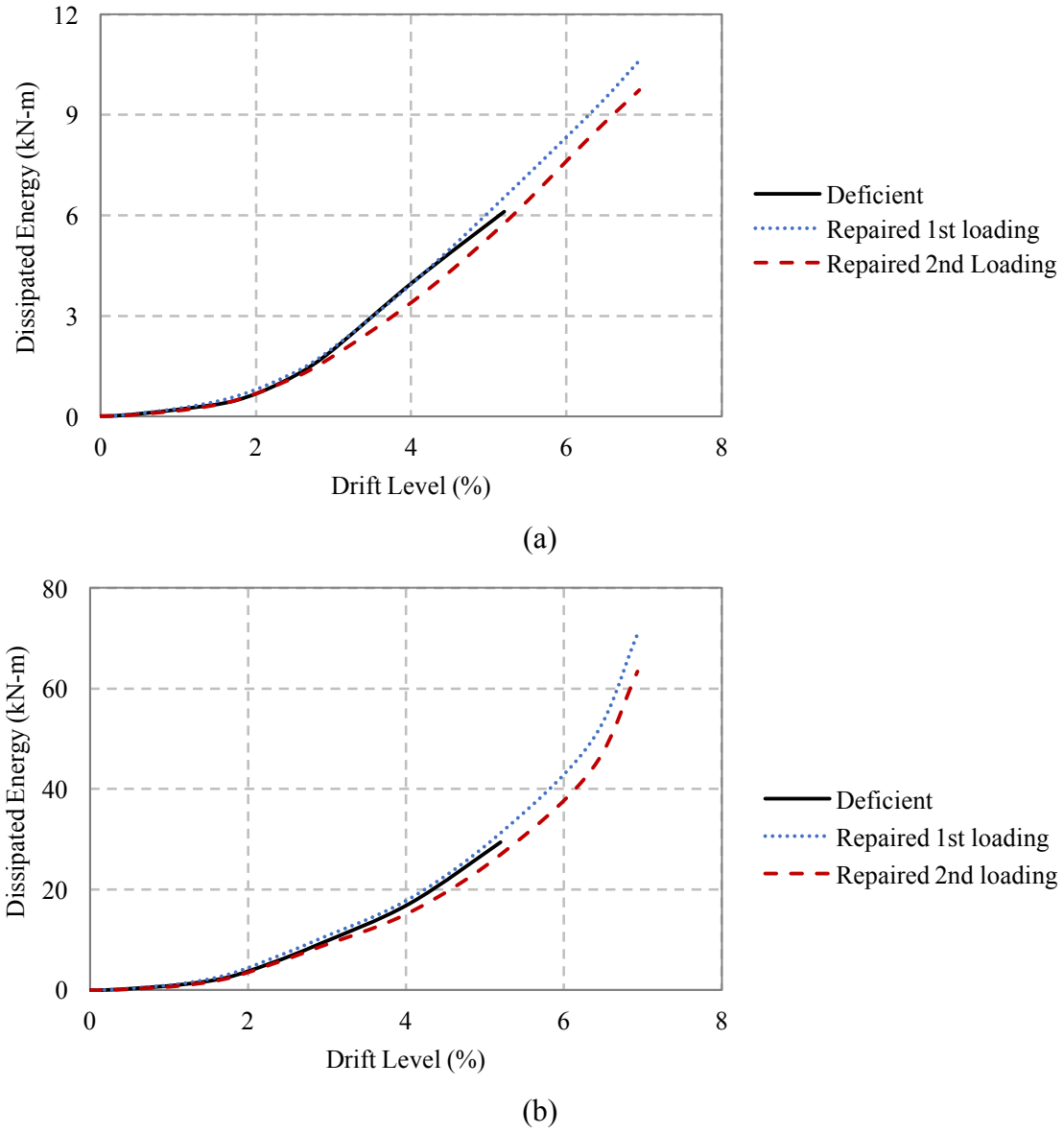

Figure 5.6: Energy dissipation capacity of repaired pier under repeated sets of loading; (a) energy per cycle; (b) cumulative energy.

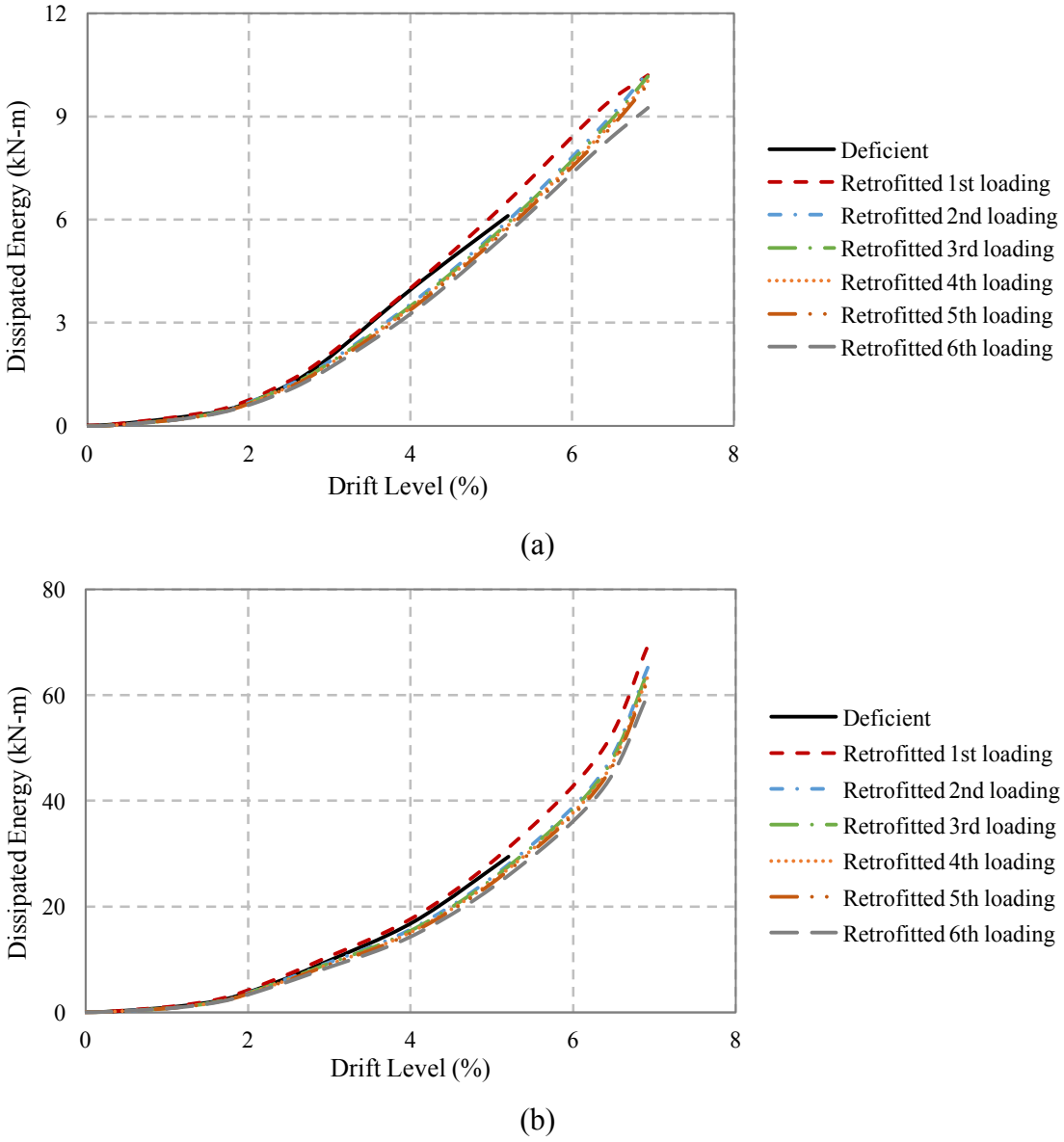

Figure 5.7: Energy dissipation capacity of retrofitted pier under repeated sets of loading; (a) energy per cycle; (b) cumulative energy.

5.4.4 Failure Mode

The failure mode for deficient specimen was characterized by the presence of horizontal cracks distributed both around and along the specimens' surface, and the diagonal shear cracks were located in the opposite direction of the loading. After reaching to maximum capacity, the spalling of concrete started and it initiated the buckling of longitudinal reinforcement. This caused hoop fracture in the plastic hinge region. The failure modes are shown in Fig. 5.8.

The repaired and retrofitted specimens were tested up to the maximum capacity of ±120 mm lateral displacement (6.9% drift). For repaired specimen, few horizontal distortions were observed during the first set of loading and the GFRP failed during the second loading with horizontal and vertical rupture. For retrofitted specimen, no significant damage was observed up to fifth set of loadings, except some distortion of vertical fibres on the extreme sides under compression. This is because of the fibres inability to take load under compression. It should be noted that these specimens were enhanced with GFRP confinement, which had a significant effect on shear and ductility. During sixth loading set, the GFRP started to fail under tension and rupture was initiated on one extreme side. Before that, the distortion under compression turned into complete rupture in the horizontal direction. The concrete started to dilate significantly which imposed more tension on the fibres and accelerated the rupturing process. The specimen was considered to be failed at this stage and no further loading was applied. No bonding failure between concrete and GFRP, and GFRP layers was observed during the failure of piers.

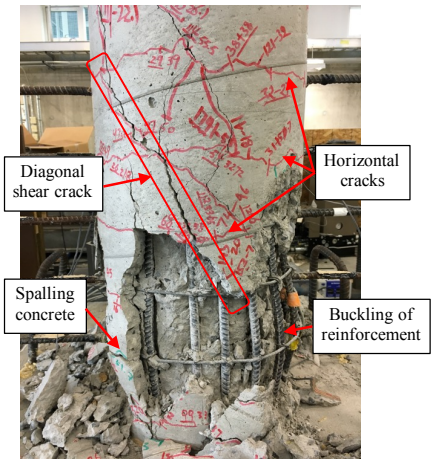

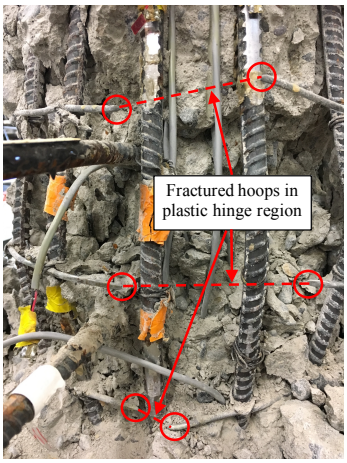

Failure of deficient specimen

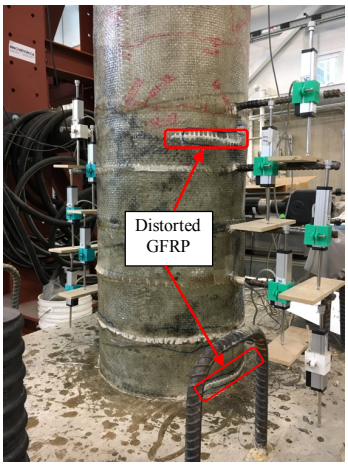

Repaired specimen after 1st loading

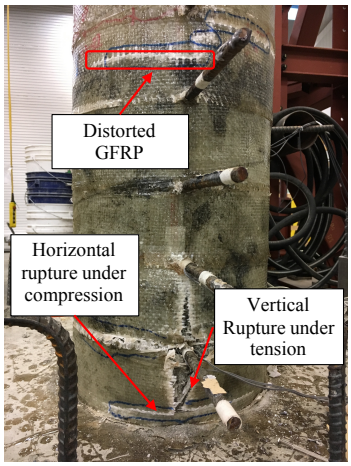

Repaired specimen after 2nd loading

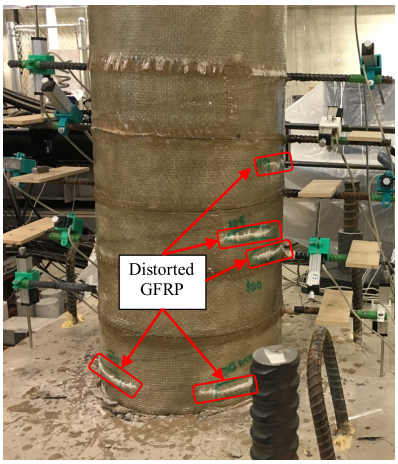

Retrofitted specimen after 1st loading

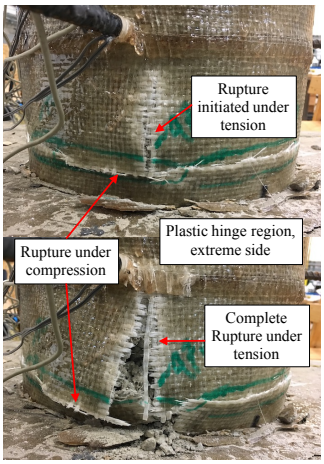

Retrofitted specimen after 6th loading

Figure 5.8: Failure mode of deficient, repaired and retrofitted specimen.

5.5 Summary

Researchers have studied different confinement technique to mitigate the problem of inadequate confinement associated with old design codes. Fibre reinforced polymer (FRP) composites have become promising retrofitting materials for improving the seismic performance of existing reinforced concrete (RC) bridge piers. This paper presented a comprehensive summary of the existing application of FRP in order to improve the seismic resistant capacity of non-seismically designed RC circular bridge piers. Investigation on the performance of scaled down specimens of 5.2 m tall bridge pier built in the 1970s under repeated cyclic loading was presented.

Chapter 6

Conclusions and Recommendations

6.1 General

Glass Fibre Reinforced Polymer (GFRP) composites are promising retrofitting material for improving the seismic behavior of existing deficient RC bridge piers. Study presented in this thesis justifies the potential capacity of low grade GFRP in repairing and retrofitting works. This thesis explores the possibility of utilizing different retrofitting techniques for improving seismic performance of non-seismically designed RC bridge piers. A state-of-the-art literature review on various retrofitting techniques and their relative advantages and disadvantages are presented. This study also demonstrates the effect of low grade GFRP confinement thickness on the compressive strength of concrete. The performance of low grade GFRP retrofitted and repaired RC circular bridge piers were investigated and compared with deficient pier. The effects of repeated seismic loading like earthquake aftershocks on the behavior of repaired and retrofitted piers are also presented in this thesis.

6.2 Limitations of this study

The limitations of this study include but not limited to:

(i) The applied axial load was assumed to be constant throughout the test, even though it could vary with the applied displacement because of column elongation and eccentricity of post-tension steel.

(ii) The direction of applied GFRP fibres was assumed to be horizontal along the periphery. There could be some misalignment because of workmanship.

(iii) The contributions of longitudinal fibres were completely ignored as small width GFRP strips are used.

(iv) The ultimate capacity of the repaired and retrofitted piers could not be obtained because of the stroke length limitation of hydraulic actuator.

(v) Dynamic behavior of the column was ignored as pseudo-static loading rate was applied during the tests.

6.3 Conclusions

6.3.1 Effect of low grade GFRP confinement thickness on the compressive strength of concrete

A combined experimental and numerical study has been conducted and presented in Chapter 3 on improving the compression carrying capacity of concrete using GFRP confinement. The following conclusions are made based on the study presented in this Chapter:

(i) GFRP with low tensile strength and modulus of elasticity can be used as a confining material for concrete. Multi-layer of GFRP showed better mechanical properties (i.e. tensile strength and modulus of elasticity) than a single layer.

(ii) The optimum overlapping length between final layers of GFRP was found 150 mm. But, for all the overlapping length provided in the coupons (25 to 200 mm) failure was due to the bonding failure between GFRP layers.

(iii) Increasing GFRP layer number (i.e. thickness of GFRP) helped improving the confinement effect thus enhanced the compression carrying capacity of low strength concrete. This kept increasing with the increasing number of layers. But the failure mode changed to more brittle type for higher layer number (3 layers).

(iv) As GFRP thickness was increased, flexural strength and ductility of the retrofitted piers also increased. However, the strength gaining started to be saturated with increased number of layers (2 layers in this study).

6.3.2 Performance of low grade GFRP repaired and retrofitted RC bridge piers

A detailed experimental investigation on the seismic performance enhancement of non-seismically designed RC circular bridge pier is presented in this paper. The effect of low grade GFRP retrofitting and repairing on the seismic response of scaled down specimens of a 5.2 m tall bridge pier built in the 1970s was investigated. Performance of repaired and retrofitted specimens was compared with deficient specimen. Based on the results presented, the following conclusions can be made:

(i) For the seismically damaged RC circular piers, repairing and retrofitting technique using passive confinement demonstrated the purpose of restoring flexural and shear strength and also the ductility of piers.

(ii) Market available low-grade glass fibres proved to be effective for confining deficient reinforced concrete piers for enhanced performance under lateral loading.

(iii) The deficient pier once retrofitted with GFRP jacketing showed increased lateral strength (27%), ductility (73%) and energy dissipation capacity (140%).

(iv) From the experimental results it was found that, initial stiffness did not change for passive confinement techniques like GFRP jacketing.

(v) The repaired and retrofitted pier had 140% improvement in energy dissipation capacity when compared with the deficient pier. This is because of the

improvement of drift capacity that enabled these piers to take more loading cycles.

(vi) Up to the maximum load capacity of deficient pier (62 kN at 3.9% drift), all the specimen had similar residual displacement. After that, the deficient pier started collapsing and its residual drift started to increase logarithmically. On the other hand, the repaired and retrofitted specimen had a liner relationship between applied drift and residual drift. The retrofitted specimen showed slightly better performance when compared with repaired one.

(vii) Damaged column repaired and strengthened with GFRP can perform similar to a retrofitted column under constant axial load and cyclic lateral load. This can be concluded based on the performance observed for repaired pier which showed 25% improvement in lateral load capacity and 73% improvement in drift capacity.

(viii) Except some horizontal distortions under compression, GFRP repaired and retrofitted pier did not show any significant damage up to the applied drift of 6.9% in the test.

(ix) The experimental results reported that material restoration technique (i.e. replacing damaged concrete with new repair concrete and keeping the buckled reinforcement straightened in place) following GFRP jacketing is an effective repairing technique to restore the strength and ductility of damaged piers.

6.3.3 Performance of GFRP retrofitted bridge pier under repeated sets of cyclic loadings

Investigation on the performance of scaled down specimens of a 5.2 m tall bridge pier built in the 1970s and repaired and retrofitted with low grade GFRP under simulated earthquake aftershocks was presented. Performance of the specimens was compared under repeated sets of cyclic loading. Based on the results presented, the following conclusions can be made:

(i) GFRP retrofitted pier can withstand multiple major earthquakes or aftershocks and prevent collapse of bridges.

(ii) GFRP retrofitted pier showed better performance by maintaining its strength up to six consecutive loading sets compared to the repaired specimen which could take only two sets of loading.

(iii) Once loaded, the stiffness of the retrofitted column was reduced drastically but the maximum load carrying capacity reduced gradually with cycles of loading sets.

(iv) GFRP retrofitted piers under multiple sets of loadings cycles showed similar energy dissipation capacity which is 140% higher than deficient pier. This is because, GFRP confinement enhanced columns ability to take more loading cycles at higher drift level by improving the strain carrying capacity of concrete.

(v) The failure of GFRP retrofitted column was initiated by horizontal rupturing at distorted location and then vertical rupturing under extreme tension.

6.4 Recommendations for future research

Based on the experimental study conducted in this thesis, the following recommendations can be made for future research:

- The effect of thickness of different kinds of FRPs on the seismic performance of RC circular piers can be experimentally investigated and compared with numerical studies.
- The effect of unidirectional and bidirectional fibres can be investigated, compared and their suitable type can be proposed for different type of design consideration.
- The test of different GFRP repaired and retrofitted RC bridge piers can be conducted on a shake table under real earthquake loading data and their performance under different design level earthquake can be investigated.
- Continuous GFRP sheets can be applied throughout the length of piers by using a single sheet or providing overlap between two adjacent sheets.

References

ACI 549.1R. (1993). Guide for design, construction & repair of ferrocement. ACI Committee 549.1R-93, American Concrete Institute, Michigan, USA.

Afifi, M. Z., Mohamed, H. M., and Benmokrane, B. (2015). "Theoretical stress–strain model for circular concrete columns confined by GFRP spirals and hoops", Engineering Structures, V. 102, pp 202–213.

Aire, C., Gettu, R., Casas, J. R., Marques, S., and Marques, D. (2010). "Concrete laterally confined with fibre-reinforced polymers (FRP): experimental study and theoretical model". Journal of Construction Materials, 60(297): 19-31.

Anderson, D. L., Mitchell, D., and Tinawi, R. (1996). "Performance of concrete bridges during the Hyogoken Nanbu (Kobe) earthquake of January 17, 1995", Canadian Journal of Civil Engineering, 23 (3): 714-726.

ATC-32. (1996). Improved seismic design criteria for California Bridges: provisional recommendation. Applied Technology Council, Redwood City, California, USA.

Bakis, C. E., Bank, L. C., Brown, V. L., Cosenza, E., Davalos, J. F., Lesko, J. J., Machida, A., Rizkalla, S. H., and Triantafillou, T. C. (2002). "Fibre-Reinforced Polymer Composites for Construction—State-of-the-Art Review." Journal of Composites for Construction, ASCE, 6(2), 73–87.

Benzaid, R., Mesbah, H., and Chikh, N. E. (2010). "FRP-confined concrete cylinders: axial compression experiments and strength model." Journal of Reinforced Plastics and Composites, 29(16), 2469–2488.

Billah, A.H.M.M. (2011). "Seismic Performance Evaluation of Multi Column Bridge Bent Retrofitted with Different Alternatives." MASc thesis, University of British Columbia, Kelowna, Canada.

Billah, A.H.M.M., and Alam, M.S. (2014). “Seismic performance evaluation of multi-column bridge bents retrofitted with different alternatives using incremental dynamic analysis.” Engineering Structures, 62–63, 105–117

Billah, A.H.M.M., Alam, M.S. and Bhuiyan, M.A.R. (2013). “Fragility Analysis of Retrofitted Multicolumn Bridge Bent Subjected to Near-Fault and Far-Field Ground Motion.” Journal of Bridge Engineering, ASCE, 18(10), 992-1004.

Binici, B. (2005). “An analytical model for stress–strain behavior of confined concrete.” Engineering Structures, 27(7), 1040–1051.

Boshoff, W. P. (2014). “Cracking behavior of strain-hardening cement based composites subjected to sustained tensile loading.” ACI Material Journal, 111, 553–560.

Bousias, S., Spathis, A. L., and Fardis, M. N. (2006). “Concrete or FRP jacketing for columns with lap-splices for seismic rehabilitation.” Journal of Advanced Concrete Technology, 4(3), 431–441.

Boys, A., Bull, D., and Pampanin, S. (2008). Seismic performance assessment of inadequately detailed reinforced concrete columns. In: New Zealand Society of Earthquake Engineering (NZSEE) Conference, Wairakei, New Zealand.

Bruneau, M. (1990). “Preliminary report of structural damage from Loma Prieta earthquake of 1989 and pertinence to Canadian structural engineering practice”, Canadian Journal of Civil Engineering, 17 (2): 198-208.

CALTRANS (2004). California Department of Transportation, Seismic Design Criteria, Sacramento, CA.

Canbolat, B., Parra-Montesinos, G., and Wight, J. (2005). “Experimental study on seismic behavior of high-performance fibre-reinforced cement composite coupling beams”, ACI Structural Journal, 102 (1): 159-166.

CAN/CSA-S6. (1974). Canadian highway bridge design code. Canadian Standards Association, Rexdale, Ontario, Canada.

CAN/CSA-S6. (2006). Canadian highway bridge design code. Canadian Standards Association, Rexdale, Ontario, Canada.

CAN/CSA-S6. (2014). Canadian highway bridge design code. Canadian Standards Association, Rexdale, Ontario, Canada.

Chai, Y. H., Priestley, M. J. N., and Seible, F. (1991). "Seismic retrofit of circular bridge columns for enhanced flexural performance." ACI Structural Journal, 88(5), 572–584.

Chang, S. Y., Li, Y. F., and Loh, C. H. (2004). "Experimental study of seismic behaviors of as-built and carbon fibre reinforced plastics repaired reinforced concrete bridge columns." Journal of Bridge Engineering, ASCE, 9(4), 391–402.

Chun, S. S., and Park, H. C. (2002). "Load carrying capacity and ductility of RC columns confined by carbon fibre reinforced polymer." In Proc. 3rd int. conf. on composites in infrastructure, University of Arizona, San Fanscisco, USA, in CD-Rom format.

Coffman, H. L., Marsh, M. L., and Brown, C. B. (1991). Seismic Durability of Retrofitted R. C. Columns, Washington State Department of Transportation.

CSA A23.2-9C (2014). Concrete materials and methods of concrete construction / Test methods and standard practices for concrete, Canadian Standard Association.

CSA/CAN3-S6-M. (1978). Canadian highway bridge design code. Canadian Standards Association, Rexdale, Ontario, Canada.

CSA S806 (2012). Design and construction of building structures with fibre-reinforced polymers, Canadian Standard Association.

De Lorenzis, L., and Tepfers, R. (2003). "Comparative study of models on confinement of concrete cylinders with fibre reinforced polymer composites." Journal of Composites for Construction, 7(3), 219–237.

Elsanadedy, H. M., and Haroun, M. (2005). “Seismic design criteria for circular lap-spliced reinforced concrete bridge columns retrofitted with fibre-reinforced polymer jackets”. ACI Structural Journal, 102(3), 354–362.

Fam, A. Z., and Rizkalla, S. H. (2001). “Confinement model for axially loaded concrete confined by circular fibre-reinforced polymer tubes.” ACI Structural Journal, 98(4), 451–461.

Fardis, M. N., and Khalili, H. (1982). “FRP-encased concrete as a structural material.” Magazine of Concrete Research, 34(122), 191–202.

Fischer, G., and Li, V. (2003). “Deformation behavior of fibre-reinforced polymer reinforced engineered cementitious composite flexural members under reversed cyclic loading conditions”, ACI Structural Journal, 100 (1): 25-35.

Gallardo-Zafra, R., and Kawashima, K. (2009). “Analysis of carbon fibre sheet retrofitted RC bridge piers under lateral cyclic loading.” Journal of Earthquake Engineering, 13, 129–154.

Gamble, W. L., Hawkins, N. M., and Kaspar, I. I. (1996). “Seismic retrofitting experience and experiments in Illinois.” Proc., 5th National Workshop on Bridge Research in Progress, National Center for Earthquake Engineering Research (NCEER), State Univ. of New York at Buffalo, Buffalo, NY, USA, 245–250.

Ghannoum, W., Saouma, V., Haussmann, G., Polkinghorne, K., Eck, M., and Kang, D.H. (2012). “Experimental Investigations of Loading Rate Effects in Reinforced Concrete Columns.” ASCE Journal of Structural Engineering, 138(8), 1032-1041.

Gu, D. S., Wu, G., Wu, Z. S., and Wu, Y. F. (2010). “Confinement effectiveness of FRP in retrofitting circular concrete columns under simulated seismic load”. Journal of Composites for Construction, ASCE, 14(5), 531–540.

Han, Q., Wen, J., Du, X., and Jia, J. (2014). “Experimental and numerical studies on seismic behavior of hollow bridge columns retrofitted with carbon fibre reinforced polymer.” Journal of Reinforced Plastic and Composites, 33(24), 2214–2227.

Haroun, M. A., and Elsanadedy, H. M. (2005). “Fibre reinforced plastic jackets for ductility enhancement of reinforced concrete bridge columns with poor lap-splice detailing”. Journal of Bridge Engineering. ASCE, 10(6), 749–757.

Haroun, M. A., Mosallam, Ayman, S., Feng, M. Q., and Elsanadedy, H. M. (2003). “Experimental investigation of seismic repair and retrofit of bridge columns by composite jacket”. Journal of Reinforced Plastics and Composites, 22(14).

Harries, K. A., and Carey, A. (2002). “Shape and ‘gap’ effects on the behavior of variably confined concrete.” Cement and Concrete Research, 33(6), 873–880.

Housner, G. W. (1971). General features of the San Fernando earthquake, Edited by P.C. Jennings, Report no: 71-02, Earthquake engineering laboratory, California Institute of Technology, Pasadena, CA.

Huijbregts, R. (2012). “To modernize Canada’s public infrastructure – every bridge needs a switch.” Cisco Canada, <http://canadablog.cisco.com/2012/12/13/to-modernize-canadas-public-infrastructure-every-bridge-needs-a-switch/>.

Intelligent Sensing for Innovative Structures (ISIS) Canada. (2008). Design manual no. 4: FRP rehabilitation of reinforced concrete structures, Version 2, Winnipeg, Canada.

Kaushik, S., Prakash, A., and Singh, A. (1990). “Inelastic buckling of ferrocement encased columns.” Proceedings of the fifth international symposium on ferrocement, Swamy, ed., In: Nedwell, 327–341.

Kawashima, K. (2011). “Lecture notes from “Seismic design of urban infrastructure.” Engineering characterization of ground motion, Seismic damage in the past earthquakes, Seismic design}, Tokyo Institute of Technology, Division of Civil Engineering, Japan.

Kesner, K. E., and Billington, S. L. (2004). Tension, compression and cyclic testing of engineered cementitious composite materials. Technical Report MCEER-04-0002 (Multidisciplinary Center for Earthquake Engineering Research).

Kesner, K. E., and Billington, S. L. (2005). "Investigation of Infill Panels Made from Engineered Cementitious Composites for Seismic Strengthening and Retrofit", Journal of Structural Engineering, 113 (11): 1712-1720.

Kumar, P. R., Oshima, T., Mikami, S., and Yamazaki, T. (2005). "Seismic retrofit of square reinforced concrete piers by ferrocement jacketing", Structure and Infrastructure Engineering, 1 (4): 253-262.

Lam, L., and Teng, J. G. (2003a). "Design-oriented stress-strain model for FRP-confined concrete in rectangular columns." Journal of Reinforced Plastic Composites, 22(13), 1149–1186.

Lam, L., and Teng, J. G. (2003b). "Design-oriented stress–strain model for FRP-confined concrete." Construction and Building Materials, 17(6-7), 471–489.

Lam, L., and Teng, J. G. (2004). "Ultimate Condition of Fibre Reinforced Polymer-Confined Concrete." Journal of Composites for Construction, 8(6), 539–548.

Li, V. C. (1992). "Performance driven design of fibre reinforced cementitious composites." 4th Int. Symposium on Fibre Reinforced Concrete, R N Swamy, ed., 12–30.

Li, V. C., Wang, S., and Wu, C. (2001). "Tensile strain-hardening behavior of polyvinyl alcohol engineered cementitious composite (PVAECC)." ACI Material Journal, 98, 483–492.

Li, Y. F., and Sung, Y. Y. (2004). "A study on the shear-failure of circular sectioned bridge column retrofitted by using CFRP jacketing". Journal of Reinforced Plastics and Composites, 23(8), 811–830.

Ma, R., and Xiao, Y. (1997). "Seismic retrofit and repair of circular bridge columns with advanced composite materials." Earthquake Spectra, 15(4), 747–764.

Maekawa, K., and An, X. (2000). "Shear failure and ductility of RC columns after yielding of main reinforcement." Engineering Fracture Mechanics, 65(2), 335–368.

Mander, J. B., Priestley, M. J. N., and Park, R. (1988). “Theoretical stress-strain model for confined concrete.” Journal of Structural Engineering, ASCE, 114(8), 1804–1825.

Marques, S. P. C., Marques, D. C. dos S. C., Silva, J. L. da, and Cavalcante, M. A. A. (2004). “Model for analysis of short columns of concrete confined by fibre reinforced polymer.” Journal of Composites for Construction, ASCE, 8(4), 332–340.

Matthys, S., Taerwe, L., and Audenaert, K. (1999). “Tests on axially loaded concrete columns confined by fibre reinforced polymer sheet wrapping.” Proceedings of the 4th International Symposium on FRP for Reinforced Concrete Structures, Baltimore, USA, 217–228.

Matthys, S., Toutanji, H., and Taerwe, L. (2006). “Stress–strain behavior of large-scale circular columns confined with FRP composites.” Journal of Structural Engineering. ASCE, 132(1), 123–133.

Menegotto, M., and Pinto, P. E. (1973). “Method of analysis for cyclically loaded R.C. plane frames including changes in geometry and non-elastic behavior of elements under combined normal force and bending.” In: Symposium on the resistance and ultimate deformability of structures acted on by well-defined repeated loads, International Association for Bridge and Structural Engineering, Zurich, Switzerland, 15–22.

Mirmiran, A. and Shahawy, M. (1997). “Behavior of concrete columns confined by fibre composites”. Journal of Structural Engineering, ASCE 123(5), 583–590.

Mirmiran, A., Shahawy, M., Samaan, M., Echary, H., Mastrapa, J., and Pico, O. (1998). “Effect of column parameters on FRP-confined concrete.” Journal of Composites for Construction, ASCE, 2(4), 175–185.

Mitchell, D., Bruneau, M., Williams, M., Anderson, D. L., and Sexsmith, R. G. (1995). “Performance of bridges in 1994 Northridge Earthquake”, Canadian Journal of Civil Engineering, 22 (2): 415-427.

Mitchell, D., Sexsmith, R. G., and Tinawi, T. (1994). “Seismic retrofit techniques for bridges- A state of the art report”, Canadian Journal of Civil Engineering, 21 (5): 823-835.

Mitchell, D., Tinawi, T., and Sexsmith, R. G. (1991). “Performance of bridges in 1989 Loma Prieta Earthquake- Canadian design concerns”, Canadian Journal of Civil Engineering, 18 (4): 711-734.

Moran, D. and Pantelides, C. (2002). “Stress-strain model for fibre reinforced polymer-confined concrete”. Journal of Composites for Construction, ASCE 6(4), 233–240.

Mortezaei, A., and Ronagh, H. R. (2012). “Plastic hinge length of FRP strengthened reinforced concrete columns subjected to both far-fault and near-fault ground motions.” Scientia Iranica, 19(6), 1365–1378.

Nanni, A., Alkhrdaji, T., Chen, G., Barker, M., Yang, X., and Mayo, R. (1999). “Testing failure program for highway bridge strengthened with fibre reinforced polymer composites”, Proceedings of the 4th Int. Symposium on Fibre Reinforced Polymer Reinforcement for Reinforced Concrete Structures, Selected Presentation Proceedings, American Concrete Institute, Farmington Hills, Mich., 69-80.

Norris, T., Saadatmanesh, H., and Ehsani, M. R. (1997). “Shear and flexural strengthening of R/C beams with carbon fibre sheets.” Journal of Structural Engineering, ASCE, 123(7), 903–911.

Ozbakkaloglu, T., and Oehlers, D. J. (2008). “Manufacture and testing of a novel FRP tube confinement system.” Engineering Structures, 30(9), 2448–2459.

Parghi, A. and Alam, M.S. (2016). “Seismic behavior of deficient reinforced concrete bridge piers confined with FRP – A fractional factorial analysis.” Engineering Structures, 126, 531–546.

Parghi, A. and Alam, M.S. (2017). “Seismic collapse assessment of non-seismically designed circular RC bridge piers retrofitted with FRP composites.” Composite Structures, 160, 901–916.

Parra-Montesions, G., and Wight, J. K. (2000). “Seismic response of exterior RC column-to-steel beam connections”, ASCE Journal of Structural Engineering, 1113-1121.

Pessiki, S., Harries, K., Kestner, J., Sause, R., and Ricles, J. M. (2001). “The axial behavior of concrete confined with fibre reinforced composite jackets.” Journal of Composites for Construction, 5(4), 237–245.

Priestley, M. J. N., and Park, R. (1984). "Strength and Ductility of Bridge Substructures," Road Research Unit Bulletin 71, New Zealand National Roads Board, Wellington, 120 pp.

Priestley, M. J. N., and Seible, F. (1991). Seismic assessment and retrofit of bridges. Research Report SSRP-91/03, Department of Applied Mechanics and Engineering Sciences, University of California, San Diego, USA.

Priestley, M. J. N., and Seible, F. (1993). Repair of shear column using fibre glass / epoxy jacket and epoxy injection. Rep. No. 93-04. Job No. 90-08, Seqad Consulting Engineers, Salona Beach, CA.

Priestley, M. J. N., and Seible, F. (1995). “Design of seismic retrofit measures for concrete and masonry structures.” Construction and Building Materials, 9(6), 365–377.

Priestley, M. J. N., Seible, F., and Calvi, G. M. (1996). Seismic design and retrofit of bridges. John Wiley & Sons, Inc., New York, USA, Chichester, Brisbane, Toronto, Singapore.

Priestley, M. J. N., Seible, F., Xiao, Y., and Verma, R. (1994). “Steel jacket retrofitting of reinforced concrete bridge columns for enhanced shear strength-Part 1: Theoretical considerations and test design.” ACI Structural Journal, 91(4), 394–405.

Rodriguez, M., and Park, R. (1994). “Seismic load tests of reinforced concrete columns strengthened by jacketing.” ACI Structural Journal, 91(2), 150–159.

Saadatmanesh, H., Ehsani, M. R., and Jin, L. (1994). “Strength and ductility of concrete columns externally reinforced with fibre composite straps.” ACI Structural. Journal, 91(4), 434–447.

Saadatmanesh, H., Ehsani, M. R., and Jin, L. (1997). “Repair of earthquake-damaged RC columns with FRP wraps.” ACI Structural Journal, 94(2), 206–2014.

Saatcioglu, M., and Yalcin, C. (2003). “External prestressing concrete columns for improved seismic shear resistance.” Journal of Structural Engineering, ASCE, 129(8), 1057–1070.

Samaan, M., Mirmiran, A., and Shahawy, M. (1998). “Model of concrete confined by fibre composites.” Journal of Structural Engineering, ASCE, 124(9), 1025–1031.

Seffo, M., and Hamcho, M. (2012). “Strength of Concrete Cylinder Confined by Composite Materials (CFRP).” Energy Procedia, Elsevier B.V., 19, 276–285.

Seible, F., and Priestley, M. J. N. (1999). Lessons learned from bridge performance during Northridge earthquake, ACI special publication, SP-187: 29-56.

Seible, F., Priestley, M. J. N., Hegemier, G., and Innamorato, D. (1997). “Seismic retrofit of RC columns with continuous carbon fibre jackets.” Journal of Composites for Construction, ASCE, 1(2), 52–62.

Seismosoft (2016) "SeismoStruct 2016 – A computer program for static and dynamic nonlinear analysis of framed structures," available from http://www.seismosoft.com.

Sheikh, S. A., and Yau, G. (2002). “Seismic behavior of concrete columns confined with steel and fibre reinforced polymers.” ACI Structural Journal, 99(1), 72–80.

Shin, M., and Andrawes, B. (2011). “Emergency repair of severely damaged reinforced concrete columns using active confinement with shape memory alloys.” Smart Materials and Structures, 20(6), 065018.

Spoelstra, M. R., and Monti, G. (1999). “FRP-confined concrete model.” Journal of Composites for Construction, ASCE, 3(3), 143–150.

Taylor, A. W. (1999). Performance of reinforced concrete bridge in January 1995 Hyogoken Nanbu (Kobe) earthquake, ACI special publication, SP-187: 57-68.

Teng, J. G., Huang, Y. L., Lam, L., and Ye, L. P. (2007). "Theoretical Model for Fibre-Reinforced Polymer-Confined Concrete." Journal of Composites for Construction, ASCE, 11(2), 201–210.

Teng, J. G., and Lam, L. (2002). "Compressive behavior of carbon fibre reinforced polymer-confined concrete in elliptical columns." Journal of Structural Engineering, ASCE, 128(12), 1535–1543.

Theriault, M., Neale, K., and Claude, S. (2004). "Fibre-reinforced polymer-confined circular concrete columns: investigation of size and slenderness effects." Journal of Composites for Construction, 8(4), 323–331.

Tsai, K. C., and Lin, M. L. (2001). Steel jacket retrofitting of rectangular RC bridge columns to prevent lap-splice and shear failure. Technical report national centre for research on earthquake engineering, National Taiwan University, Taiwan.

Wang, Z. Y., Wang, D. Y., Dheikh, S. A., and Liu, J. T. (2010). "Seismic performance of FRP-confined circular RC columns". CICE 2010 - The 5th International Conference on FRP Composites in Civil Engineering, A. in F. C. in C. E. L. Ye et al., ed., Tsinghua University Press, Beijing and Springer-VerlagBerin Heidelberg, Beijing, China, 810–814.

Williamson, R. B., and Fisher, F. L. (1983). Fire resistance of a load bearing ferrocement wall. Report no. UCBFRG-83-1, Department of Civil Engineering, University of California, Berkeley, USA.

Xiao, Y., and Wu, H. (2000). "Compressive behavior of concrete confined by carbon fibre composite jackets." Journal of Materials in Civil Engineering. ASCE, 12, 139–146.

Xiao, Y., and Wu, H. (2001). "Concrete stub columns confined by various types of FRP jackets." In: Proceedings of the international conference on FRP composites in Civil Engineering, T. JG, ed., Hong Kong, China, 293–300.

Xiao, Y., Wu, H., and Martin, G. R. (1999). “Prefabricated composite jacketing of RC columns for enhanced shear strength.” Journal of Structural Engineering, ASCE, 125(3), 255–264.

Xiong, G. J., Wu, X. Y., Li, F. F., and Yan, Z. (2011). “Load carrying capacity and ductility of circular concrete columns confined by ferrocement including steel bars.” Construction and Building Materials, 25, 2263–2268.

Yen, W. H. (2002). Lessons Learned about Bridges from Earthquake in Taiwan. Vol. 65, 4, Public Roads, U.S. Department of Transportation, Federal Highway Administration, Washington, DC 20402-9325 USA.

Yoneda, K., Kawashima, K., and Shoji, G. (2001). “Seismic retrofit of circular reinforced bridge columns by wrapping of carbon fibre sheets”. Journal of Structural Engineering and Earthquake Engineering, JSCE 682/I56, 41–56 (in Japanese).

Youssef, M. N., Feng, M. Q., and Mosallam, A. S. (2007). “Stress–strain model for concrete confined by FRP composites.” Composite Part B: Engineering, 38(5-6), 614–628.

Yun, H., Kim, S., Jeon, E., and Park, W. (2005). Effects of Matrix Ductility on the Shear Performance of Precast Reinforced HPHFRCC Coupling Beams, Proceedings of the 2nd Korea-Japan International Joint Symposium on Manufacture/ Construction/ Structural Applications of High-Performance Fibre Reinforced Cementitious Composites, Daejon, Korea.

Zong-Cai, D., Daud, J. R., and Hu, L. (2014). “Seismic behavior of short concrete columns with prestressing steel wires.” Advances in Materials Science and Engineering, Article ID (180193), 10.

Zulfiqar, N., and Filippou, F. C. (1990). “Models of critical regions in reinforced concrete frames under earthquake excitations”. Report No. EERC 90-06, University of California, Berkeley, USA.